BOND BEHAVIOR OF 15.2-MM (0.6-INCH) DIAMETER PRESTRESSING STRANDS IN SAN ANGELO BRIDGE RESEARCH BEAMS

by

Michael Owen Braun, B.S.

THESIS

Presented to the Faculty of the Graduate School of

The University of Texas at Austin

in Partial Fulfillment

of the Requirements

for the Degree of

MASTER OF SCIENCE IN ENGINEERING

The University of Texas at Austin

December 2002

BOND BEHAVIOR OF 15.2-MM (0.6-INCH) DIAMETER PRESTRESSING STRANDS IN SAN ANGELO BRIDGE RESEARCH BEAMS

Approved by
Supervising Committee:

Michael E. Kreger

Ned H. Burns

Acknowledgements

Abstract

BOND BEHAVIOR OF 15.2-MM (0.6-INCH) DIAMETER PRESTRESSING STRANDS IN SAN ANGELO BRIDGE RESEARCH BEAMS

by

Michael Owen Braun, M.S.E.

The University of Texas at Austin, 2002

Supervisors: Michael E. Kreger and Ned H. Burns

The objective of this research was to determine the transfer and development lengths for fully bonded, 15.2 mm (0.6 in.) diameter strand on a 51 mm (2 in.) grid in full-size, I-shaped concrete beams. Two Texas Type C beams were fabricated with high-strength concrete and two were fabricated with normal-strength concrete. The high-strength and normal-strength concrete had 56-day and 28-day compressive strengths of approximately 90 MPa (13,000 psi) and 48 MPa (7000 psi), respectively. The laboratory research beams were intended to have characteristics similar to the AASHTO Type IV beams of a bridge under design, and now completed, in San Angelo, Texas. Also, to assess the surface condition of the strand and its effect on bond, pull-out tests were performed on strand samples embedded in concrete blocks .

Results from transfer and development length tests performed on the laboratory research beams were compared with values predicted by equations from the American Concrete Institute code and the American Association of State Highway Transportation Officials specifications. Results also were compared with values predicted by equations proposed by other researchers.

TABLE OF CONTENTS

LIST OF TABLES

LIST OF FIGURES

CHAPTER ONE

Introduction

1.1 BACKGROUND AND PROBLEM DEFINITION

The use of 12.7 mm (1/2 inch) diameter prestressing strands at a 51 mm (2 in.) spacing is common practice in the prestressed, precast concrete industry. High-strength, high-performance concrete ($f'_c > 69$ MPa [10,000 psi]), which has been studied and has grown in use in recent years, requires a larger prestress force than normal-strength concrete to be used efficiently. One way to provide a larger prestress force without expensive new or modified concrete forms is to use larger 15.2 mm (0.6 in.) diameter strands on the standard 51 mm (2 in.) grid. However, in October 1988, the Federal Highway Administration (FHWA) issued a memorandum that placed the following restrictions on the use of prestressing strands for pretensioned prestressed concrete members in highway bridge applications:

1. The use of 15.2 mm (0.6 in.) diameter strand in a pretensioned application shall not be allowed.

2. Minimum strand spacing (center-to-center of strand) will be four times the nominal strand diameter.

3. Development length for all strand sizes up to and including 9/16 inch special strand shall be determined as 1.6 times the AASHTO equation 9-32.

4. Where strand is debonded (blanketed) at the end of a member, and tension at service load is allowed in the precompressed tensile zone, the development length shall be determined as 2.0 times AASHTO equation 9-32 as currently required by AASHTO article 9.27.3.

This memorandum was issued, because research just completed at that time suggested that, for pretensioned strands, the transfer and development length provisions of the American Association of State Highway and Transportation Officials (AASHTO)

Specifications[2] were unconservative. To address this concern, the FHWA funded additional research projects in the United States. This report describes one of those research projects.[1]

1.2 OBJECTIVES

This project was part of a larger research program funded by the FHWA and the Texas Department of Transportation (TxDOT). The objective of this phase of the research program was to determine the transfer and development lengths of straight, fully bonded 15.2 mm (0.6 in.) diameter strands at a 51 mm (2 in.) spacing in full-sized, I-shaped concrete beams. The test beams were to have characteristics similar to the AASHTO Type IV beams of the then proposed San Angelo Bridge on U.S. Highway 67 over U.S. Highway 87 and the North Concho River in San Angelo, Texas. That bridge was designed and built with high-performance concrete (HPC) beams as well as normal-strength concrete (NSC) beams. Similarly, this study tested beams fabricated with both types of concrete.

1.3 SCOPE

Four TxDOT Type C beams (two HPC beams and two NSC beams) were fabricated and tested. The TxDOT Type C beam section is 1016 mm (40 in.) deep with a 178 mm (7 in.) thick web. Transfer length was determined at the fabrication plant from concrete strain measurements and end slip measurements at both ends of each beam.

The beams were transported to the Ferguson Structural Engineering Laboratory at The University of Texas at Austin where a 191 mm (7.5 in.) thick composite slab was added to each beam in preparation for a series of development length load tests. There was one series of load tests for the HPC beams and another for the NSC beams. The development length was determined from an iterative procedure in which each end of

---

[1] In 1996 after the results of this and other studies were known, the strict development length requirements and the ban on 15.2 mm (0.6 in.) diameter strands in pretensioned members were removed by the FHWA.

each beam in a series was load tested with a different embedment length based on the failure mode of the preceding test.

Strand pull out tests also were performed to assess the strand surface condition. Six strand samples were embedded 508 mm (20 in.) into a large HPC test block, and six were embedded into a NSC test block. The strands were individually pulled to their ultimate load. The failure mode and the ultimate load were recorded.

1.4 RESULTS – EXPECTED AND ACTUAL

The researchers expected to obtain development lengths between 1980 to 2130 mm (78 to 84 in.), which were the values obtained for 15.2 mm (0.6 in.) diameter strands in the rectangular and I-shaped beams, respectively, of a previous research project conducted at The University of Texas at Austin.[17] The researchers of this study also expected to find that development length decreased for higher strength concrete.

An upper bound of 1830 mm (72 in.) was determined for the development length of the 15.2 mm (0.6 in.) diameter strands in the I-shaped beams of this study. The upper bound development length was the same for normal-strength and high-strength concrete. This upper bound was about 25% less than values predicted by the ACI/AASHTO development length equations.

Exceptionally good results were also obtained for transfer length measurements and pull out tests. The consistently good results for all tests suggest that the surface condition of the strand might have been especially favorable for bond.

1.5 RESEARCH PERSONNEL

Carlos Cordova and Analbhai Shah were graduate students at The University of Texas at Austin who also fulfilled part of the requirements for a Master of Science in Engineering by working on this research study. Cordova[22] completed his thesis in 1996 on the transfer and development length of 15.2 mm (0.6 in.) diameter strand in normal-strength concrete excluding the end slip data. Shah[23] completed his report in 1996 on the transfer length for normal-strength and high-strength concrete based on end slip data.

Portions of their work have been incorporated into this thesis. A concerted effort has been made to credit them for their contributions. None of their work has been knowingly used without acknowledgement.

1.6　TOPICAL OUTLINE

The outline of this thesis is the same as that for the thesis by Cordova as the subject matter is the same. Chapter Two briefly discusses basic concepts and previous research on the transfer and development length of pretensioned strand. The test program is described in Chapter Three, and the results are presented in Chapter Four. A discussion of the results and the conclusions are presented in Chapter Five and Chapter Six, respectively.

CHAPTER TWO

Literature Review

2.1 INTRODUCTION

This chapter presents background information about bond between concrete and prestressing strand in pretensioned prestressed concrete members. Definitions of transfer and development length are given along with a brief description of the mechanisms of bond and a list of factors that affect transfer and development length. Summaries of previous experimental research programs are presented. Transfer and development length formulas proposed by various researchers are listed in the table at the end of this chapter. The notation used throughout this report is listed in Appendix G.

2.2 DEFINITIONS

Transfer length is the length of bond needed to develop the effective prestress, f_{se}, in the strand.[10,13,20] See Figure 2.1.

Flexural bond length is the additional length required to develop the increase in strand stress from the effective prestress, f_{se}, to the stress at the nominal flexural strength of the cross section, f_{ps}.[10,13,20] Flexural bond results from the application of external loads.[9,22]

Development length is the total length of bond required to develop the strand stress at the nominal flexural strength of the cross section, f_{ps}. Development length is taken as the algebraic sum of transfer length and flexural bond length.[13,20]

Embedment length is the length of bond from the beginning of bond of the strand to the critical section. The critical section is located at the point of maximum moment where the strand stress is maximum. The beginning of bond in fully bonded strands is located at the ends of the beam, while for debonded strands, it is located where the debonding ends. To prevent bond failure, the embedment length should exceed the development length.[1,2,20,22]
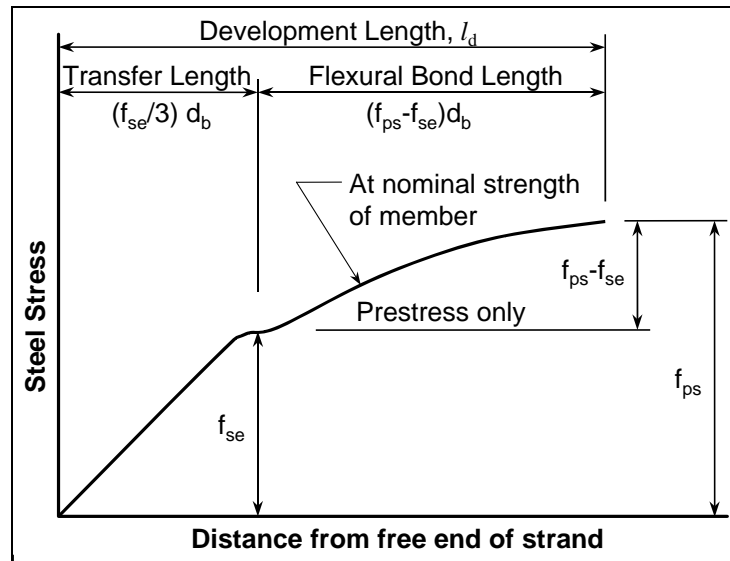
Figure 2.1   Steel stress vs. distance from free end of strand [1]

2.3   NATURE OF BOND OF PRETENSIONED STRAND

2.3.1   Bond Mechanisms

Adhesion, Hoyer's effect, and mechanical interlock are the mechanisms that develop bond between concrete and pretensioned steel strand.

Adhesion — The concrete adheres to the surface of clean strand.   The contribution of this mechanism is small.   The behavior of this mechanism is rigid-brittle (i.e., not ductile).   Once the strand slips, adhesion is lost.[10,17,20,22]

Hoyer's Effect — When a steel strand is prestressed, its diameter decreases as a function of Poisson's ratio.   When the prestress force is released, the strand extending from the end of the member returns to its original diameter.   Inside the member where bonding begins, the strand returns partially to its original diameter and imposes a normal pressure on the surrounding concrete.   This normal pressure induces friction, which acts against shortening of the strand and holds the strand in tension.[10,17,20,22]   The strand diameter varies from its original size at the free end where its stress is zero to some

slightly smaller size where its stress equals the effective prestress. For this reason, this mechanism is sometimes called wedging action.[17,20]

Mechanical Interlock — This mechanism is similar to the pull out resistance of deformed reinforcing bars in concrete. Seven-wire prestressing strand has a center wire wrapped by six outer wires in a helical pattern. The hardened concrete provides essentially perfect encasement for the strands. If twisting is prevented, straight pull out of prestressing strand is resisted by the narrow ridges of concrete in the corrugations of the strand's outer surface.[10,17,20,22]

2.3.2   Bond Stresses

Bond stresses in pretensioned prestressed concrete are often classified as transfer bond stresses or flexural bond stresses depending upon their function.

Transfer bond stresses transfer the effective prestress force from the strand to the concrete. These stresses occur at the ends of the bonded portion of a pretensioned strand and extend for a certain length called the transfer length. Transfer bond stresses are developed by Hoyer's effect and mechanical interlock. Adhesion does not contribute to bond in the transfer zone, because the strand slips relative to the concrete in that region.[10,17,20,22]

Flexural bond stresses develop the increase in strand stress due to external loads applied to the member. Flexural bond stresses are developed from the point where the load is applied to the end of the transfer length. This length is called the flexural bond length. Prior to cracking, the flexural bond stresses are small, because stress in the strand increases very little in an uncracked section. Once cracks form, stress in the strand increases dramatically at each crack and the flexural bond stresses become significant.[9,10,17,20,22] Janney observed that there is little interaction between the transfer bond stresses and the flexural bond stresses.[10,22]

2.3.3   General Bond Failure

Various researchers have mentioned different causes for a general bond failure. Janney[10] concluded that final bond failure occurs when a wave of high flexural bond stresses (from increased loading) progress toward the end of the beam and encroach upon the region of the transfer bond stresses. Hanson and Kaar[9] stated that bond failure is attributed to a reduction of the diameter of the strand in the transfer region. When flexural bond stresses reach the transfer zone, they increase the stress of the strand, so its diameter is reduced and the strand tends to slip. Russell and Burns[17] observed that bond failure occurred when web shear cracks propagated across the strands in the transfer zone.

2.4   FACTORS AFFECTING TRANSFER AND DEVELOPMENT LENGTH

Zia and Mostafa[20] listed the following factors that affect transfer and development length of prestressing steel.

1. Type of steel, e.g. wire, strand
2. Steel size (diameter)
3. Steel stress level
4. Surface condition of steel -- clean, oiled, rusted
5. Concrete strength
6. Type of loading, e.g., static, repeated, impact
7. Type of release, e.g., gradual, sudden (flame cutting, sawing)
8. Confinement reinforcement around steel, e.g., helix or stirrups
9. Time-dependent effect
10. Consolidation and consistency of concrete around steel
11. Amount of concrete coverage around strand

As noted by Cordova[22], detailed discussion of each point can be found in papers written by Cousins et al.[5], Deatherage et al.[6], Hanson[8], Kaar et al.[11], Mitchell et al.[15], and Russell and Burns.[17]

2.5 PREVIOUS RESEARCH

Many experimental programs have investigated the transfer and development length of prestressing strands. A brief summary of related research is presented below.

2.5.1 Hanson and Kaar – Portland Cement Association (1959)

Hanson and Kaar[9] tested small beam specimens with strand sizes up to 12.7 mm (1/2 in.) in diameter. The ACI[1]/AASHTO[2] expressions for transfer and development length are based mainly on the results of these tests.[14]

2.5.2 Janney – Portland Cement Association (1959)

Janney[10] conducted transfer and development length tests of small prism and beam specimens with strand sizes up to 12.7 mm (1/2 in.) in diameter.

2.5.3 Kaar, LaFraugh and Mass – Portland Cement Association (1963)

The transfer length research by Kaar et al.[11] was conducted on small test specimens with strand sizes up to 12.7 mm (1/2 in.) in diameter and several concrete strengths up to 34 MPa (5000 psi). Concrete strength did not consistently affect transfer length, but strand size did. Transfer lengths were longer for the larger diameter prestressing strands.

2.5.4 Martin and Scott — The Consulting Engineers Group, Illinois (1976)

Martin and Scott[14] proposed revisions to the ACI provisions for transfer and development length. The proposed revisions were based on a review of the test results of Hanson and Kaar.[9]

2.5.5 Zia and Mostafa — North Carolina State University (1977)

Zia and Mostafa[20] conducted an extensive review of literature and proposed transfer and development length equations that include the effects of strand size, initial

concrete strength, initial prestress and effective prestress. The equations are valid for initial concrete strengths from 14 to 55 MPa (2000 to 8000 psi).

2.5.6 Cousins, Johnston and Zia — North Carolina State University (1990)

Cousins et al.[5] presented a summary of their transfer and development length research results and proposed equations to predict transfer and development length. Their research tested three sizes of strand with the largest being 15.2 mm (0.6 in.) diameter strand. Some strands were coated with epoxy and grit, and other strands were uncoated. The test specimens were small with only one strand each.

The average transfer length of the uncoated strands was about twice as long as the epoxy-coated strands. The average transfer length of the uncoated strand exceeded the value predicted by the simplified ACI/AASHTO expression (50 times the strand diameter) by 85%. The authors' proposed transfer length equation tended to slightly underestimate the measured transfer lengths from their research and to overestimate them for the results of other researchers. The proposed development length equation and the current ACI/AASHTO expression tended to underestimate the results of their research for the two larger strand sizes and to overestimate it for the smallest strand size.

2.5.7 Shahawy, Issa and Bachelor — Florida Dept. of Transportation (1992)

Shahawy et al.[18] measured the transfer length of 12.7 and 15.2 mm (1/2 and 0.6 in.) diameter strands in full-scale AASHTO Type II prestressed concrete beams. The average transfer lengths were about 20% greater than predicted by the simplified ACI/AASHTO expression. The recommended transfer length was one third of the initial prestress times the strand diameter, $(f_{si}/3)d_b$. A center-to-center strand spacing of 51 mm (2 in.) was satisfactory for the 15.2 mm (0.6 in.) diameter strands, which is less than the spacing of four times the strand diameter mandated in the 1988 FHWA memorandum.

2.5.8 Lane — Federal Highway Administration (1992)

Lane[12] measured the transfer length of small test specimens containing one or four strands. Three strand sizes were tested with and without an epoxy and grit coating. The transfer lengths were longer for larger strand sizes and for more strands per test specimen. Considering all sizes of epoxy-coated strands, the average transfer length was approximately 50 times the strand diameter. For 15.2 mm (0.6 in.) diameter strands, the transfer length was only 43 times the strand diameter. The uncoated strands had transfer lengths about 60% longer than the epoxy-coated strands.

2.5.9 Mitchell, Cook, Tham and Khan — McGill University (1993)

Mitchell et al.[15] tested small rectangular beams containing a single strand. The primary variables were concrete strength and the strand diameter. Higher strength concrete had consistently shorter transfer lengths. Based on their test results, the authors proposed transfer and development length equations that predict values shorter than the ACI/AASHTO expressions.

2.5.10 Russell and Burns — The University of Texas at Austin (1993)

The transfer and development length research by Russell and Burns[17] investigated the effect of the number of strands, strand size (12.7 or 15.2 mm [1/2 or 0.6 in.] diameter strand), debonding, confining reinforcement, specimen size, and type of cross section (rectangular or I-shaped). Although concrete strength was not one of the design variables, transfer lengths were consistently longer in lower strength concrete specimens. Specimen size affected transfer length as large I-shaped beams had shorter transfer lengths than small prism test specimens. For small test specimens, more strands per specimen increased the transfer length. A center-to-center strand spacing of 51 mm (2 in.) was sufficient for 15.2 mm (0.6 in.) diameter strands based on measured transfer lengths.

Transfer lengths were longer for the larger diameter strand. The average measured transfer lengths were longer than predicted by the simplified ACI/AASHTO

expression. The authors recommended a transfer length of one half of the effective prestress times the strand diameter, $(f_{se}/2)d_b$. This is 50% more than the ACI/AASHTO expression.

The development lengths determined for the larger strand were equal to or less than specified by the ACI/AASHTO expression. For the smaller strand, the results were mixed. The development length of the smaller strand in I-shaped beams was less than specified by the ACI/AASHTO expression. In the rectangular beams, the development length of the smaller strand exceeded the ACI/AASHTO specified length possibly due to an unusually poor strand surface condition. The authors found that flexural and/or shear cracks that cross the strands in the transfer zone cause strand slip. Instead of a development length expression, the authors recommended a design provision that prevents cracks from forming in the transfer zone.

2.5.11 Deatherage, Burdette and Chew — University of Tennessee (1994)

Deatherage et al.[6] tested full-scale AASHTO Type I beams to determine the transfer and development length for various strand sizes, the largest being 15.2 mm (0.6 in.) in diameter. The transfer length was approximately proportional to the strand diameter, except for the largest strand. The average transfer length for that strand was shorter than suggested by results from the smaller strand sizes. The average transfer length for 15.2 mm (0.6 in.) diameter strand was shorter than the value predicted by the simplified ACI/AASHTO expression, while the smaller strand sizes had average transfer lengths longer than predicted. The authors found that a transfer length expression based on the initial prestress, f_{si}, was consistent with the test results. The ACI/AASHTO expression for development length predicted values that were slightly unconservative compared to the development lengths determined from the load tests. The authors proposed an increase in the flexural bond length term of the ACI/AASHTO development length expression.

The strand surface was in "milled" condition except for one series of tests. Strand weathered for three days had no visible rust, yet the transfer lengths decreased by

5% to 40%. Center-to-center strand spacing of 3.5 times and 4.0 times the strand diameter were tested for 12.7 mm (1/2 in.) diameter strand. The smaller strand spacing was satisfactory based on the ultimate moment capacity from load tests.

2.5.12 Gross and Burns — The University of Texas at Austin (1995)

Gross and Burns[7] measured the transfer and development length of 15.2 mm (0.6 in.) diameter strands in large rectangular, high-performance concrete beams. The ACI/AASHTO expressions and proposed equations by various researchers predict transfer and development lengths that were longer than the measured values.

2.5.13 Tawfiq — Florida State University (1995)

Tawfiq[19] conducted field and laboratory tests on full-scale AASHTO Type II prestressed concrete beams with 12.7 mm (1/2 in.) diameter strand. The parameters of this study were concrete strength and the amount of shear reinforcement. The objective was to measure the transfer length and the shear capacity of high-performance concrete beams. The measured transfer lengths were inversely proportional to the concrete compressive strength.

2.5.14 Buckner — Federal Highway Administration (1995)

Buckner[3] reviewed recent literature, analyzed the data to understand and explain differences between conclusions, and recommended expressions to predict the transfer and development lengths of Grade 270 (1860 MPa [270 ksi] guaranteed ultimate tensile strength), low-relaxation, seven-wire strand. The recommended transfer length expressions were 20% longer than the ACI/AASHTO provisions. The recommended general expression is one third of the initial prestress times the strand diameter, $(f_{si}/3)d_b$. The simplified expression is 60 times the strand diameter.

The recommended development length expression includes the recommended transfer length expression plus a term for the flexural bond length. From a review of development length load test results, the author found that test beams often failed

prematurely due to bond as the applied moment approached the nominal flexural strength of the cross section. The author recommended increasing the ACI/AASHTO flexural bond length term by the factor, λ. This factor increases from 1.0 to 2.0 as the strand strain approaches 0.035, which is the guaranteed minimum elongation of the strand. A transfer and development length multiplier of 1.3 is recommended for strands in the upper third of the member with at least 305 mm (12 in.) of concrete below.

2.6 EQUATIONS FOR TRANSFER AND DEVELOPMENT LENGTH

2.6.1 ACI Code and AASHTO Specifications Requirements

The American Concrete Institute (ACI) Building Code Requirements for Reinforced Concrete[1] and the American Association of State Highway and Transportation Officials (AASHTO) Standard Specifications for Highway Bridges[2] have nearly identical requirements for development length of prestressing strands. In both, there is a provision for a minimum embedment length, which is calculated by a simple expression that only accounts for the strand diameter, d_b, the effective prestress, f_{se}, and the strand stress at the nominal flexural strength of the cross section, f_{ps}. The ACI Code provisions are shown below. The AASHTO Specification provisions 9.27.1 and 9.27.2 are essentially identical with the only significant differences being the notation, which is shown in Appendix G.

12.9.1 — Three- or seven-wire pretensioning strand shall be bonded beyond the critical section for a development length, in inches, not less than

$$\left(f_{ps} - \frac{2}{3} \cdot f_{se}\right) \cdot d_b$$

where $\mathbf{d_b}$ is strand diameter in inches, and $\mathbf{f_{ps}}$ and $\mathbf{f_{se}}$ are expressed in kips per square inch.

12.9.2 — Limiting the investigation to cross sections nearest each end of the member that are required to develop full design strength under specified factored loads shall be permitted.

The expression presented above was developed based on tests of clean 6.4 to 12.7 mm (1/4 to 1/2 in.) diameter strands in normal weight concrete members with a minimum cover of 51 mm (2 in.) to the center of the strands. This expression can be rewritten as:

$$L_d = \frac{f_{se}}{3} \cdot d_b + \left(f_{ps} - f_{se}\right) \cdot d_b$$

where the first term represents the transfer length of the strand and the second term represents the additional length needed to develop the strand stress at the nominal flexural strength of the cross section, f_{ps}.[1]

A requirement for transfer length is not explicitly specified in the ACI Code nor the AASHTO Specifications. However, when calculating the nominal web shear strength of the concrete, V_{cw}, provisions 11.4.4 of the ACI Code and 9.20.2.4 of the AASHTO Specification suggest a transfer length of 50 times the strand diameter. This expression is the transfer length term presented above for an assumed effective prestress, f_{se}, of 150 ksi (1034 MPa).

2.6.2   Proposed Equations for Transfer and Development Length

Equations to predict the transfer and development length of prestressing strand have been proposed by several researchers. Table 2.1, which was taken from Gross and Burns[7], presents some of them. As Cordova[22] mentioned, most of these equations are empirical. None of them account for all of the variables that can affect transfer and development length. As a result, no single equation stands out as the best or the most accurate.

Only the equation proposed by Cousins et al.[5] explicitly includes a term for the surface condition of the strand. The strand surface condition may be an important variable. In almost all of the past experimental studies, the reported strand surface conditions were based on visual inspections. Yet, there is some indication that differences not detectable from a visual inspection may have affected some of the

15

measured transfer and development lengths and, consequently, some of the proposed equations.

Table 2.1   Transfer and development length equations [7]

Author	Year	Transfer Length	Development Length
ACI[1] AASHTO[2 (1)]	1963	$L_t = \dfrac{f_{se}}{3} \cdot d_b$ $L_t \approx 50 \cdot d_b$	$L_d = L_t + \left(f_{ps} - f_{se}\right) \cdot d_b$
Martin and Scott[14 (3)]	1976	$L_t = 80 \cdot d_b$	$f_{ps} \leq \dfrac{L_e}{80 \cdot d_b} \cdot \left(\dfrac{135}{d_b^{1/6}} + 31\right)$ for $L_e \leq 80 \cdot d_b$ $f_{ps} \leq \dfrac{135}{d_b^{1/6}} + \dfrac{0.39 \cdot L_e}{d_b}$ for $L_e > 80 \cdot d_b$
Zia and Mostafa[20 (2)]	1977	$L_t = 1.5 \cdot \dfrac{f_{si}}{f_{ci}} \cdot d_b - 4.6$	$L_d = L_t + 1.25 \cdot \left(f_{pu} - f_{se}\right) \cdot d_b$
Cousins, Johnston and Zia[5 (4)]	1990	$L_t = \dfrac{U_t' \cdot \sqrt{f_{ci}'}}{2 \cdot B}$ $+ \dfrac{f_{si} \cdot A_{ps}}{\pi \cdot d_b \cdot U_t' \cdot \sqrt{f_{ci}'}}$	$L_d = L_t + \left(f_{ps} - f_{se}\right) \cdot \left(\dfrac{\dfrac{A_{ps}}{\pi \cdot d_b}}{U_d' \cdot \sqrt{f_c'}}\right)$
Russell and Burns[17 (5)]	1993	$L_t = \dfrac{f_{se}}{2} \cdot d_b$	$M_{cr} > L_t \cdot V_u$ Fully Bonded $\dfrac{L_b + L_t}{Span} \leq \dfrac{1}{2}\left[1 - \sqrt{1 - \dfrac{M_{cr}}{M_u}}\right]$ Debonded
Mitchell et al.[15 (6)]	1993	$L_t = \dfrac{f_{si} \cdot d_b}{3} \cdot \sqrt{\dfrac{3}{f_{ci}'}}$	$L_d = L_t + \left(f_{ps} - f_{se}\right) \cdot d_b \cdot \sqrt{\dfrac{4.5}{f_c'}}$
Deatherage, Burdette and Chew[6 (7)]	1994	$L_t = \dfrac{f_{si}}{3} \cdot d_b$	$L_d = L_t + 1.50 \cdot \left(f_{ps} - f_{se}\right) \cdot d_b$
Buckner (FHWA)[3]	1994	$L_t = \dfrac{1250 \cdot f_{si} \cdot d_b}{E_c}$ $L_t \approx \dfrac{f_{si}}{3} \cdot d_b$	$L_d = L_t + \lambda \cdot \left(f_{ps} - f_{se}\right) \cdot d_b$ $\lambda = \left(0.6 + 40 \cdot \varepsilon_{ps}\right)$ or $\left(0.72 + 0.102 \cdot \dfrac{\beta_1}{\varpi_p}\right)$ $\left(1.0 \leq \lambda \leq 2.0\right)$

Table 2.1 (continued)   Transfer and development length equations [7]

Notes:	Notation was changed in some cases to provide consistency between equations. All equations shown are expressed in terms of standard English units unless noted otherwise.
(1)	The second approximate equation for transfer length is from shear provisions of ACI 318, Section 11.4.4 and AASHTO Section 9.20.2.4. These provisions are still current.
(2)	Zia & Mostafa's equations are valid for initial concrete strengths of 2000 to 8000 psi.
(3)	Martin & Scott's development length equations limit f_{ps} as a function of L_e.
(4)	B = 300 (psi/in) on average; U', and U'_d are functions of strand surface conditions.
(5)	Russell & Burns' development length equations are based on preventing cracking in the transfer zone. L_b = Length of debonding for debonded strands.
(6)	The units for f'_{ci} and f'_c in the equations proposed by Mitchell et al. are kip/in^2.
(7)	Shahawy et al.[18] proposed the same transfer length equation in 1992.

CHAPTER THREE

Test Program

3.1 OVERVIEW

The primary purpose of this test program was to determine the development length of fully bonded, 15.2 mm (0.6 in.) diameter prestressing strand on a 51 mm (2 in.) grid in full scale, I-shaped beams. The transfer length of the prestressing strand was measured using the same beams.

The transfer and development length tests were performed on four beams. The beams conformed to the Texas Department of Transportation (TxDOT) Type C section, which is an I-shaped section 1016 mm (40 in.) deep with a 178 mm (7 in.) thick web. The surface condition of the strand was "bright". The only design variable was the concrete strength. Two beams were fabricated with normal-strength concrete (NSC), and two were fabricated with high-performance concrete (HPC). Though high-performance concrete has many properties of interest to designers, compressive strength and its effect on bond were the properties of particular interest in this study.

The beams were fabricated in July 1995 by Texas Concrete Company in Victoria, Texas. The HPC beams were 15.85 m (52 ft.) long, and the NSC beams were 16.46 m (54 ft.) long. The beams were delivered to the Phil M. Ferguson Structural Engineering Laboratory (FSEL) at The University of Texas at Austin where a 191 mm (7.5 in.) thick concrete slab was cast in place on each beam.

Load tests to determine the development length were performed on the composite beams at FSEL in late 1995 and early 1996. A series of four load tests was performed for each concrete type. As development length cannot be measured directly, the procedure used was iterative. An embedment length was chosen and the beam was loaded short of collapse, but enough to establish a bond or flexural failure. Then, depending upon the failure type, a longer or shorter embedment length was chosen for the next load test in the series.

The transfer length was determined from two types of data: concrete strain at the level of the bottom strands and strand end slip. Initial and final measurements were taken at the fabrication plant. A second set of final measurements was collected a few months later at FSEL.

Pull out tests were performed on untensioned strand specimens to assess the possibility of residues from the manufacturing process that might reduce bond. Concrete test blocks with embedded strands were made and tested at the fabrication plant.

3.2   TEST BEAM DESIGN

The dimensions of the TxDOT Type C section and the composite slab are shown in Figure 3.1. The HPC beams and the NSC beams were designed with the same strand pattern, so all beams could be made concurrently in the fabricator's 124.4 m (408 ft.) long prestressing bed. For a beam with a tightly packed grid of strands, cracks could develop along planes formed by horizontal or vertical rows of strands resulting in a bond failure prior to attaining the ultimate flexural capacity of the cross section. Thus, one goal of the beam design was to fill all available strand positions in the bottom two rows, or as many as possible. Another goal was to attain a strand strain at ultimate moment equal to or greater than the guaranteed minimum elongation of the strand, 3.5%. This latter goal assured that flexural failures would be ductile. These two goals were conflicting. Modifying the beam design to enhance one diminishes the other, so a balance was sought.

The resulting design had 20 fully bonded, 15.2 mm (0.6 in.) diameter strands in four rows. The rows were designated A through D, where Rows A and B were in the bottom flange, and Rows C and D were in the top flange as shown in Table 3.1 and Figure 3.1. The top strands in Rows C and D were provided to reduce the high tensile stresses at the top fibers of the NSC beams just after transfer of the prestress force. Two #5 bars in the top flange of the beams also helped control concrete stresses at transfer.

All mild reinforcement in the test beams except the shear reinforcement conformed to the TxDOT Type C beam standard drawing. The desired modes of failure during development length load tests were flexure or bond. To minimize the chance of shear failures, vertical shear reinforcement of double U-shaped #4 bars (4 vertical legs) was placed at a 102 mm (4 in.) spacing along the entire length of the beams. The mild reinforcement in the beams is shown in the fabricator's shop drawings

Table 3.1   No. and position of the strands

Row Designation	Number of Strands per Row	Location – Top or Bottom Flange
A	10	Bottom
B	6	Bottom
C	2	Top
D	2	Top
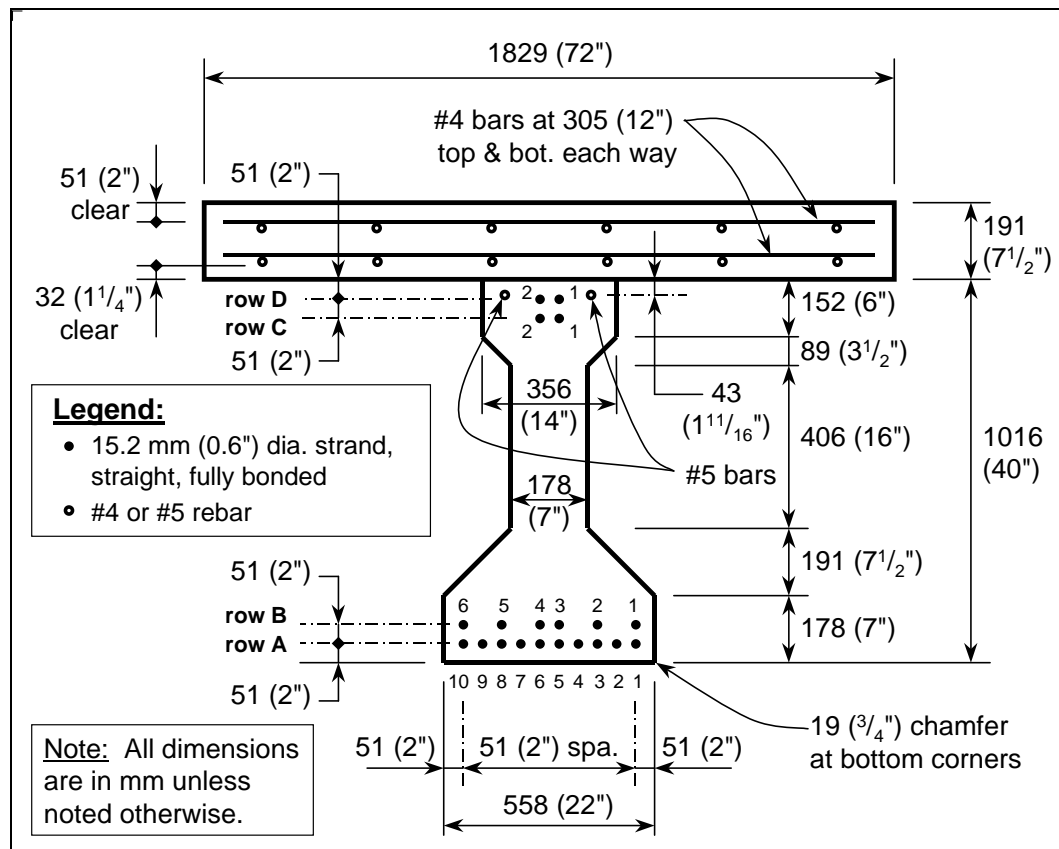
Figure 3.1   Test beam cross section (south end)

in Appendix A. The nominal shear strength of this reinforcement, V_s, exceeded the maximum of $8\sqrt{f_c'}\, b_w d$ allowed by the ACI[1] and AASHTO[2] specifications where f'_c is in pounds per square inch. The nominal shear strength provided was about 2 to 2.75 times the maximum allowed for the HPC and NSC beams, respectively, based on the design concrete strengths.

3.3 MATERIAL PROPERTIES

The prestressing steel was 15.2 mm (0.6 in.) diameter, Grade 270 (1860 MPa [270 ksi] guaranteed ultimate tensile strength), low-relaxation, seven-wire strand. The strand was manufactured by Shinko Wire America Inc. (SWAI). The strand for the beams was taken from two spools at the fabrication plant. The strand surface was "bright" with no visible rust. This condition generally results in longer transfer and development lengths. Independent tensile tests were performed by SWAI and by the researchers of this study. The tensile test results are shown in Appendix B and are summarized in Table 3.2.

Table 3.2   Summary of tensile tests of prestressing strand

Item	Units	CMRG	SWAI	Average
Ultimate Load	kN (kip)	264 (59.3)	270 (60.6)	267 (60.0)
Stress at Ultimate Load	MPa (ksi)	1884 (273.3)	1925 (279.3)	1905 (276.3)
Load at 1% Strain	kN (kip)	236 (53.1)	251 (56.5)	244 (54.8)
Stress at 1% Strain	MPa (ksi)	1687 (244.7)	1795 (260.4)	1741 (252.5)
Ultimate Strain	%	8.4%	9.2%	8.8%
Strain at 195.5 kN (43.94 kips)	%	0.712%	0.730%	0.721%
Modulus of Elasticity	GPa (ksi)	195.8 (28,400)	191.0 (27,700)	193.4 (28,100)

The tensile tests by the researchers were performed at the Concrete Materials Research Group (CMRG) Laboratory at The University of Texas at Austin. After seating the prestressing chucks with a pre-load of approximately 13 kN (3 kips), the ultimate strain was determined by measuring the length of the strand specimen between the nearest edges of the prestressing chucks with a steel tape measure. An extensometer with a gauge length of 102 mm (4 in.) was used to electronically plot load versus elongation in the elastic range. The modulus of elasticity shown was for a load of 195.5 kN (43.94 kips) which corresponded to a stress of 1396 MPa (202.5 ksi), that is, $0.75 f_{pu}$.

All mild reinforcing steel was Grade 60 (420 MPa [60 ksi] yield strength) with an assumed modulus of elasticity of 200 GPa (29,000 ksi). No material tests were performed on the mild reinforcing steel by the researchers.

The mix designs for both types of concrete, HPC and NSC, were provided by the fabricator and are shown in Appendix B. The concrete for the beams was mixed on-site by the fabricator in 3 cubic meter (4 cubic yard) batches. For each concrete type, a set of 100x200 mm (4x8 in.) cylinders was cast from the second of four concrete batches. A pair of cylinders for each concrete type was match-cured, that is, their temperature was adjusted to match the internal temperature of the beams. The maximum heat of hydration was 74°C and 54°C (165°F and 130°F) in the HPC and NSC beams, respectively. The match-cured cylinders were tested the next morning. The remaining cylinders were cured overnight adjacent to and under the same conditions as the beams. The next day those cylinders were transported to FSEL where they were air-cured inside the laboratory building, which was open during the day and closed overnight. Meanwhile, the beams were stored in an open yard at the fabrication plant for one to four months before shipment to FSEL.

The concrete for the composite slabs was batched and mixed at Capitol Aggregates in Austin, Texas, and delivered to FSEL. The mix design, shown in Appendix B, was used for all slabs. A set of 100x200 mm (4x8 in.) cylinders was cast from concrete corresponding to each slab. For comparison purposes, a set of 150x300

Table 3.3   Concrete compressive strengths

Beam Conc Type	Design Strength			Measured Concrete Strength and Age At Transfer and During Load Tests				
	Beam		Slab	Beam		Slab	Avg. Beam Age	Avg. Slab Age
	Transfer	28 or 56 days	28 days	Transfer	Load Tests	Load Tests		
	MPa (psi)	MPa (psi)	MPa (psi)	MPa (psi)	MPa (psi)	MPa (psi)	days	days
HPC	55-62 (8000-9000)	69-90 (10,000-13,000)	38-45 (5500-6500)	72.5 (10,520)	92.0 (13,340)	37.0 (5370)	134	91
NSC	28-34 (4000-5000)	34-48 (5000-7000)	38-45 (5500-6500)	30.0 (4360)	50.0 (7250)	48.7 (7070)	225	31

mm (6x12 in.) cylinders was cast from the concrete corresponding to each slab of the NSC beams. All cylinders were cured under the same conditions as the slabs.

The concrete compressive strengths are listed in Table 3.3. The design concrete strengths shown were the expected values at transfer and at 28 or 56 days. The HPC strength was the 56-day strength. The measured concrete strengths were determined at transfer and during the development length load tests. Average ages of the beams and slabs during the load tests also are shown. Appendix B contains plots of concrete strength versus time (beams and slabs), plots of modulus of elasticity versus time (beams only), and tables of the plotted data. The moduli of elasticity were measured for the HPC and NSC concrete beams, but not for the concrete slabs. The measured values fluctuated some over time, but they did not increase much after the first day. The measured moduli of elasticity were approximately 39 GPa (5,700 ksi) and 34 GPa (5,000 ksi) for the HPC and NSC beams, respectively.

3.4   FABRICATION OF BEAMS

The beams were fabricated on July 10, 1995 at Texas Concrete Company in Victoria, Texas. The strands were pretensioned around 12:00 noon before the researchers arrived at the fabrication plant. The strands were individually pretensioned and power

seated at a load of 4.4 kN (1.0 kip) per strand corresponding to a prestress of 32 MPa (4.6 ksi). Next, all strands in the top and bottom flanges were pulled simultaneously to a calculated elongation. The calculated elongation of 880 mm ($34^5/_8$ in.) was based on an increase in prestress from 32 to 1396 MPa (4.6 to 202.5 ksi) and a modulus of elasticity of 193 GPa (28,000 ksi) for the strands. The actual prestress before the anchorage loss was 1372 MPa (199.0 ksi) based on the pressure gauge reading and the calibration tables for the hydraulic jacks. Finally, the strands were elongated an additional amount to offset slippage during seating of the grips. The estimated and measured slippage was 10 mm (3/8 in.). Consequently, the initial prestress after anchorage loss, f_{po}, was 1372 MPa (199.0 ksi). The difference between the intended and the actual initial prestress of approximately 24 MPa (3.5 ksi), or 2%, had no significant effect on the transfer and development length tests.

The concrete was batched and placed between 5:30 PM and 6:30 PM. The weather was hot and dry with approximate temperatures of 38^oC (100^oF) during the day and 24^oC (75^oF) late at night, so accelerated curing with steam was not utilized. The beams were covered with moist burlap and tarps overnight. On the next day, concrete cylinders were tested at 6:00 AM and the formwork was removed by 9:00 AM. During the rest of the morning and the afternoon, the beams were instrumented for concrete strain and strand end slip measurements as discussed later in this chapter. After taking initial measurements, the prestress force was released gradually and simultaneously for all strands at 9:00 PM. After detensioning, the strands were flame-cut approximately 450 mm (18 in.) from the ends of each beam.

A composite slab was constructed on each beam prior to the development length load tests. The slab was reinforced with #4 bars at 305 mm (12 in.) center-to-center each way top and bottom. The slab dimensions and the placement of the reinforcing bars are shown in Figure 3.1. The beam was shored when the slab was cast, because the forms for the slab were supported on the laboratory floor. The beam shores were nominal 100 mm (4 in.) square wood posts spaced at 1.5 m (5 ft.) center-to-center with shims to assure a tight fit and full support. The ends of the beams were supported by neoprene bearing

pads on a large concrete pedestal. The slab was cured by covering it with polyethylene sheets. The shores and forms were removed after the slab had cured three days.

3.5 TRANSFER LENGTH MEASUREMENTS

Transfer lengths were determined from two types of data: concrete strains on the beam surface and end slip of the strands. Data were obtained from each beam end. As shown in Table 3.4, each beam end was assigned a label consisting of the concrete type, an arbitrary beam number, and a north or south designation. The north or south designation was based on the beam's orientation during fabrication.

Concrete strains were measured on the surface of the beam at the level of the bottom strands. The concrete strains were plotted versus distance from the end to obtain concrete strain profiles. Transfer length was determined for each beam end from its concrete strain profile. The transfer length is the dimension from the beginning of bond to the location where the entire prestress force has been transferred from the strand to the concrete. For the fully bonded strands of this study, the beginning of bond was the end of a beam. The end of the transfer zone was where the concrete strain ceased to increase and became constant.

Concrete strains were measured with the DEMEC Mechanical Strain Gauge system. A DEMEC gauge was used to precisely measure the change in length between a pair of DEMEC points spaced approximately 200 mm (7.87 in.) apart. A DEMEC "point" is a machined, conical hole in a small stainless steel disk. The disks were epoxied to both sides of the concrete beam at a spacing of 50 mm (1.97 in.) so the DEMEC gauge measurements would overlap. The DEMEC gauge readings were recorded in units of gauge divisions where each gauge division was equivalent to a

Table 3.4 Beam end labels

Beam End Label	Concrete Type	Beam No.	North or South End
H1S	HPC	1	South
H1N	HPC	1	North
H2S	HPC	2	South
H2N	HPC	2	North
N1S	NSC	1	South
N1N	NSC	1	North
N2S	NSC	2	South
N2N	NSC	2	North

dimension of 0.0016 mm (0.000063 in.). The recorded value was the average of two readings taken by removing and immediately reapplying the gauge. If the readings were not within two gauge divisions, additional readings (usually just one) were taken until the tolerance was met. The strain on the concrete surface was determined from the difference between gauge readings
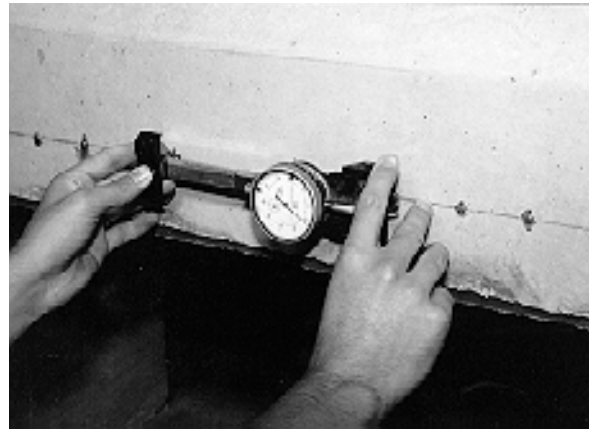
Figure 3.2   DEMEC gauge reading

before and after release of the prestress force multiplied by the gauge factor of 8.0×10^{-6}. Figure 3.2 shows a DEMEC gauge used to obtain a reading between a pair of DEMEC points.

The strand end slips at transfer were related to the decrease in the strand prestress at the beam ends. The transfer lengths determined from the strand end slip data assumed the prestress in the strands after transfer varied linearly from zero at the end of the beam to the effective prestress, f_{se}, at L_t from the end, where L_t is the transfer length. Thus, the strand prestress
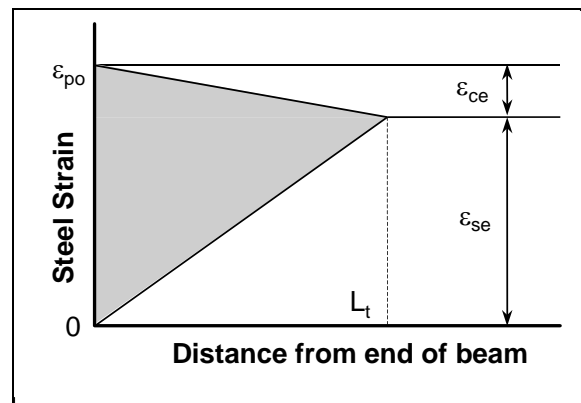
Figure 3.3   Transfer length as a function of end slip[17]

decreased from the initial strand prestress before release, f_{po}, to zero at the end of the beam, and from f_{po} to f_{se} at L_t from the end. It is easier to explain in terms of strain, as illustrated in Figure 3.3 from Russell and Burns[17], where the strand prestress is divided

by the modulus of elasticity, E_{ps}. The amount that the strand shortened can be calculated from the following expression.

$$\text{Strand shortening} = [\tfrac{1}{2} \cdot \varepsilon_{po} + \tfrac{1}{2} \cdot (\varepsilon_{po} - \varepsilon_{se})] \cdot L_t$$

The concrete also shortens in the transfer zone. There is no relative slip between the strand and the concrete at L_t from the end of the beam, so the concrete strain at that location equals the change in strain of the strand, that is, $\varepsilon_{ce} = \varepsilon_{po} - \varepsilon_{se}$. The shortening of the concrete can be calculated from the following expression.

$$\text{Concrete shortening} = \tfrac{1}{2} \cdot (\varepsilon_{po} - \varepsilon_{se}) \cdot L_t$$

The strand end slip is the difference between the shortening of the strand and the concrete in the transfer zone. The difference between the preceding two expressions yields the following expression for transfer length.

$$L_t = \frac{2 \cdot \text{Slip} \cdot E_{ps}}{f_{po}}$$

The derivation of this expression is explained more thoroughly by Russell and Burns.[17]

To measure end slips, an aluminum U-shaped guide was clamped to each strand approximately 50 to 100 mm (2 to 4 in.) from the end of the beam. The distance from the guide to the face of the beam was measured with the wire probe of a micrometer. Holes through the upturned legs of the guide aligned the wire probe so it contacted the bare concrete at the same point for each
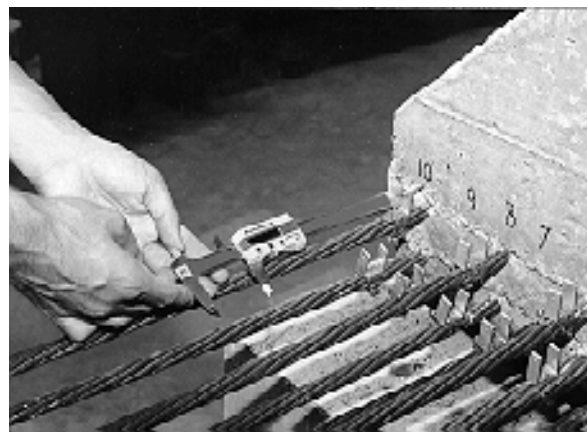
Figure 3.4   End slip measurements at transfer

measurement. The recorded distance was the average of two measurements. If the measurements differed by more than 0.02 mm (0.0008 in.), additional measurements were taken. Measurements were taken before and after the prestress force was released. The end slip was the difference between the two measurements with an adjustment to account for the initial prestress in the exposed strand. The method of end slip measurement described above was suggested by and the equipment was borrowed from researchers at the Federal Highway Administration (FHWA). Figure 3.4 shows an end slip measurement with the micrometer.

3.6 DEVELOPMENT LENGTH MEASUREMENTS

Development length cannot be measured directly or exactly. Instead, it must be determined indirectly from a series of load tests using an iterative procedure. For each concrete type, HPC and NSC, four load tests were performed, one on each end of each beam. The embedment length of the strand was different for each test in a series. The embedment length is the dimension from the beginning of bond to the critical section. For the beams with fully bonded strands and the load test setup of this study, it was the dimension from the end of the beam to the

Table 3.5   Load test designations

Load Test Designation	Test No.	Beam End	Embedment Length inches
1-H1S-120	1	H1S	120
2-H1N-93	2	H1N	93
3-H2N-78	3	H2N	78
4-H2S-72	4	H2S	72
5-N1S-120	5	N1S	120
6-N1N-93	6	N1N	93
7-N2S-78	7	N2S	78
8-N2N-72	8	N2N	72

first load point. If a load test ends with a bond failure, then the development length is longer than the embedment length and a longer embedment length is chosen for the next load test. Similarly, if a test ends with a flexural failure, then the development length is shorter and a shorter embedment length is chosen for the next test.
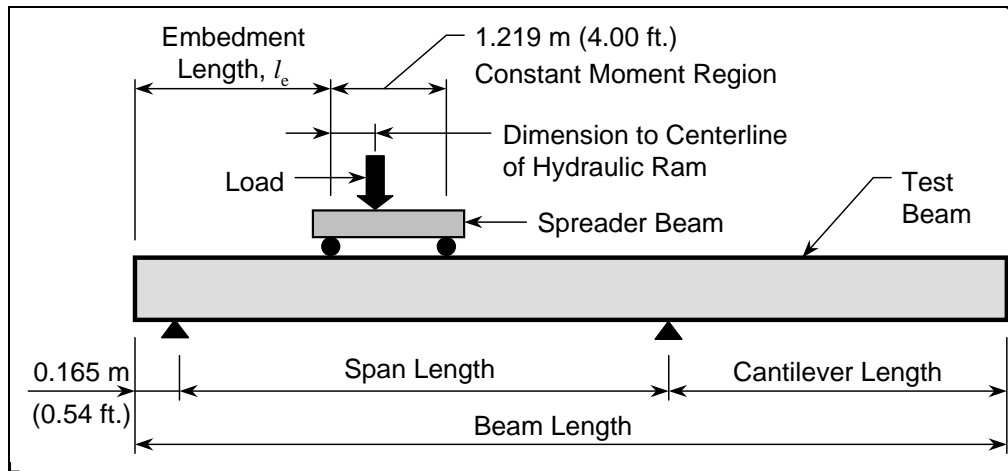
Figure 3.5   Schematic diagram of the development length load test setup

Table 3.5 shows the development length load test designations. The designations include the load test number in sequential order, the beam end, and the embedment length in inches.

When a load test was performed on one end of a beam, the opposite end was cantilevered to protect it from damage. A diagram of the development length test setup is

Table 3.6   Development length test setup parameters

Test Designation	Beam Length m (ft.)	Span Length m (ft.)	Embedment Length mm (in.)	Dimension to Centerline of Hydraulic Ram mm (in.)
1-H1S-120	15.850 (52.00)	7.874 (25.83)	3050 (120)	559 (22)
2-H1N-93	15.850 (52.00)	7.874 (25.83)	2360 (93)	422 ($16^5/_8$)
3-H2N-78	15.850 (52.00)	7.874 (25.83)	1980 (78)	349 ($13^3/_4$)
4-H2S-72	15.850 (52.00)	7.823 (25.67)	1830 (72)	321 ($12^5/_8$)
5-N1S-120	16.459 (54.00)	8.179 (26.83)	3050 (120)	530 ($20^7/_8$)
6-N1N-93	16.459 (54.00)	8.179 (26.83)	2360 (93)	403 ($15^7/_8$)
7-N2S-78	16.459 (54.00)	8.179 (26.83)	1980 (78)	333 ($13^1/_8$)
8-N2N-72	16.459 (54.00)	8.179 (26.83)	1830 (72)	305 (12)

shown in Figure 3.5. The beam was set on 64 x 229 x 610 mm (2.5 x 9 x 24 in.) steel-reinforced neoprene bearing pads with a simple span length of approximately 7.9 m (26 ft.) for the HPC beams and 8.2 m (27 ft.) for the NSC beams. The exact dimensions are listed in Table 3.6. Load was applied by a hydraulic ram to the top of a steel spreader beam. The spreader beam transmitted each of its reactions to the test beam through a 70 mm (2.75 in.) diameter steel roller and a 51 x 203 x 711 mm (2 x 8 x 28 in.) steel plate on a grout leveling bed. The position of the spreader beam was established by the chosen embedment length for that test. The hydraulic ram was positioned to account for the cantilevered end, so the moment in the test beam between load points was uniform.

Each test was instrumented to measure applied load, beam deflection, strand end slip and concrete strain of the slab at the top surface. The applied load was measured with two devices: an electronic load cell between the hydraulic ram and the spreader beam, and a pressure transducer attached to the hydraulic line. Deflections were determined from displacements measured with linear potentiometers. The linear potentiometers were placed at both load points and at both neoprene bearing pad supports. End slips were measured by linear potentiometers clamped to each strand. A glass plate was epoxied to the concrete surface at the plunger tip of each potentiometer to obtain accurate measurements.

Concrete strains were measured on top of the concrete slab in the constant moment region of each test with electronic resistance strain gauges (ERSG's). A couple of different ERSG
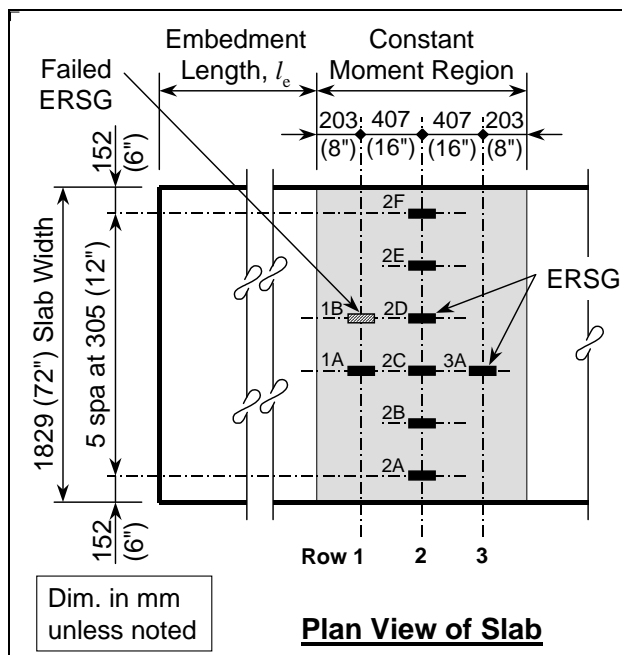
Figure 3.6 ERSG locations for test no. 1-H1S-120

arrangements were tried for the first two tests. Figures 3.6 and 3.7 show the locations of the ERSG's for those tests. The remaining six tests used the ERSG arrangement shown in Figure 3.8, which had three pairs of ERSG's over the beam and one at each edge of the slab to observe shear lag effects. Only one ERSG failed during all tests.

All of the electronic equipment and instruments had been calibrated prior to the development length load tests.

Figure 3.7 ERSG locations for test no. 2-H1N-93

Each piece of equipment was connected to the data acquisition system that read voltages, converted them to engineering units, and recorded the data on a computer disk.

Load was applied in increments of 180 kN (40 kips) until the formation of the first flexural or shear crack. The loading was immediately stopped when the first crack was observed. After the first crack, the load increment was reduced to 90 kN (20 kips) until the loss of the member's stiffness was apparent. Thereafter, the load was increased based on increments of deflection.

Readings were taken from all instruments at each increment of load. The beam was examined for flexural and shear cracks during and after each increment of load. Once initiated, the cracks were marked at every other increment of load. The test continued until a flexural or bond failure was established, but it was terminated, if at all possible, before a total collapse occurred. At the completion of each test, the load was removed in three or four steps.

A failure was classified as flexural if the nominal flexural strength of the cross section was achieved and the beam exhibited ductile behavior. A failure would have been attributed to bond if there had been significant strand end slips and the beam could not attain the nominal flexural strength, but none occurred. One failure was classified as a compression strut failure. The observed failures are discussed with the other test results in the next chapter.

3.7 PULL OUT TESTS

Pull out tests were performed on strand samples cut from three locations from each of two reels. The samples were tied
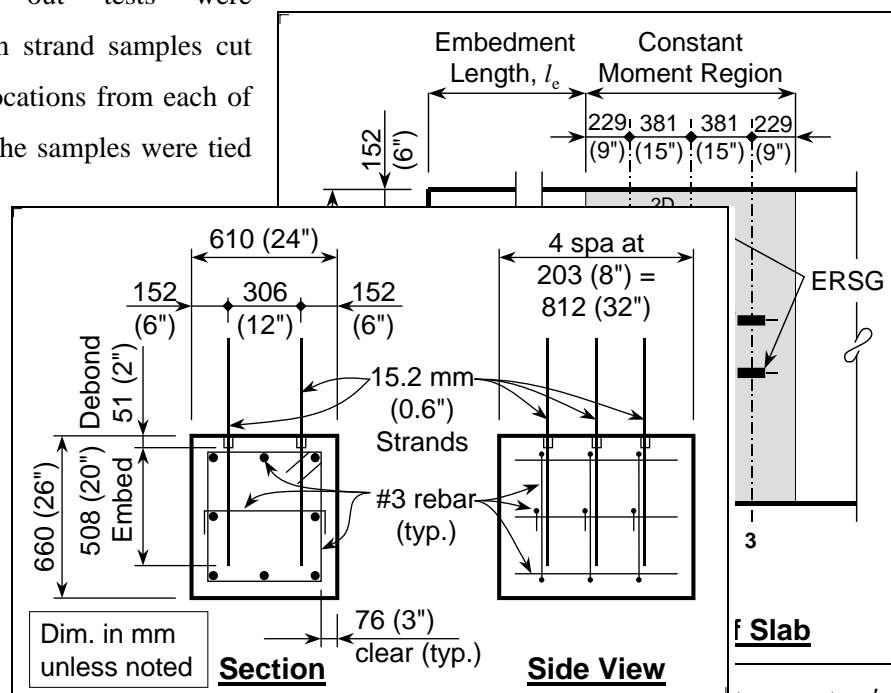
Figure 3.8 ERSG locations for all tests except no's.
Figure 3.9 Concrete block reinforcement detail for pull out test 18+20 and 2-H 18+93

32

in place vertically with a 508 mm (20 in.) embedment and debonded an additional 51 mm (2 in.) at the surface as shown in Figure 3.9.   A concrete block was made for each concrete   type,   HPC   and   NSC.   The   concrete

was taken from the last batch of each concrete type used to fabricate the full-sized test beams. Pull out tests were performed three days later using the setup shown in Figure 3.10. The measured HPC and NSC strengths on that day were 82.7 MPa (11,990 ksi) and 35.9 MPa (5200 ksi), respectively.
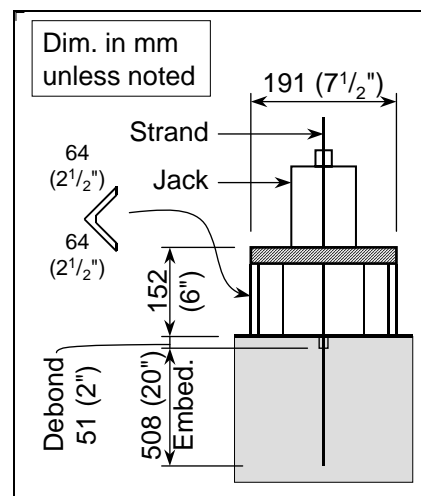
Figure 3.10 Pull out test setup

CHAPTER FOUR

Test Results

4.1 INTRODUCTION

Results of transfer and development length measurements are presented in this chapter. A brief explanation of the method used for data reduction is also described. Additional tables and graphs of the transfer and the development length measurements are shown in Appendices E and F. Factors that could have negatively affected the results are briefly discussed.

4.2 TRANSFER LENGTH MEASUREMENTS

Concrete strain measurements were taken with the DEMEC Mechanical Strain Gauge system at each beam end using the procedure described in Section 3.5. Two sets of final DEMEC readings were taken. The first set was taken just after release of the prestress force. The second set was taken one to six months later at the Phil M. Ferguson Structural Engineering Laboratory (FSEL) shortly before each composite slab was constructed.

At each beam end, the strains of the east face were averaged with the strains of the west face. These average values were then smoothed to reduce the variability in the data so the strain profile was easier to interpret. The technique used for smoothing consisted of taking the average over three gauge lengths.

$$Average\ \ Strain_n = \frac{Strain_{n-1} + Strain_n + Strain_{n+1}}{3}$$

The smoothed concrete strain profiles for half of the beam ends are shown in Figures 4.1 through 4.4. The strain profiles for the other beam ends are shown in Appendix E.
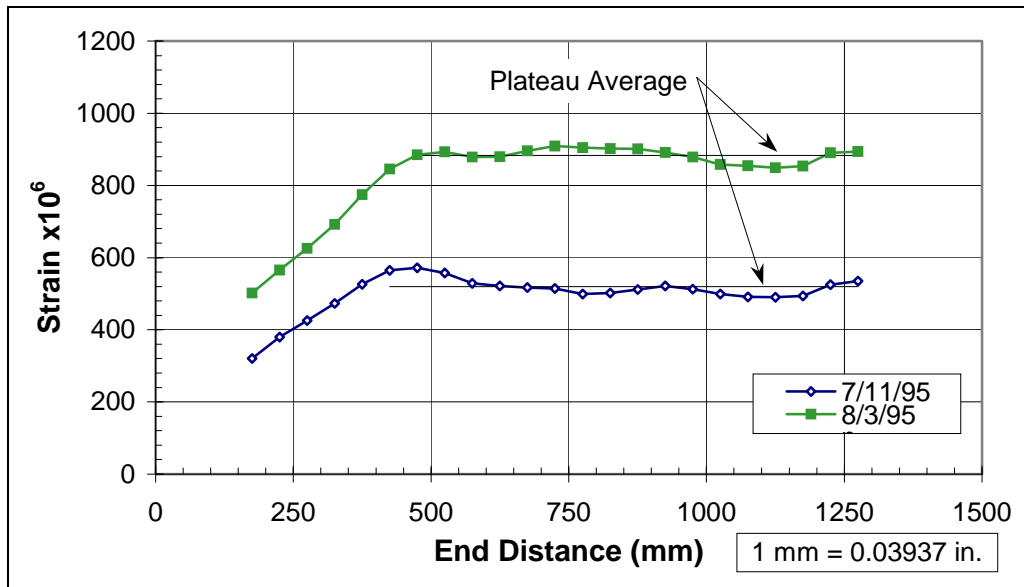
Figure 4.1   Concrete strain profile for beam end H1S
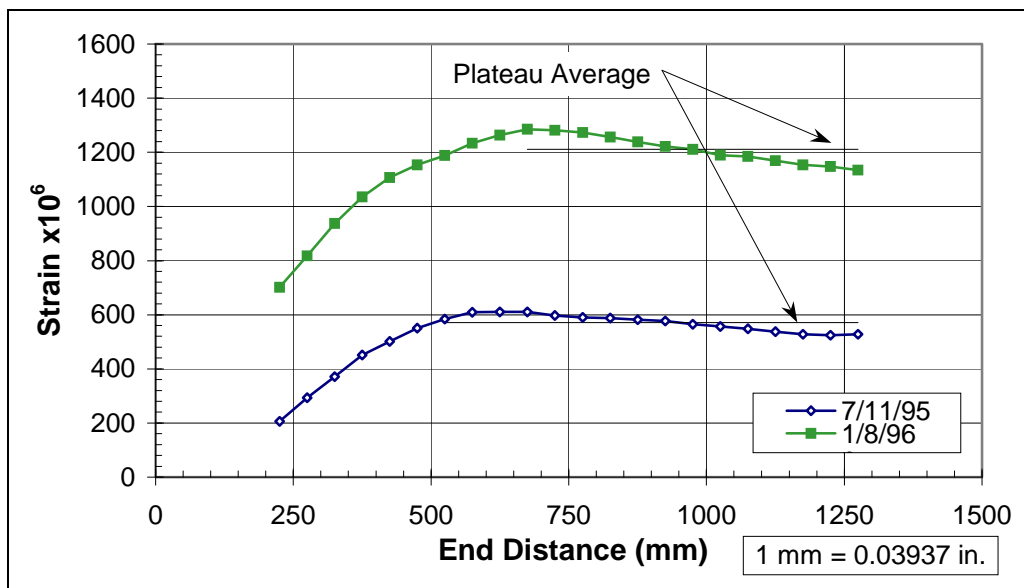
Figure 4.2   Concrete strain profile for beam end N1S
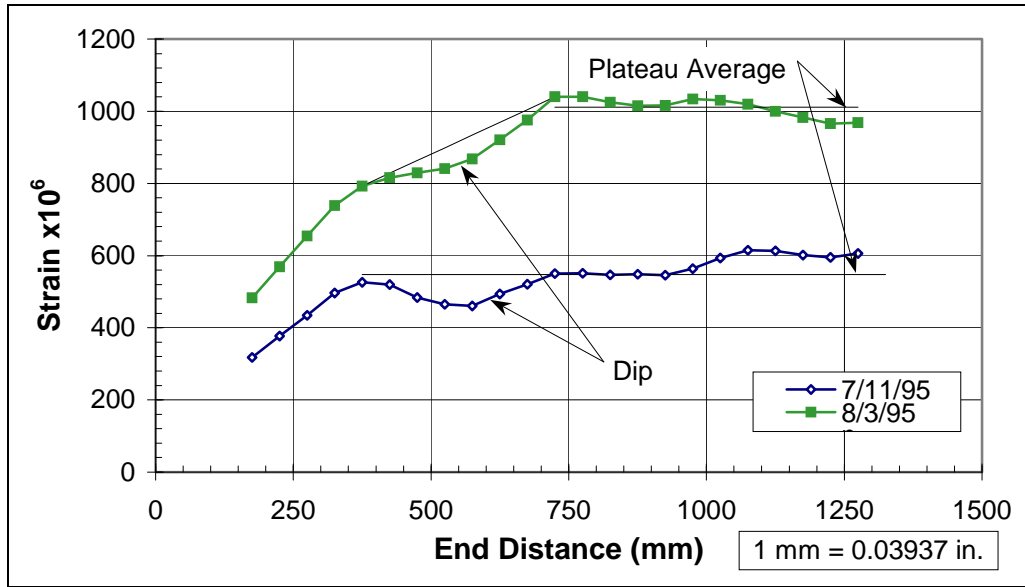
Figure 4.3   Concrete strain profile for beam end H2N
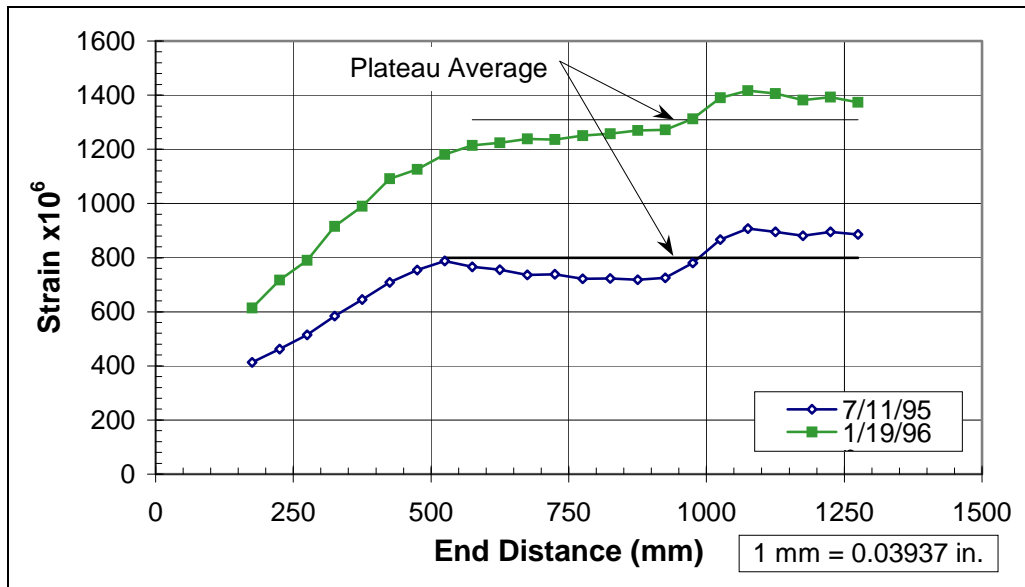
Figure 4.4   Concrete strain profile for beam end N2S

The strain profiles in Figures 4.1 and 4.2 were reasonably typical for six of the eight beam ends. The concrete strain increased linearly in the transfer zone and formed a plateau beyond. The data were not adjusted to account for the effect of the gravity load moment, so the plateaus should decline slightly toward midspan. The concrete strains increased and the profiles shifted upward for the second set of data collected one to six months after release. Creep and shrinkage most likely were the primary causes of the concrete strain increases.

The concrete strain profiles for two beam ends deviated some from the expected shape. They are shown in Figures 4.3 and 4.4. The strain profiles shown in Figure 4.3 for beam end H2N have a dip located about 600 mm (24 in.) from the end. In Figure 4.4, beam end N2S appears to have a second, slightly higher plateau beginning approximately 1000 mm (39 in.) from the end.

The transfer lengths were determined from the concrete strain profiles using the 95% plateau method. The beginning of the transfer zone was the end of each test beam as all strands were fully bonded. A horizontal line was plotted at 95% of the plateau average. The end of the transfer zone was located at the intersection of the 95% plateau line and the curve formed by the data. The transfer lengths are reported in Table 4.1.

Table 4.1   Transfer lengths

Beam End	Just After Release		1-7 Months After Release	
	From Concrete Strain	From Strand End Slip	From Concrete Strain	From Strand End Slip
	mm (in.)	mm (in.)	mm (in.)	mm (in.)
H1S	340 (14)	420 (17)	420 (17)	540 (21)
H1N	360 (14)	420 (17)	480 (19)	590 (23)
H2S	320 (13)	340 (13)	400 (16)	470 (19)
H2N	360 (14)	310 (12)	660 (26)	500 (20)
HPC (avg.)	350 (14)	370 (15)	490 (19)	520 (21)
N1S	470 (18)	490 (19)	470 (19)	no data
N1N	440 (17)	440 (17)	440 (17)	no data
N2S	480 (19)	570 (22)	490-970 (19-38)	670 (27)
N2N	470 (18)	530 (21)	480 (19)	560 (22)
NSC (avg.)	460 (18)	510 (20)	470 (19) [1]	620 (24)
Note: [1] Does not include data for beam end N2S.				
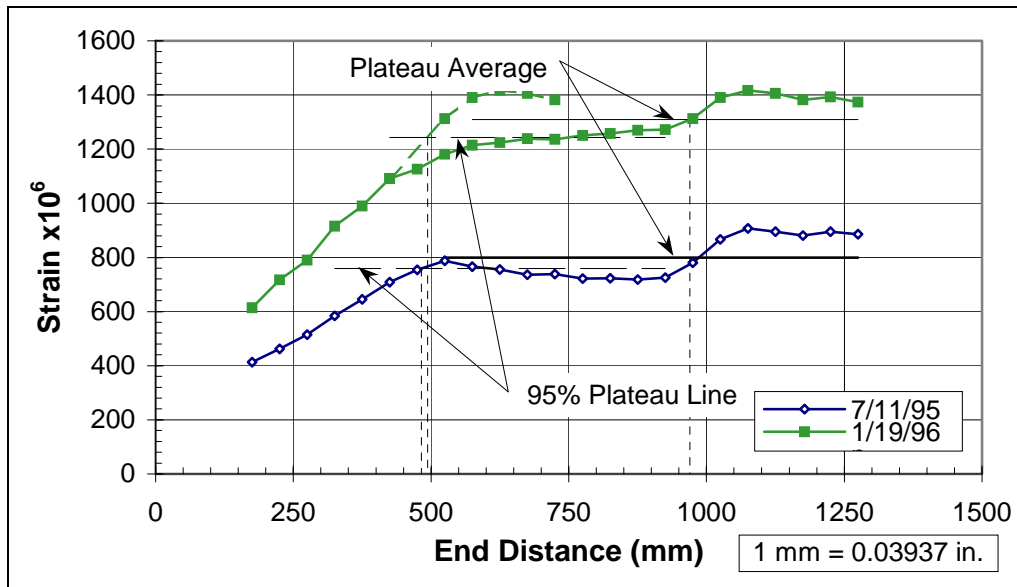
Figure 4.5   Transfer length from concrete strain profile of beam end N2S

For the upper concrete strain profile of beam end N2S in Figure 4.5, the 95% plateau line runs along the data of the lower plateau, which makes the determination of the transfer length unreliable using the 95% plateau method. The transfer length for this case was bracketed between two extremes. The lower bound was determined from the 95% plateau method except the data in the transfer zone were projected along the same slope. The upper bound was determined from the intersection of the 100% plateau line and the curve formed by the measured data.

Table 4.1 also lists transfer lengths determined from strand end slip measurements. The end slip measurements were taken at each beam end using the procedure described in Section 3.5. Two sets of final end slip readings were taken. One set of final readings was taken at the fabrication plant just after release of the prestress force and a second set was taken a few months later after each composite concrete slab had been constructed. The end slip data were adjusted to account for the shortening of the exposed strand from the aluminum U-shaped guide to the end of the beam, so the reported data are the "true" strand slips measured from the beam end inward. The strand prestress after anchorage, 1372 MPa (199.0 ksi), was used to make this adjustment.

End slip data for some strands are missing, because some aluminum U-shaped guides were dislodged when they caught on formwork during release of the prestress force. Some U-shaped guides also were dislodged during transportation of the beams to FSEL. The U-shaped guides were inadvertently removed from beam ends N1S and N1N before a second set of final end slip readings was taken.

The measured end slip data are shown in Appendix E and are summarized in Table 4.2. The end slips were roughly 25% smaller for the HPC beams than the NSC beams, which might suggest that end slip is a function of concrete strength. The average end slip was roughly 30% smaller for the bottom strands compared to the top strands, except for beam end N2S just after transfer. This trend probably is partially due to less prestress in the bottom strands as a result of precompression of the bottom fibers of the beam, but the prestress in the bottom strands was only 10% smaller. Another factor might have been the entrapment of air and bleed water on the underside of the top strands from more than 300 mm (12 in.) of concrete below, similar to the effect on the

Table 4.2   Average strand end slips

Concrete Type	Just After Transfer		After Placing Composite Slab	
	Bottom Strands mm (in.)	Top Strands mm (in.)	Bottom Strands mm (in.)	Top Strands mm (in.)
H1S	1.51 (0.059)	1.78 (0.070)	1.90 (0.075)	2.41 (0.095)
H1N	1.50 (0.059)	2.14 (0.084)	2.10 (0.083)	2.61 (0.103)
H2S	1.20 (0.047)	1.62 (0.064)	1.67 (0.066)	2.06 (0.081)
H2N	1.09 (0.043)	1.70 (0.067)	1.79 (0.070)	2.20 (0.087)
HPC (avg.)	1.33 (0.052)	1.81 (0.071)	1.86 (0.073)	2.32 (0.091)
N1S	1.73 (0.068)	2.12 (0.083)	no data	no data
N1N	1.58 (0.062)	2.43 (0.096)	no data	no data
N2S	2.02 (0.080)	1.98 (0.078)	2.40 (0.094)	2.56 (0.101)
N2N	1.88 (0.074)	2.65 (0.104)	1.99 (0.078)	2.98 (0.117)
NSC (avg.)	1.80 (0.071)	2.30 (0.090)	2.19 (0.086)	2.77 (0.109)

development length of mild reinforcing bars. Average end slip increased with time. However, the data for individual strands shown in Appendix E incorrectly suggested that end slip decreased with time for 14% of the strands. The apparent end slip decrease varied from 1% to 23%. The erroneous data occurred primarily for beam end N2N. It was not determined if there were offsetting errors, such that the average end slips were approximately correct, or if errors only decreased the average.

Typical plots of strand end slip data are shown in Figures 4.6 and 4.7. In Figure 4.6, one strand had an end slip about twice the average, which was not uncommon for many beam ends. The plots of strand end slips for the other beams ends are shown in Appendix E.

In Table 4.1, the transfer lengths, L_t, from strand end slips were determined using the following equation.

$$L_t = \frac{2 \cdot \text{Slip} \cdot E_{ps}}{f_{po}}$$

The end slips used in this equation were the values for the bottom strands shown in Table 4.2. The modulus of elasticity of the prestressing steel, E_{ps}, was taken as 193 GPa (28,000 ksi). The strand prestress before release, f_{po}, was 1372 MPa (199.0 ksi).

The initial prestress, f_{si}, was calculated for the bottom strands at the end of a beam and is presented in Table 4.3. The initial prestress for the top strands is shown in

Table 4.3   Calculated bottom strand prestress and losses

Concrete Type	Elastic Shortening Loss MPa (ksi)	Initial Prestress $f_{si,calc}$ MPa (ksi)	Total Losses MPa (ksi)	Effective Prestress $f_{se,calc}$ MPa (ksi)
HPC	92 (13.4)	1280 (185.6)	218 (31.6)	1154 (167.4)
NSC	102 (14.8)	1270 (184.2)	249 (36.1)	1123 (162.9)

41
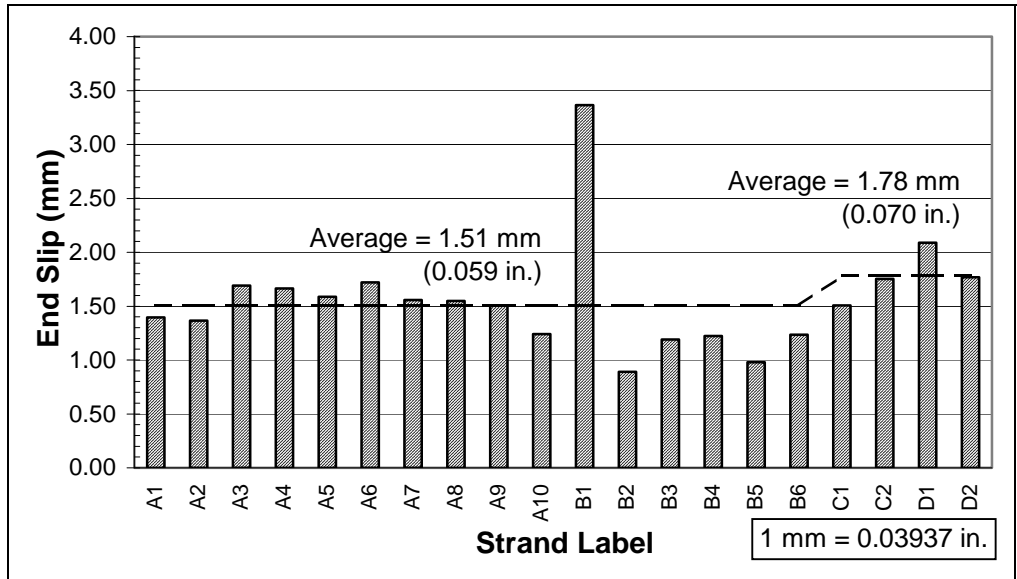
Figure 4.6   Strand end slips for beam end H1S measured just after transfer
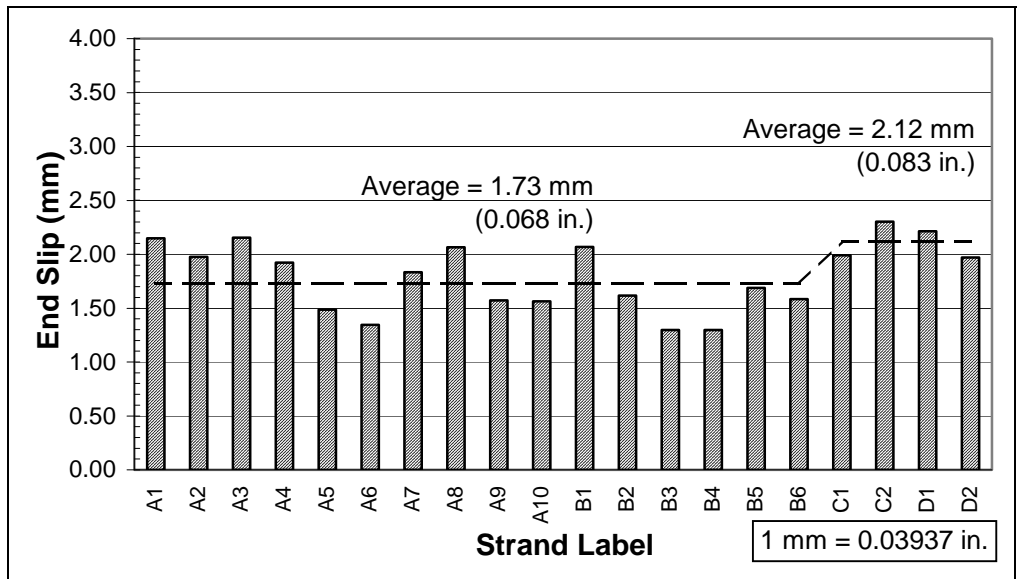
Figure 4.7   Strand end slips for beam end N1S measured just after transfer

Appendix C. The initial prestress includes the losses due to anchorage and elastic shortening only.

Table 4.3 also shows the total losses and the effective prestress, f_{se}, for the bottom strands at midspan. The effective prestress was needed for analysis of the development length load tests discussed in the next section. The total losses and the effective prestress were calculated in accordance with the PCI General (Time-Step) Method[16] for the average age of the beams during the load tests. Appendix C lists the material properties and the section properties used in the prestress loss calculations along with summaries of the calculations.

The prestress and the prestress losses of the bottom strands were also determined from concrete strain measurements mentioned at the beginning of this section. After bonding, the change in strain of the concrete and the prestressing steel were assumed equal in the region beyond the transfer zone. Prestress losses were determined from the average concrete strain of the plateaus. The prestress and the prestress losses determined from concrete strain measurements are listed in Table 4.4.

The prestress determined from measured concrete strains compared well to the calculated values. The values determined from the measured concrete strains, f_{meas}, are shown in Table 4.4, and the calculated values, f_{calc}, are shown in Table 4.3. The ratios of f_{meas}/f_{calc} listed in Table 4.4 varied from 0.96 to 1.05.

Several factors might have affected the accuracy of the concrete strain measurements. Concrete forms are never perfectly flat, so the concrete beam surfaces most likely had some waviness, which might prevent the conical points of the gauge from seating squarely in the holes of the stainless steel disks. Uniform pressure must be applied for each reading with the gauge set square to the surface to obtain consistent results. Even though one might apply nearly uniform pressure for a pair of readings, the pressure might be unintentionally varied in a series of readings along the beam. The physically awkward and fatiguing position needed to take the readings exacerbated the difficulty in maintaining uniform pressure for all readings. The stainless steel disks were low, about 300 mm (12 in.) above the ground, and there were steam pipes and steel

Table 4.4   Bottom strand prestress and losses from concrete strain measurements

Beam End	Just After Transfer				Before Placing Composite Slab			
	Average Concrete Strain of Plateau	Elastic Shortening Loss	Initial Prestress $f_{si,meas}$	$\dfrac{f_{meas}}{f_{calc}}$	Average Concrete Strain of Plateau	Total Losses	Effective Prestress $f_{se,meas}$	$\dfrac{f_{meas}}{f_{calc}}$
	με	MPa (ksi)	MPa (ksi)		με	MPa (ksi)	MPa (ksi)	
H1S	520	100 (14.6)	1272 (184.4)	0.99	883	170 (24.7)	1202 (174.3)	1.04
H1N	538	104 (15.1)	1268 (183.9)	0.99	952	184 (26.7)	1188 (172.3)	1.03
H2S	509	98 (14.3)	1274 (184.7)	1.00	844	163 (23.6)	1209 (175.4)	1.05
H2N	547	106 (15.3)	1266 (183.7)	0.99	1011	195 (28.3)	1177 (170.7)	1.02
HPC (avg.)	529	102 (14.8)	1270 (184.2)	0.99	923	178 (25.8)	1194 (173.2)	1.03
N1S	571	110 (16.0)	1262 (183.0)	0.99	1211	234 (33.9)	1138 (165.1)	1.01
N1N	640	124 (17.9)	1249 (181.1)	0.98	1212	234 (33.9)	1138 (165.1)	1.01
N2S	799	154 (22.4)	1218 (176.6)	0.96	1309	253 (36.7)	1119 (162.3)	1.00
N2N	741	143 (20.7)	1229 (178.3)	0.97	1283	248 (35.9)	1124 (163.1)	1.00
NSC (avg.)	688	133 (19.3)	1239 (179.7)	0.98	1254	242 (35.1)	1130 (163.9)	1.01

formwork appurtenances where one knelt to take gauge readings. Direct summer sunlight on one side of the beams might have affected the concrete surface strains. Readings were taken on both sides of the beams to mitigate this factor, but one to three hours passed between initial measurements on opposite sides of the same beam end. Initial readings were taken during the afternoon and early evening, while the first set of final readings was taken after sunset and the second set of final readings was taken under shelter.

Some end slip measurements were not as consistent as desired. The desired tolerance was 0.02 mm (0.0008 in.) for a pair of readings taken just seconds apart. The desired tolerance was met only 60% of the time. A couple readings differed by as much as 0.19 mm (0.0075 in.). On average, the difference between a pair of readings was 0.03 mm (0.0012 in.). Sometimes the desired tolerance could not be met because sand grains were dislodged from the concrete surface with each measurement. A 25 mm (1 in.)

square glass or plastic plate epoxied to the concrete surface would have solved this problem.

In spite of these factors, the concrete strain data and the strand end slip data yielded fairly reasonable and consistent results. In the concrete strain profiles, the strain increased more or less linearly in the transfer region followed by an approximately constant plateau.

4.3 DEVELOPMENT LENGTH TEST RESULTS

The development length tests were performed using the procedure described in Section 3.6. The applied load was recorded when the first web shear crack and the first flexural crack were observed during each load test. Those applied loads and the final applied load of each test are shown in Table 4.5. The applied loads do not include the self-weight of the test beam nor the weight of the spreader beam. The total weight of the spreader beam and the bearing plates was 9.3 kN (2.1 kips).

The applied loads were measured with an electronic load cell positioned between the hydraulic ram and the spreader beam, and a pressure transducer attached to the hydraulic lines. The load cell was monitored continuously during each test. The pressure transducer was checked occasionally. The readings of the two devices differed by less than 1.5% for loads greater than 1300 kN (300 kips). A third device, the pressure gauge mounted on the hydraulic pump, was deemed unreliable

Table 4.5   Applied loads

Test Designation	At First Web Shear Crack	At First Flexural Crack	At Final Load
	kN (kips)	kN (kips)	kN (kips)
1-H1S-120	2150 (483)	2090 (470)	3030 (682)
2-H1N-93	2150 (483)	2420 (545)	3410 (766)
3-H2N-78	2050 (461)	2620 (590)	3680 (827)
4-H2S-72	2090 (470)	2770 (622)	3910 (880)
5-N1S-120	2050 (460)	2050 (460)	3000 (674)
6-N1N-93	2420 (545)	2420 (545)	3350 (753)
7-N2S-78	2040 (458)	2480 (558)	3740 (841)
8-N2N-72	1960 (440)	2490 (560)	3870 (871)

for accurate readings.

The applied loads in Table 4.5 were measured with the load cell (the primary device) for all load tests except one. For load test 6-N1N-93, the applied loads were measured with the pressure transducer (the backup device), because the load cell readings were too low by a factor of approximately five. This discrepancy was not discovered until the first shear and flexural cracks had been observed during what was thought to be the third 180-kN (40-kip) load increment. The applied load actually was much higher. Since cracks were not expected so early in the load test, the hydraulic pump applying the load was not stopped immediately when cracks first occurred. Once the loading was stopped, there were several web shear cracks and four flexural cracks instead of the usual one or two of each crack type. The pressure transducer indicated an applied load of 2460 kN (552 kips). The applied load at the onset of the shear and flexural cracks was estimated to be 2420 kN (545 kips) based on observations of the hydraulic pump's pressure gauge while the loading was in progress.

The nominal flexural strength, M_n, of each typical cross section at midspan was calculated using a moment-curvature analysis and is shown in Table 4.6. The concrete strain at the top slab surface was taken as 0.003. Additional details of the moment-curvature analyses are discussed in Appendix D. The nominal flexural strength of the NSC beam cross section was slightly larger due to the higher concrete compressive strength of its slab. The concrete strengths of the beams and slabs are shown in Table 3.3.

The final loads from Table 4.5 and the test setups shown in Section 3.6 were used to calculate the maximum total moment acting on each test beam, M_{test}. The maximum total moments are shown in Table 4.7. The maximum total moment includes the moment caused by the maximum

Table 4.6   Nominal flexural strengths

Concrete Type	Strand Strain at Nominal Flexural Strength ε_{ps}	Strand Stress at Nominal Flexural Strength f_{ps}	Nominal Flexural Strength M_n
	%	MPa (ksi)	kN-m (k-ft)
HPC	3.51%	1850 (268.3)	4800 (3540)
NSC	4.21%	1853 (268.8)	4880 (3600)

applied load, the self-weight of the composite test beam, and the weight of the spreader beam. The table lists the ratio of the maximum total moment to the nominal flexural strength, M_{test}/M_n. All ratios were 1.00 or larger, so all beams met or exceeded the nominal flexural strength of their respective cross sections.

Table 4.7 also lists the maximum total end slips. These values are relative to the beginning of each load test and do not include the end slips from transfer of the prestress force discussed in the previous section. The end slips shown were recorded just prior to the termination of each load test. None of the end slips were significant.

The intended failure mode for each load test was either flexural or bond failure. To classify a failure as a flexural failure, the nominal flexural strength of the cross section should be achieved and the beam should demonstrate ductile behavior. A failure would be classified as a bond failure if the beam could not achieve and/or sustain the nominal flexural strength and if strand end slips were significant.

No failure was attributed to bond. All tests were classified as flexural failures except test 8-N2N-72, which was a compression strut failure. In tests 4-H2S-72 and

Table 4.7   Summary of development length load tests

Test Designation	M_{test} kN-m (k-ft)	$\dfrac{M_{test}}{M_n}$	Max. Total End Slip mm (in.)	Type of Failure
1-H1S-120	4890 (3600)	1.02	0.28 (0.011)	Flexural
2-H1N-93	4980 (3670)	1.04	1.22 (0.048)	Flexural
3-H2N-78	4840 (3570)	1.01	0.97 (0.038)	Flexural
4-H2S-72	4850 (3580)	1.01	1.22 (0.048)	Flexural
5-N1S-120	4990 (3680)	1.02	0.16 (0.006)	Flexural
6-N1N-93	5000 (3690)	1.03	0.54 (0.021)	Flexural
7-N2S-78	5000 (3690)	1.03	1.24 (0.049)	Flexural
8-N2N-72	4890 (3610)	1.00	1.40 (0.055) [1]	Compr. Strut
Note: [1] The maximum total end slip was 31.5 mm (1.24 in.) immediately after the compression strut failure.				

8-N2N-72, the embedment length was only one and a half times the height of the composite section. A compressive strut developed between the first load point and the bearing pad. In test 8-N2N-72, the compressive force crushed the concrete cover over the web reinforcement causing a sudden loss of the beam's strength. A maximum total end slip of 31.5 mm (1.24 in.) was recorded immediately after the compression strut failure, but that was a result of the failure, not the cause. Just prior to the failure, the maximum total end slip was only 1.40 mm (0.055 in.), which was comparable to the end slip for the HPC beam test with the same embedment length.

In addition to achieving the nominal flexural strength of the cross section and having no significant strand end slip, all test beams exhibited satisfactory ductile behavior based on the calculated strain of the bottom strands at the final load. The guaranteed minimum elongation of the strands was 3.5%. The calculated strain of the bottom strands was approximately 2.9% or more for the HPC beam tests and 3.3% or more for the NSC beam tests. The approximate strand strains at the final load are shown in Table 4.8.

The strand strain was calculated using two methods. During each load test, the strand strain was calculated from the measured concrete strain of the top slab surface and the measured depth to the neutral axis. This was an approximate but quick method to check whether or not the strand strain had reached the target value of 3.5%. The second method was the moment-curvature analysis mentioned previously in this section. Both methods assumed plane sections remain plane and strain compatibility between steel and concrete after bonding. The calculated strains for both methods include a strand strain of approximately 0.6% due to the effective prestress at the beginning of each test. The effective prestress is shown in Table 4.3.

The average concrete strains were used to determine the strand strains for both methods of calculation. The concrete strains were measured by electronic resistance strain gauges (ERSG's). The maximum and average concrete strains for each test are shown in Table 4.8. The average concrete strain shown is for one of three rows of ERSG's. Sometimes a "row" had only one ERSG; most rows had only two. Refer to

Figures 3.5 through 3.7 for the number and locations of the ERSG's for each load test. The final concrete strain readings for all ERSG's are shown in Appendix F.

The measured depth to the neutral axis listed in Table 4.8 was the average dimension from the top of the slab to the tips of a pair of flexural cracks. The selected cracks were on opposite sides of the slab at the same approximate location from the beam end. After every other increment of load, the crack tips were marked and the uncracked slab depth was measured.

The crack tips were observed with a magnifying glass. Even so, the measurements were approximate at best, because the slab surface was not perfectly flat and the edge of the slab was irregular. The crack heights almost certainly varied across the width of the slab due to shear lag effects and the inherent variability of concrete. About half the time, the crack was not at the location of the ERSG row used to measure the average concrete strain. These factors affected the accuracy of the strand strains calculated using the first method.

Table 4.8   Calculated strain of bottom strands at the final load

Test Designation	Measured Concrete Strain at Top of Slab		Measured Depth to Neutral Axis	Calculated Strand Strain	
	Max. (ERSG no.)	Average (ERSG row)		From Measured Depth to N.A.	From Moment-Curvature Analysis
			mm (in.)	%	%
1-H1S-120	0.00308 (1A)	0.00308 (1)	117 (4.63)	3.3%	3.6%
2-H1N-93	0.00267 (2B)	0.00252 (2)	102 (4.03)	3.2%	2.9%
3-H2N-78	0.00298 (1A)	0.00267 (1)	106 (4.16)	3.2%	3.1%
4-H2S-72	0.00273 (1B)	0.00248 (1)	105 (4.13)	3.0%	2.9%
5-N1S-120	0.00292 (2B)	0.00286 (1)	103 (4.06)	3.5%	4.0%
6-N1N-93	0.00263 (3A)	0.00254 (1)	92 (3.63)	3.5%	3.5%
7-N2S-78	0.00267 (3A)	0.00249 (1)	84 (3.31)	3.7%	3.4%
8-N2N-72	0.00272 (1B)	0.00243 (1)	87 (3.44)	3.5%	3.3%

The NSC beam tests were terminated after the bottom strands had attained a strain of 3.5% based on the first method of calculation. The HPC beam tests were terminated slightly before. It was more difficult to attain higher strand strains with the HPC beams as the compressive strength of the concrete slab for each beam was less than that of the NSC beam slabs and less than the design value. To attain higher strand strains in the HPC beams, the tests would have had to continue until the average concrete strain at the top slab surface had attained the ultimate value of 0.003. For tests 1-H1S-120 and 3-H2N-78, the maximum concrete strain was about 0.003 and minor crushing of the concrete slabs was observed on their top surfaces during post-test inspections.

Displacements were measured with linear potentiometers at the neoprene bearing pad supports and at both load points. These displacements were used to calculate deflections. Plots of applied load versus deflection are shown in Figures 4.8 and 4.9 for the HPC and NSC beam load tests, respectively. The deflections shown are at the load point nearest midspan. An inspection of the plot for test 6-N1N-93 suggests the estimated load of 2420 kN (545 kips) probably was more than the true load when the first flexural crack occurred. For test 8-N2N-72, the plot shows a large drop in the applied load when the compression strut failure occurred.

Plots of load versus deflection are shown for each individual load test in Appendix F. Examples of these individual plots are shown in Figures 4.10 and 4.11. The individual load versus deflection plots also display the end slips of one strand as the load test progressed. The end slips shown are for the strand with the largest end slip at the final load. As previously mentioned, the end slips are relative to the beginning of the test and do not include end slip from transfer of the prestress force.

Flexural and shear cracks were traced with permanent markers on the concrete surfaces at every other increment of load and were sketched on grid paper following each test. Typical crack patterns are shown in Figures 4.12 and 4.13. The crack patterns for the other tests are presented in Appendix F. Cordova[22] noted that the NSC beams exhibited "ductile behavior with cracks well distributed both within and outside the
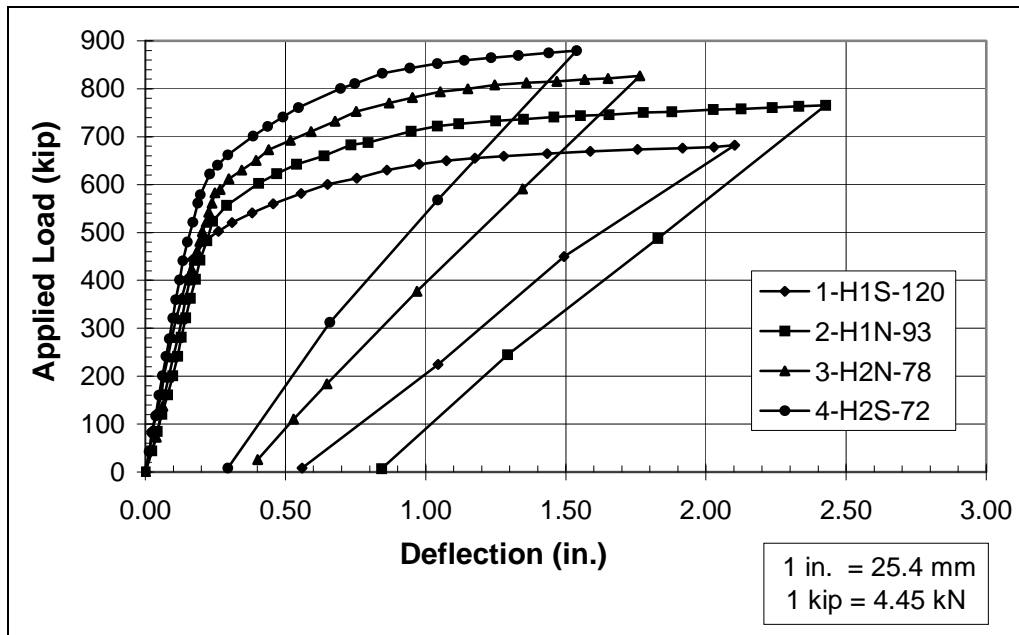
Figure 4.8 Deflections of HPC beams during load tests
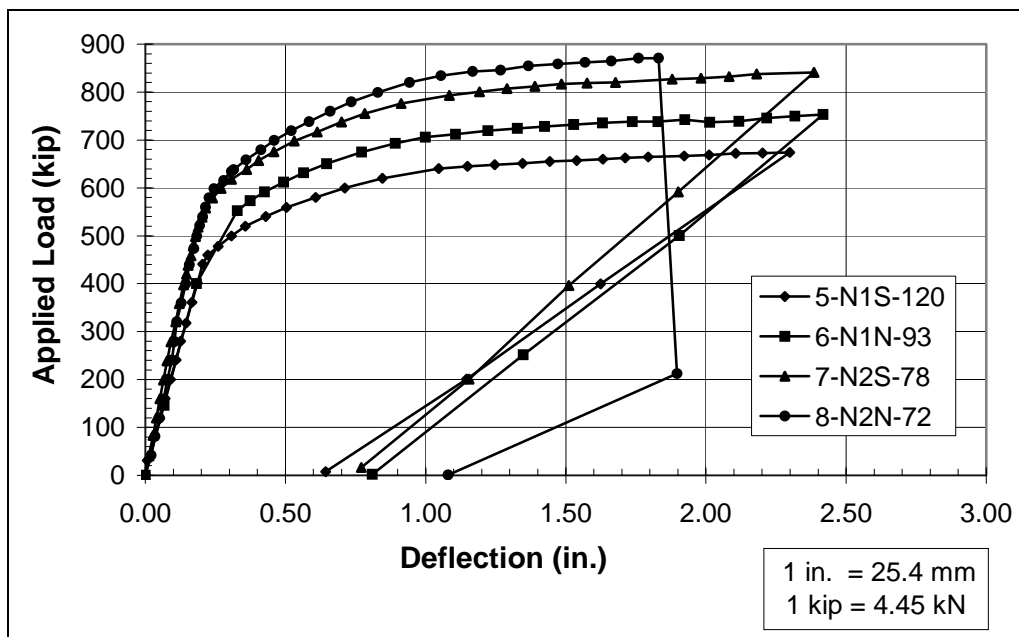
Figure 4.9 Deflections of NSC beams during load tests
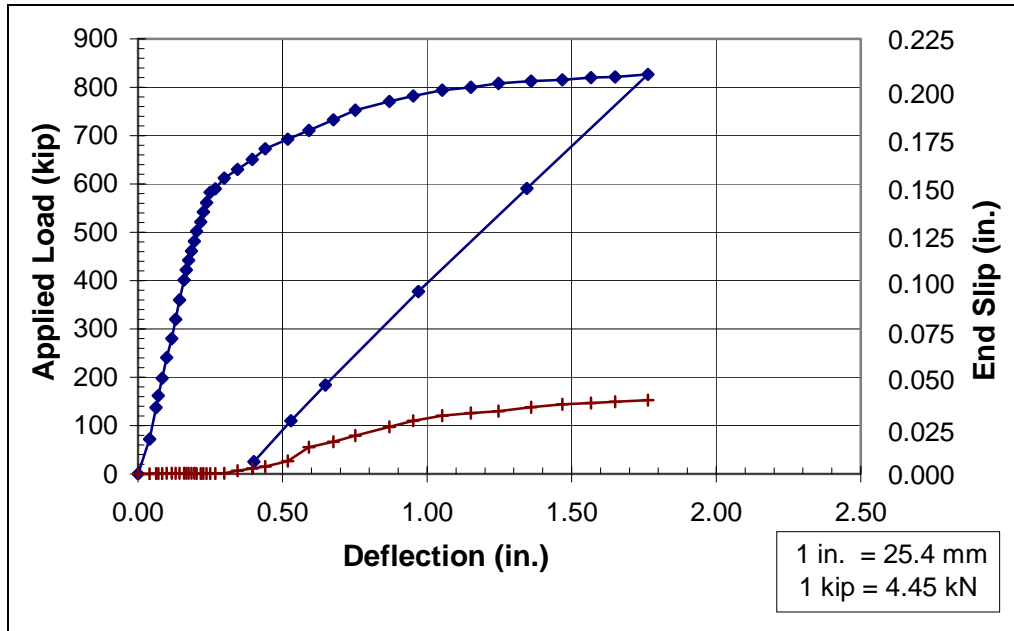
Figure 4.10 Load vs. deflection plot for load test 3-H2N-78
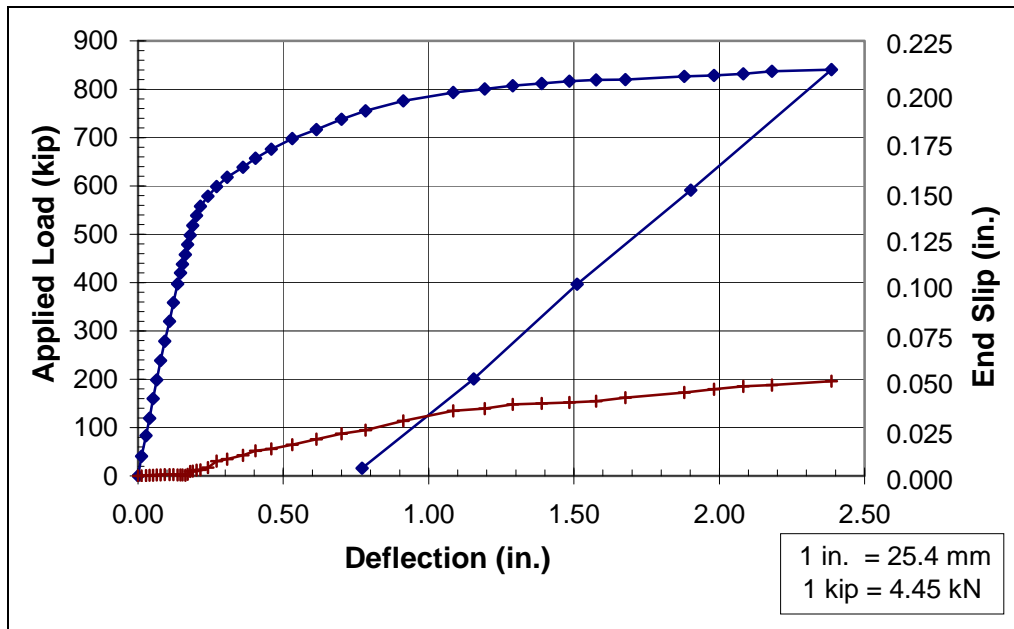
Figure 4.11 Load vs. deflection plot for load test 7-N2S-78
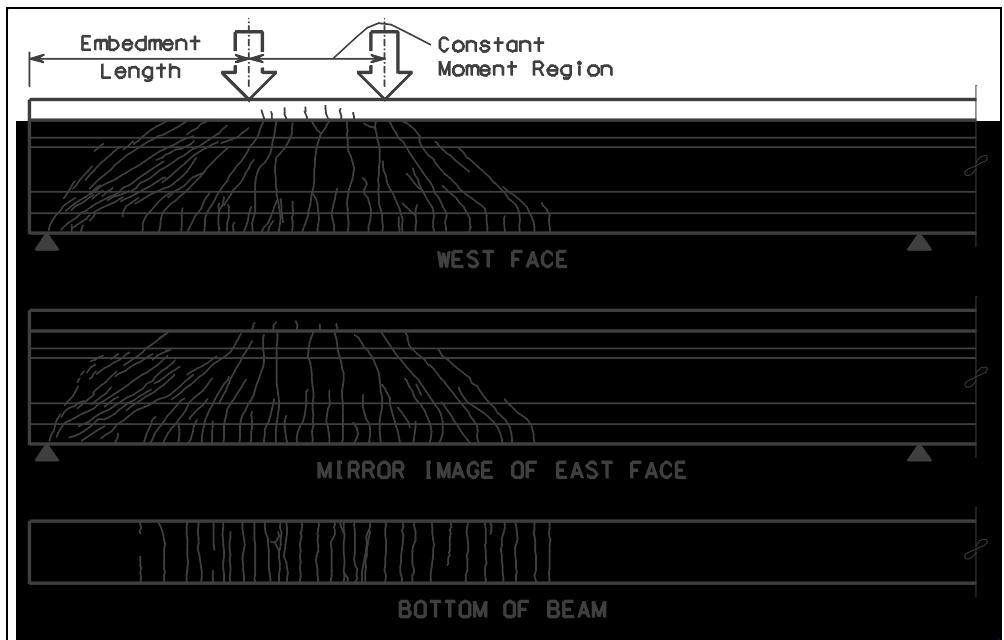
Figure 4.12 Crack pattern for test no. 3-H2N-78

Figure 4.13 Crack pattern for test no. 7-N2S-78

constant moment region." This statement applies equally well to the HPC beams. In each test, one or more cracks propagated from the web to the bottom rows of strands in the transfer zone. In some cases the cracks arrested just beyond the strands and in other cases the cracks continued to the bottom of the section. The cracks appeared to have no significant effect on end slip or on the development of the strands.

Cracking moments determined from the load tests, $M_{cr,test}$, were compared to theoretical values calculated for the cross section, $M_{cr,calc}$. This was not one of the primary interests of this study, but flexural cracking can have an effect upon beam deflections and corrosion of strands.

The load test cracking moments were determined from the applied loads (at the first observed flexural crack) in Table 4.5 and the test setups shown in Section 3.6. The load test cracking moments are listed in Table 4.9.

Table 4.9   Cracking moments during development length load tests

Test Designation	$M_{cr,test}$	$M_{cr,test}$ / $M_{cr,calc}$			
		Without Slab Shrinkage		With Slab Shrinkage	
	kN-m (ft-k)	$f_r = 7.5\sqrt{f_c'}$ [1]	$f_r = 10\sqrt{f_c'}$ [1]	$f_r = 7.5\sqrt{f_c'}$ [1]	$f_r = 10\sqrt{f_c'}$ [1]
1-H1S-120	3340 (2470)	1.02	0.94	1.07	0.98
2-H1N-93	3530 (2600)	1.08	0.99	1.13	1.03
3-H2N-78	3440 (2540)	1.05	0.97	1.10	1.01
4-H2S-72	3420 (2530)	1.05	0.96	1.10	1.00
HPC (avg.)	3440 (2530)	1.05	0.96	1.10	1.01
5-N1S-120	3390 (2500)	1.10	1.02	1.14	1.06
6-N1N-93	3610 (2660)	1.17	1.09	1.21	1.13
7-N2S-78	3310 (2440)	1.08	1.00	1.11	1.03
8-N2N-72	3140 (2320)	1.02	0.95	1.05	0.98
NSC (avg) [2]	3280 (2420)	1.07	0.99	1.10	1.03
Notes: [1] The units of f'_c are pounds per square inch. [2] The values from test 6-N1N-93 are excluded from the averages.					

Ratios of the load test cracking moment to the calculated cracking moment, $M_{cr,test}$/$M_{cr,calc}$ also are shown in Table 4.9. The calculated cracking moments are presented in Table 4.10 and are discussed below. The cracking moment ratios for test 6-N1N-93 were significantly larger than the ratios for the other NSC beam tests. This tends to confirm that the recorded load for the first flexural crack of test 6-N1N-93 was too large. The results of that test were omitted from the computed averages for the NSC beams.

The calculated cracking moments in Table 4.10 were determined from the composite cross section properties and a bottom fiber tensile stress equal to the modulus of rupture, f_r. Values of $7.5\sqrt{f_c'}$ and $10\sqrt{f_c'}$ were used for the modulus of rupture where f'_c is in pounds per square inch. The coefficient of 7.5 is generally accepted for normal weight, normal-strength concrete. A value of $10\sqrt{f_c'}$ was used to calculate the cracking moment of HPC beams in a research report by Gross and Burns[7]. The coefficient of 10 was based on test results by Carrasquillo, Nilson, and Slate[4] for high-performance concrete.

The calculated cracking moments were determined with and without consideration of slab shrinkage effects. The net effect of slab shrinkage is a residual tensile stress at the bottom of the beam. This residual tension consumes some of the tensile capacity of the bottom concrete fibers, so the moment that can be applied which initiates flexural cracking is reduced.

Table 4.10 Calculated cracking moments

Concrete Type	$M_{cr,calc}$			
	Without Slab Shrinkage		With Slab Shrinkage	
	$f_r = 7.5\sqrt{f_c'}$ [1]	$f_r = 10\sqrt{f_c'}$ [1]	$f_r = 7.5\sqrt{f_c'}$ [1]	$f_r = 10\sqrt{f_c'}$ [1]
	kN-m (ft-k)	kN-m (ft-k)	kN-m (ft-k)	kN-m (ft-k)
HPC	3270 (2410)	3560 (2630)	3120 (2300)	3410 (2520)
NSC	3080 (2270)	3300 (2440)	2980 (2200)	3200 (2360)
Note: [1] Units of f'_c are pounds per square inch.				

In research by Russell and Burns[17], including the effects of slab shrinkage in calculations was significant and beneficial. They performed tests on three composite beams with a cross section nearly identical to the cross section used in this study. They compared cracking loads instead of cracking moments. The theoretical load that caused the first flexural crack was calculated for a bottom fiber tensile stress of $7.5\sqrt{f_c'}$ where f'_c is in pounds per square inch. The calculated cracking load decreased 9% when the slab shrinkage effects were included. On average, the ratio of the measured cracking load to the calculated cracking load improved from 0.94 to 1.03.

They determined the residual tensile stress indirectly by measuring beam deflections caused by slab shrinkage. The curvature of the beam was calculated from the deflections. Strains and stresses of the composite cross section were calculated from the curvature. A similar procedure was used for this study. Deflection measurements and a discussion of the calculations are presented in Appendix D.

Unlike the research results reported by Russell and Burns, the consideration of slab shrinkage in this study was not significant. Slab shrinkage effects had a minor impact of only 3% to 5% on the calculated cracking moment. In addition, considering the effects of slab shrinkage was not always beneficial. It was hoped the results would show that assuming a value of $7.5\sqrt{f_c'}$ for the modulus of rupture was accurate for the NSC beams and assuming a value of $10\sqrt{f_c'}$ was accurate for the HPC beams. The results for the HPC beams were as hoped. The value of $10\sqrt{f_c'}$ yielded the most accurate results, and they improved slightly when slab shrinkage effects were included. However, a value of $7.5\sqrt{f_c'}$ was not the best for the NSC beams. Results for the NSC beams were very similar to the results for the HPC beams. For both concrete types, a value of $7.5\sqrt{f_c'}$ was conservative, but results were better for a value of $10\sqrt{f_c'}$. Based on the limited data from this study, the generally accepted coefficient of 7.5 times $\sqrt{f_c'}$ is reasonable for normal weight concrete. The results of this study do not justify different coefficients for the different concrete types, HPC and NSC.

The nominal web shear strengths, V_{cw}, for the HPC and NSC beams were 845 kN (190 kips) and 661 kN (149 kips), respectively. These values were calculated for a principal tension stress of $4\sqrt{f'_c}$ at the centroid of the composite section, where f'_c is in pounds per square inch. For the NSC beams, the nominal web shear strength was calculated at the top of the web because the centroid of the composite section was in the flared portion of the top flange. The gross concrete section properties used in the calculations are listed in Table 4.11.

The applied shear forces, V_{test}, listed in Table 4.12 were determined from the loads shown in Table 4.5 and the test setups shown in Section 3.6. The shear forces were determined at the midpoint of the shear span because the first web shear cracks occurred slightly past that location. The shear force was nearly constant in the shear span, so the location for which the shear force is determined is not too significant. The applied shear force shown for test 6-N1N-93 almost certainly is too large. The applied load was estimated for the first web shear cracks in that test, because of the equipment failure mentioned previously. The applied shear force was noticeably larger than all the others, which seems to confirm that the estimate for the applied load was too large.

The ratio of applied shear force to nominal web shear strength, V_{test}/V_{cw}, shown in Table 4.12 was substantially larger than 1.00 for all tests. The diagonal tensile strength of the beam concrete probably was greater than $4\sqrt{f'_c}$. This is consistent with the finding that the extreme fiber tensile stress was greater than $7.5\sqrt{f'_c}$ for flexural cracking.

Table 4.11 Gross concrete section properties for web shear strength

Item	Units	Beam only	Composite Section	
			HPC beams	NSC beams
A	mm^2 (in^2)	319×10^3 (495)	576×10^3 (893)	654×10^3 (1013)
y_b	mm (in)	434 (17.09)	736 (28.97)	780 (30.73)
I	mm^4 (in^4)	$34,400 \times 10^6$ (82,600)	$100,400 \times 10^6$ (241,300)	$110,300 \times 10^6$ (265,000)
Q	mm^3 (in^3)	---	109.6×10^6 (6691)	118.9×10^6 (7255)

The ratio of V_{test}/V_{cw} tended to become larger as the shear span became shorter and the overall depth to clear span ratio approached a value of 4/5. Some applied load may have transferred directly to the support due to arching action.

From the beginning of this study it was decided to minimize the possibility of a shear failure in the beams, so the amount of shear reinforcement was not limited. ACI[1] and AASHTO[2] limit the contribution of the nominal shear strength of the shear reinforcement, V_s, to a maximum of $8\sqrt{f'_c}\,b_w d$. Cordova[22] noted that "this limit is intended to prevent non-ductile failures from occurring, like the compression strut failure experienced in this study." The shear reinforcement that was provided had a nominal shear strength equal to $15\sqrt{f'_c}\,b_w d$ and $20\sqrt{f'_c}\,b_w d$ for the HPC and NSC beams, respectively. Based on the results of these load tests, it appears that the ACI/AASHTO equation contains a factor of safety of more than two. The test beams could have been designed with fewer strands in the bottom flange resulting in less moment strength and less applied load during tests. Consequently, the applied shear would have been controlled so the required shear reinforcement would not have exceeded the ACI/AASHTO limit.

In reference to the NSC beams, Cordova[22] noted that a "major inconvenience encountered in the development length tests of this study was that a bond failure did not occur, [so] the development length … could not be determined precisely." This was also true for the HPC beams. The shortest embedment length in this study was 1830 mm (72 in.). A shorter embedment length would have been meaningless because the overall

Table 4.12   Web shear from load tests

Test Designation	Applied Shear Force V_{test} kN (k)	$\dfrac{V_{test}}{V_{cw}}$
1-H1S-120	1193 (268)	1.41
2-H1N-93	1423 (320)	1.68
3-H2N-78	1479 (333)	1.75
4-H2S-72	1554 (349)	1.84
HPC (avg.)	1412 (317)	1.67
5-N1S-120	1176 (264)	1.78
6-N1N-93	1643 (369)	2.49
7-N2S-78	1495 (336)	2.26
8-N2N-72	1481 (333)	2.24
NSC (avg.)[(1)]	1384 (311)	2.09
Note: [(1)] The values for test 6-N1N-93 are excluded from the averages.		

depth to clear span ratio would have exceeded 4/5, so the composite section would have been classified as a deep flexural member. The compression strut failure observed in the last NSC beam test demonstrated that shorter embedment lengths could not be tested with the composite TxDOT Type C beam section. Development length load tests on shallower I-shaped beam section, such as the AASHTO Type I or the TxDOT Type A section, could use shorter embedment lengths without contending with deep flexural member behavior.

4.4 PULL OUT TEST RESULTS

Strand pull out tests were performed at the precast concrete fabrication plant using the test setup shown in Figure 3.10. The tests were performed three days after the concrete pull out test blocks were cast. The concrete strengths were 82.7 MPa (11,990 psi) and 35.9 MPa (5200 psi) for the HPC and NSC blocks, respectively. The pull out test results are summarized in Table 4.13. The stress in the strand, f_{strand}, was based on a strand cross sectional area of 140 sq. mm (0.217 sq. in.). The guaranteed ultimate tensile strength of the strands, f_{pu}, was 1860 MPa (270 ksi).

All strand specimens in the HPC block failed due to fracture of the strand. Though the failure of most strand specimens in the NSC block initiated with pull out due to bond failure, their ultimate failure was due to fracture of the strand. When the strands in the NSC block fractured, the average ratio of the strand stress to ultimate strength, f_{strand}/f_{pu}, was 1.02. That was just slightly less than the average ratio of 1.04 for the strand specimens in the HPC block.

Table 4.13   Pull out test results

Test No.	Conc Type	Force kN (kip)	f_{strand} MPa (ksi)	$\dfrac{f_{strand}}{f_{pu}}$	Description of Failure
1H	HPC	269 (60.5)	1920 (278.8)	1.03	Strand fracture.
2H	HPC	275 (61.9)	1970 (285.1)	1.06	Strand fracture.
3H	HPC	269 (60.5)	1920 (278.8)	1.03	Strand fracture.
4H	HPC	272 (61.2)	1940 (282.0)	1.04	Strand fracture.
5H	HPC	269 (60.5)	1920 (278.8)	1.03	Strand fracture.
6H	HPC	272 (61.2)	1950 (282.0)	1.04	Strand fracture.
Avg	HPC	271 (61.0)	1940 (280.9)	1.04	
1N	NSC	266 (59.8)	1900 (275.6)	1.02	Strand fracture.
2N	NSC	248 (55.7)	1770 (256.6)	0.95	Pull out. Strand fracture at 0.97 f_{pu}.
3N	NSC	257 (57.8)	1830 (266.1)	0.99	Pull out plateau. Strand fracture at 0.99 f_{pu}.
4N	NSC	186 (41.9)	1330 (193.3)	0.72	Pull out began. Strand fracture at 1.04 f_{pu}.
5N	NSC	257 (57.8)	1830 (266.1)	0.99	Pull out. Strand fracture at 1.04 f_{pu}.
6N	NSC	248 (55.7)	1770 (256.6)	0.95	Pull out began. Strand fracture at 1.03 f_{pu}.
Avg	NSC	244 (54.8)	1740 (252.4)	0.93 [1]	

Note: [1] Average f_{strand}/f_{pu} = 1.02 for failures due to strand fracture.

CHAPTER FIVE

Discussion of Test Results

5.1 INTRODUCTION

Transfer and development length results from this study are compared to selected results from previous research programs. Values of transfer and development length predicted by several proposed equations are compared with the measured results.

5.2 TRANSFER LENGTH MEASUREMENTS

Transfer length results from this study are reported in the previous chapter for 15.2 mm (0.6 in.) diameter strands in two high-performance concrete (HPC) beams and two normal-strength concrete (NSC) beams. The test specimens were full-sized, I-shaped beams. The transfer length results from the concrete strain measurements are summarized in Table 5.1. The transfer lengths shown are for final measurements taken just after release of the prestress force. The strand surface condition, the initial prestress, the initial concrete strength, and the type of release are also shown in Table 5.1.

Strand size and strand prestress are recognized as two of the most important factors affecting transfer length. Most, if not all, transfer length equations proposed by

Table 5.1   Transfer lengths from this study

Concrete Type	Strand Surface Condition	Initial Prestress f_{si} MPa (ksi)	Initial Concrete Strength f'_{ci} MPa (psi)	Type of Release	Transfer Length	
					Range mm (in.)	Avg. mm (in.)
HPC	bright, free of rust	1280 (185.6)	72.5 (10,520)	gradual	320-360 (13-14)	350 (14)
NSC	bright, free of rust	1270 (184.2)	30.1 (4,360)	gradual	440-480 (17-19)	460 (18)

various researchers are functions of these two factors. Some researchers have concluded concrete strength is significant, while others have not. More data will help resolve this issue.

Concrete strength was the only variable in this study. The transfer length was 26% longer for the NSC beams compared to the HPC beams. The limited results of this study suggest that concrete strength affects transfer length, but the effect might not be significant. A comparison with the results from previous research suggests that other factors, such as the strand surface condition and the type of release, probably are equally or more significant than concrete strength.

Results of some research studies are summarized in Table 5.2. Only the transfer lengths of 15.2 mm (0.6 in.) diameter strands in test specimens with initial strand prestress greater than 1030 MPa (150 ksi) and average concrete strengths greater than 28 MPa (4000 psi) were selected. In the upper part of the table, the concrete strengths at transfer were about 48 MPa (7000 psi) and above. This could be classified as high-strength concrete. In the lower part, the concrete strengths at transfer were about 28 to 38 MPa (4000 to 5500 psi), which is a fairly typical range for what currently is considered normal-strength concrete in the prestressed, precast concrete industry.

Typically, strands are prestressed at or near the maximum limit allowed by the ACI[1] and AASHTO[2] specifications, so the initial strand prestress generally has a relatively narrow range. The initial prestress for the test specimens summarized in Table 5.2 varied from approximately 1170 to 1380 MPa (170 to 200 ksi) for Grade 270 low-relaxation strands. Table 5.2 includes the 1963 study by Kaar et al.[11], which used Grade 250 (1720 MPa [250 ksi] guaranteed ultimate tensile strength) stress-relieved strands. The least initial prestress in that research was 1056 MPa (153.1 ksi). Some data presented by Mitchell et al.[15] were omitted from Table 5.2 because the initial prestress of 871 MPa (126 ksi) was abnormally low due to stressing problems.

In the HPC and NSC beams of this study, the strands were "bright", that is, free of visible rust, and the prestress was released gradually. Of the selected studies, only

Table 5.2   Transfer lengths of 15.2 mm (0.6 in.) strand from previous research

Researchers	Strand Surface Condition	Average Initial Prestress f_{si} MPa (ksi)	Initial Concrete Strength f'_{ci} MPa (psi)	Type of Release	Transfer Length Range mm (in.)	Avg. mm (in.)
Gross & Burns[7] (1995)	rusty	1358 (197.0)	48.5 (7040)	sudden	330-430 (13-17)	360 (14)
Mitchell et al.[15][(1)] (1993)	smooth, untreated	1176 (171.0)	47.9 (6950)	gradual	430-540 (17-21)	480 (19)
Cousins et al.[5] (1990)	uncoated	1352 (196.1)	32.8 (4750)	sudden	1120-1730 (44-68)	1440 (57)
	coated with epoxy and grit	1308 (189.7)	28.9-32.8 (4190-4750)	sudden	560-980 (22-39)	810 (32)
Deatherage et al.[6] (1994)	milled (shiny and rust free)	1311 (190.1)	28.3-37.6 (4100-5450)	sudden	530-760 (21-30)	620 (24)
Kaar et al.[11] (1963)	slightly rusted before cleaning	1115[(2)] (161.7)	28.0-37.7 (4070-5470)	sudden	700-1000 (28-40)	840 (33)
Lane[12] (1992)	uncoated	1396[(4)] (202.5)	29.9 (4330)	sudden	N/A	>1460[(3)] (>58)
	coated with epoxy and grit	1396[(4)] (202.5)	29.9 (4330)	sudden	N/A	660[(3)] (26)
Russell & Burns[17] (1993)	bright	1396[(5)] (202.5)	26.5-33.0 (3850-4790)	sudden	610-1470 (24-58)	1040 (41)
Shahawy et al.[18] (1992)	weathered 3-4 days	1272 (184.5)	38.9 (5640)	sudden	810-910 (32-36)	880 (35)

Notes: [(1)] 15.7 mm (0.62 in.) strands.
[(2)] Stress-relieved strand with guaranteed ultimate strength of 1720 MPa (250 ksi).
[(3)] Published transfer lengths were for concrete age of 365 days.
[(4)] Strand prestress before elastic loss. f_{si} = 1250 MPa (181 ksi) approximately.
[(5)] Strand prestress before elastic loss. f_{si} = 1270 MPa (184 ksi) approximately.

that by Mitchell et al. had similar conditions. The concrete for the transfer length beam specimens of that study was high-strength concrete. The average transfer length from that study was about 40% longer than the results for the HPC beams of this study.

In research by Gross and Burns[7] on large rectangular HPC beams, the strands were described as rusty and the prestress was released suddenly. Those conditions were the opposite of the conditions for this study in terms of their effect on transfer length. While the rust on the strand surface should decrease the transfer length measured in that study as compared to this one, the sudden release should increase it. The net effect is unpredictable. The average transfer lengths from that study and this study were the same for high-strength concrete.

For normal-strength concrete, the average transfer lengths from the other studies were 35% to 220% longer than the results for the NSC beams investigated in this study. All those studies used strands essentially free of rust, the same as this study, but the prestress was released suddenly. The sudden release of prestress tends to increase the transfer length and might increase the scatter in transfer length data, especially for small test specimens. In research by Russell and Burns[17], the transfer length of 15.2 mm (0.6 in.) diameter strands in small rectangular test specimens was about 35% greater than the transfer length in larger I-shaped beams.

Another factor with perhaps the most significant effect on the transfer length is the surface condition of the strand. In the studies by Cousins et al.[5] and by Lane[12], the average transfer length decreased, that is, improved, by about 50% for strands coated with epoxy and grit as compared to uncoated strands in the same studies.

The surface condition of strand is assessed based on a visual inspection, but a visual inspection can miss the presence of residual stearates and/or form oil. Stearates, usually called "soaps", are used as lubricants when the wires of the strand are manufactured by pulling them through dies. If too much is used or if the excess is not removed, the stearates can negatively affect bond of concrete to the strand. Form oil inadvertently applied to the strands during the fabrication of the concrete members might have a similar effect.[17]

The scatter in the transfer length data is illustrated in Figure 5.1 where the individual data points summarized in Tables 5.1 and 5.2 are plotted. For the relatively narrow range of concrete strengths from 28 to 38 MPa (4000 to 5500 psi), the transfer length data varies wildly. The transfer lengths for high-strength concrete do not vary much, but the test specimens were massive and/or the prestress was released gradually. Also, there are few transfer length studies with high-strength concrete, so the strand surface condition might not have been representative of typical conditions.

It is interesting that virtually all data in Figure 5.1 above the line for a transfer length of 1000 mm (39 in.) are for small specimens with sudden release in the study by Russell and Burns[17] or for uncoated strands in the studies by Cousins et al.[5] and Lane[12].
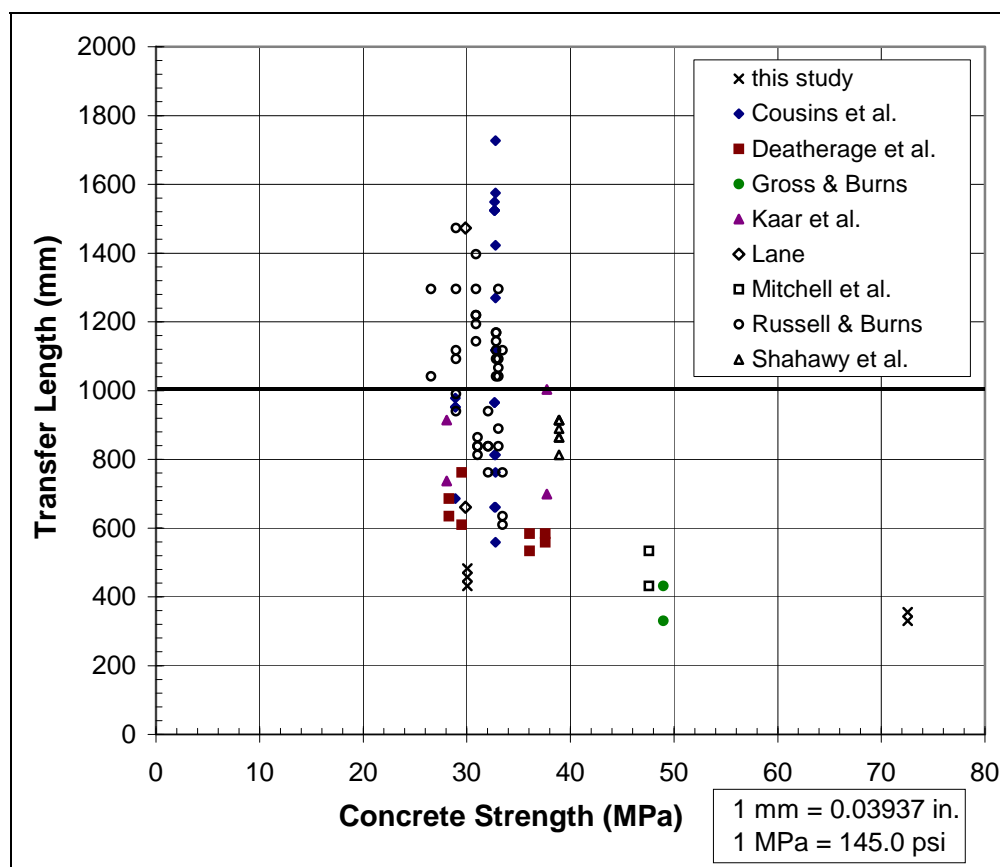
Figure 5.1   Transfer length data from literature for 15.2 mm (0.6 in.) strands

Without these data where the strand surface condition and the sudden release in small specimens are known to have had a negative effect, there is much less scatter. This helps illustrate the importance of the strand surface condition and the sudden release of prestress, especially for small test specimens.

Transfer length equations proposed by various researchers are shown in Table 2.1. These equations were used to calculate the transfer length for the HPC and NSC beams of this study. The calculated transfer lengths are listed in Table 5.3 and are plotted in Figures 5.2 and 5.3. All of the proposed equations yielded transfer lengths longer, that is, more conservative, than the measured transfer lengths. The only exception was the equation proposed by Zia and Mostaffa[20] when applied to the HPC beams, but the concrete strength of the HPC beams exceeded the limit for that equation. Note that it is desirable for the transfer lengths predicted by the simplified ACI[1]/AASHTO[2] equation to be equal to or longer than the actual transfer length. The purpose of the

Table 5.3   Transfer lengths from proposed equations

Source of Equation	HPC		NSC	
	Transfer Length	$\dfrac{L_{t,calc}}{L_{t,test}}$	Transfer Length	$\dfrac{L_{t,calc}}{L_{t,test}}$
	mm (in.)		mm (in.)	
ACI[1]/AASHTO[2]	850 (33)	2.43	830 (33)	1.81
Martin & Scott[14]	1220 (48)	3.49	1220 (48)	2.67
Zia & Mostaffa[20]	290 (11) [1]	0.82[1]	850 (33)	1.85
Cousins, Johnston & Zia [5] [2]	820 (32)	2.35	1230 (49)	2.70
Russell & Burns[17]	1270 (50)	3.64	1240 (49)	2.72
Mitchell, Cook, Khan & Tham[15]	500 (20)	1.44	780 (31)	1.70
Deatherage, Burdette & Chew[6]	940 (37)	2.71	930 (37)	2.04
Buckner[3]	620 (24)	1.78	700 (28)	1.53
Notes: [1] f'_{ci} = 72.5 MPa (10,520 psi) for the HPC beams is greater than the maximum limit of 55.2 MPa (8000 psi) allowed for this authors' transfer length equation. [2] B = 300 psi/in. U'$_t$ = 6.7 for uncoated strand.				
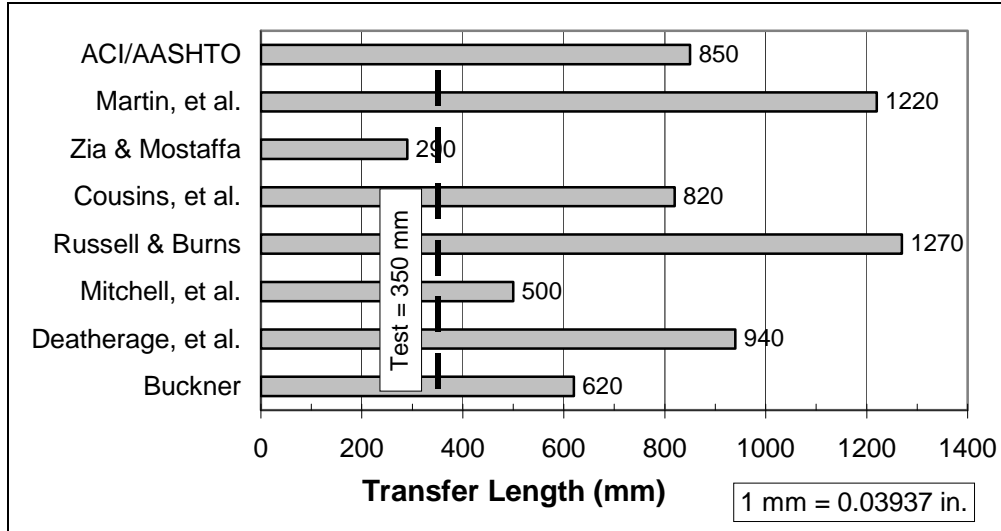
Figure 5.2   Transfer length predicted by proposed equations for HPC beams
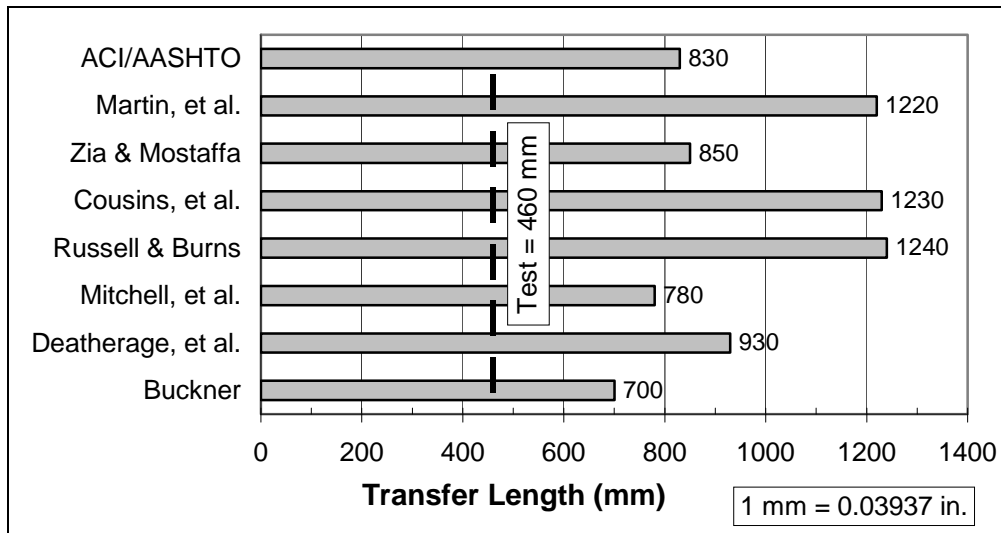
Figure 5.3   Transfer length predicted by proposed equations for NSC beams

transfer length equation in those specifications is for the calculation of the nominal web shear strength, V_{cw}, and an equation that yields a transfer length shorter than reality could be unconservative. However, a predicted transfer length that is too long could be unconservative in a check of concrete stresses at the ends of a beam just after transfer.

The transfer lengths measured in this study were exceptionally good compared to previous research, so it is not surprising that the proposed equations predict values that appear to be overly conservative. Although the surface condition of the strands in this study was classified as "bright" (i.e., no visible rust), the strand had excellent bond properties. The strand surface condition probably was free of excess stearates from the manufacturing process, and there was little or no contamination from form oil during the fabrication of the test beams. The gradual release of the prestress force in this study also contributed to short transfer lengths.

5.3 DEVELOPMENT LENGTH TESTS

An iterative procedure described in Section 3.6 was used to determine the development length. A series of four load tests was performed for each concrete type, HPC and NSC, with a different embedment length for each test in a series. The development length equals the embedment length when failure borders on flexure and bond simultaneously. In this study, embedment lengths from 1830 to 3050 mm (72 to 120 in.) were tested. All test beams failed due to flexure except the NSC beam with the shortest embedment length, which had a compression strut failure. Cordova[22] noted that, "because no bond failure was observed with the 1830 mm (72 in.) embedment length, a precise value for the development length could not be determined. It can only be stated that, for this study, the development length was less than 1830 mm (72 in.)." This was true for the HPC beams as well as the NSC beams.

Results from previous studies on the development length of 15.2 mm (0.6 in.) diameter strands with concrete strengths greater than 31 MPa (4500 psi) are summarized in Table 5.4. The upper and lower parts of the table present results from previous studies that used high-strength and normal-strength concrete, respectively.

The development length of less than 1830 mm (72 in.) for the HPC beams of this study is consistent with high-strength concrete test results reported by Gross and Burns[7] and by Mitchell et al.[15] In the study by Mitchell et al., the development length of 15.2 mm (0.6 in.) diameter strand in concrete with a compressive strength of 65.0 MPa (9430 psi) was 750 mm (30 in.), which is exceptionally short. The results were contradictory in that study because the development length was longer in test beams with a higher concrete strength. Generally, the development length is shorter for higher concrete strengths. Perhaps it would be reasonable to conclude from the results of Mitchell et al.

Table 5.4   Development lengths of 15.2 mm (0.6 in.) strand from previous research

Researchers	Average Concrete Strength f'_c MPa (psi)	Development Length mm (in.)
Gross & Burns[7] (1995)	90.7 (13,160)	<1980 (<78)
Mitchell et al.[15] (1993)	89.0 (12,900)	>980 (>38) [1]
	65.0 (9430)	750 (30) [1]
Mitchell et al.[15] (1993)	31.0 (4500)	1860 (74) [1]
Cousins et al.[5] (1990)	45.8 (6640)	3350 (132) [2]
	45.8 (6640)	1630 (64) [3]
Deatherage et al.[6] (1994)	53.2 (7720)	2160 (85)
	35.9 (5210)	2240 (88)
Russell & Burns[17] (1993)	48.1 (6980)	2130 (84) [4]
	48.4 (7020)	<1980 (<78) [5]
Notes: [1] 15.7 mm (0.62 in.) strands. [2] Uncoated strands. [3] Strands coated with epoxy and grit. [4] I-shaped beams. [5] Rectangular beams.		

and Gross and Burns, that the development length was between 980 and 1980 mm (38 and 78 in.) for high-strength concrete beams.

The development length of less than 1830 mm (72 in.) for the NSC beams of this study is shorter than reported values for almost all the normal-strength concrete test results shown in Table 5.4. Most researchers reported development lengths from 1860 to 2240 mm (74 to 88 in.) for uncoated strands. The development length of 3350 mm (132 in.) reported by Cousins et al.[5] was unusually long. That value was from the same study that also reported long transfer lengths.

The proposed development length equations in Table 2.1 were used to calculate values for the 15.2 mm (0.6 in.) diameter strands of this study. The calculated values are shown in Table 5.5 and Figures 5.4 and 5.5. All equations predicted conservative development lengths except the equation by Mitchell et al. for the HPC beams. The ACI[1]/AASHTO[2] equation conservatively predicted a development length of 2390 to 2440 mm (94 to 96 in.), which is roughly 30% greater than the minimum embedment length tested in this project.

Table 5.5   Development lengths from proposed equations

Source of Equation	HPC		NSC	
	Development Length mm (in.)	$\dfrac{L_{d,calc}}{L_{d,test}}$	Development Length mm (in.)	$\dfrac{L_{d,calc}}{L_{d,test}}$
ACI[1]/AASHTO[2]	2390 (94)	1.31	2440 (96)	1.34
Zia & Mostaffa[20]	2250 (89)	1.23	2890 (114)	1.58
Cousins, Johnston & Zia [5] [(1)]	2760 (109)	1.51	3990 (157)	2.18
Mitchell, Cook, Khan & Tham[15]	1230 (49)	0.68	2050 (81)	1.12
Deatherage, Burdette & Chew[6]	3250 (128)	1.78	3360 (132)	1.84
Buckner[3]	3700 (146)	2.02	3930 (155)	2.15
Note: [(1)] $U'_d = 1.32$ for uncoated strand.				

The good development length results of this study probably are attributable to a strand surface free of stearates and oils, and the gradual release of the prestress force. The current ACI/AASHTO development length equation is satisfactory for clean strand like that used in this study.
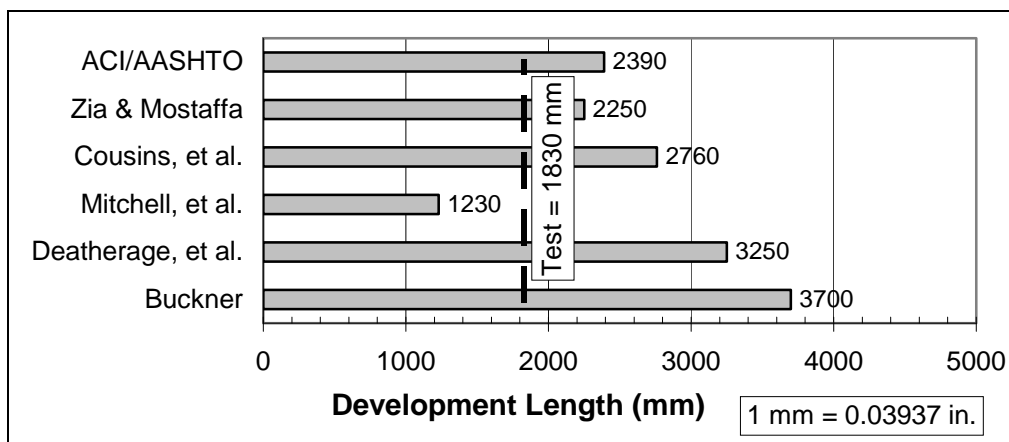
Figure 5.4   Development length predicted by proposed equations for HPC beams
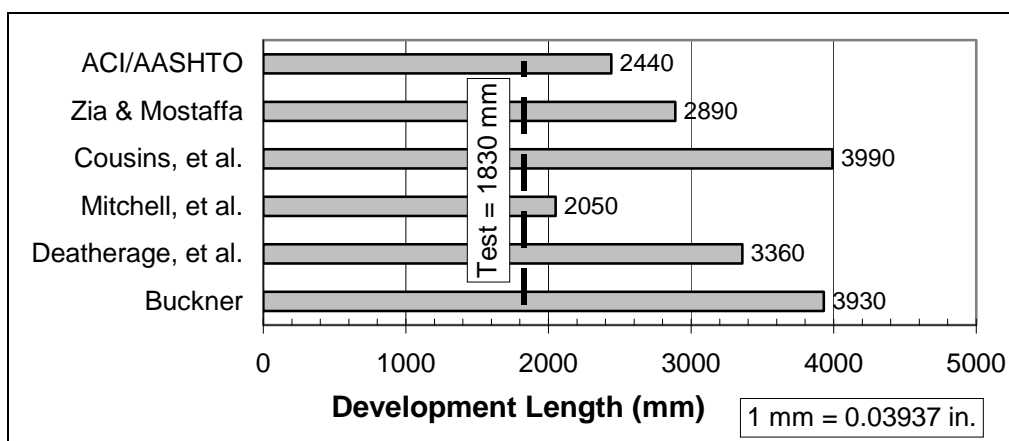
Figure 5.5   Development length predicted by proposed equations for NSC beams

5.4 PULL OUT TESTS

There was and is no standard pull out test to assess the surface condition of strand. The strand had excellent bond properties as all strands ultimately failed in fracture in the pull out tests. The good pull out test results of this study are consistent with the measured transfer and development lengths.

CHAPTER SIX

Summary and Conclusions

6.1 SUMMARY

The purpose of this research study was to determine the transfer and development lengths of 15.2 mm (0.6 in.) diameter strand on a 51 mm (2 in.) grid in I-shaped concrete beams. The only variable was the concrete strength of the beams, which was either normal-strength concrete (NSC) or high-performance concrete (HPC). Pull out tests were performed on strand samples embedded in concrete test blocks to assess the strand surface condition.

A total of four beams, two beams of each concrete type, were fabricated with straight, fully-bonded strands. Sixteen strands were placed as tightly as possible in two rows in the bottom flange. Four strands were added to the top flange to control high tensile concrete stresses at release. The prestress force was released gradually. The strands were Grade 270 (1860 MPa [270 ksi] guaranteed ultimate tensile strength), low-relaxation, seven-wire strand. The surface condition was "bright", that is, there was no visible surface rust. The beams were standard Texas Department of Transportation (TxDOT) Type C sections, which were 1016 mm (40 in.) deep with a 178 mm (7 in.) thick web. A 191 mm (7.5 in.) thick composite slab was added prior to development length load tests. The concrete strengths of the HPC and NSC beams were 92.0 MPa (13,340 psi) and 50.0 MPa (7250 psi), respectively, during the load tests. At release of the prestress force, the concrete strengths were 72.5 MPa (10,520 psi) and 30.0 MPa (4360 psi), respectively.

Transfer length was determined from concrete surface strains at the level of the bottom strands. Measurements were taken immediately before and after release using mechanical strain gauges (DEMEC gauges). Concrete strains were recorded and plotted with respect to length. The transfer length was determined from the resulting concrete

strain profile using the 95% plateau method. Transfer length also was determined from strand end slips measured with a micrometer immediately before and after release.

An upper bound for the development length was determined from a series of load tests using a different embedment length for each test in a series. Embedment length is the length of bond from the beginning of bond to the critical section. The intent was to bracket the development length between a pair of embedment lengths where the failure mode was flexure in one load test and bond in the other. In this study, flexural failure occurred or was imminent in all tests, so the development length could not be established precisely. The development length load tests were performed at the Ferguson Structural Engineering Laboratory at The University of Texas at Austin. Applied load, deflections, top fiber concrete strains, strand end slips and crack patterns were recorded for each test.

Pull out tests were performed on strand samples embedded in HPC and NSC test blocks. The samples were cut from the same spools of strand used to fabricate the test beams. The strands were unstressed and bonded for a length of 508 mm (20 in.) with an additional unbonded length of 51 mm (2 in.) at the concrete surface. At a concrete age of three days, the strands were pulled to failure and the load was recorded.

6.2 CONCLUSIONS

The following conclusions are based on the results from this study.

1. The average transfer length for the 15.2 mm (0.6 in.) diameter strands was 350 mm (14 in.) and 460 mm (18 in.) in the HPC and NSC beams, respectively, based on concrete strain. Based on the strand end slip, the average transfer lengths were about 10% longer. These transfer lengths were less than the values predicted by the simplified ACI[1]/AASHTO[2] expression of 50 times the strand diameter. This expression is suggested by ACI/AASHTO for the calculation of the concrete web shear strength, V_{cw}. The simplified ACI/AASHTO expression when applied to the test beams of this study would be conservative for the calculation of the concrete web

shear strength, V_{cw}, but could be unconservative for a check of concrete stresses near the end of the beams just after transfer.

2. An upper bound of 1830 mm (72 in.) was determined for the development length of the 15.2 mm (0.6 in.) diameter strands in the HPC and NSC beams. The ACI/AASHTO expressions conservatively predicted a development length 1.3 times the upper bound development length determined in this study.

3. In pull out tests, all strand samples in HPC and NSC test blocks ultimately failed due to strand fracture at about 1.03 times the minimum guaranteed tensile strength. This was consistent with the short transfer and development lengths measured in this study.

4. The short transfer and development lengths of the strands and the fracture of the strand in all pull out tests suggest the strand surface was clean, that is, not contaminated by an excess of stearates or form oil.

APPENDIX A

CONTRACTOR DRAWINGS FOR TEST BEAMS

REINFORCING STEEL NOTES:
1. ALL DIMENSIONS ARE CENTER TO CENTER.
2. ALL STEEL TO BE ASTM A-615,GR.60.
3. U BAR SPLICES PERMITTED (40'MIN. C-C SPLICES) NO PORTION OF BAR TO BE LESS THAN 10'. (2'-5" MIN.) DOES NOT INCLUDE LAP.

V₁ BAR   R 6 BAR   X 5 BAR   U 5 BAR

BEAM MARK	ALL BMS					REINFORCING STEEL SCHEDULE & DIMENSIONS						
BAR	SIZE	NO. REQ'D.				TOTAL	LENGTH	Ø	A	B	C	D	R
R6	#4	314				628	8'-3"	——	3 1/4"	3'-8"	4"	——	1"
X5	#3	54				108	1'-9"	——	——	11"	6"	——	1"
W5	#5	4				8	6'-0"	——	——	1'-6"	2'-3"	——	1"
Y5	#6	4				8	4'-4"	——	——	2'-10"	9"	——	3"
V1	#4	142				284	3'-2"	——	1'-1"	5 1/4"	1' 7 1/4"	——	1"
U5	#5	2				4	54'-0"	——	——	—STRAIGHT—		——	

STRANDS

C.L. SECTION   END VIEW

cg=9.60" e=7.49"
CGC CGS
11 SPA. @ 2" = 1'-10"

STRAND PATTERN

NUMBER OF STRANDS	: 20 6/10"Ø 270K @ 43.95K EA.
NUMBER OF STRAIGHT STRANDS	: 20
INITIAL LOAD STRAIGHT STRANDS	: 3000 LBS
CLASS OF CONCRETE	: H
CONCRETE RELEASE STRENGTH	: 8000-9000 PSI
CONCRETE DESIGN STRENGTH @ 56 DAYS	: 10,000-13,000 PSI

SUBMITTED FOR APPROVAL   DATE: 6/27/95

RELEASED FOR FABRICATION   DATE: _____

BEAM MARK FF-1

"C" BEAM DETAIL

52' TEST BEAM

TEXAS CONCRETE COMPANY
P.O. DRAWER 1070   VICTORIA, TEXAS 77901

CUSTOMER	UNIV OF TEXAS-FERGUSON LAB	DVN. I.H. / CHKD R.D.B.
OWNER	UNIVERSITY OF TEXAS	DATE 6/27/95
ENGINEER	PHILL M. FERGUSON STRUCTURAL ENG. LAB.	SHEET NO. F-1
STRUCTURE	TEST BEAMS	DWG. NO. D-2311
LOCATION	AUSTIN, TX.	JOB NO. 567
PROJECT	RESEARCH BEAMS	

3 DELETED H BARS & ADDED MORE R BARS-7/3/95
2 CHANGED V1 BARS-6/29/95
1 ADD V1,V2 & H BARS-6/28/95

Figure A.1   High-performance concrete test beam shop drawing (Part 1 of 3)

END VIEW C.L. SECTION END VIEW

⊕ DENOTES CAST CORRECTION ADDED

BEAM SCHEDULE & DIMENSIONS

BEAM MARK	NO. REQ'D	BEAM LENGTHS (ALONG CENTERLINE OF BM.)			INTERIOR DIAFRAMS CHAINED FROM MARKED END (CAST CORRECTION ADDED)									PLAN TYPE
		A	B	C	1	⊕ 1A	2	⊕ 2A	3	⊕ 3A	4	⊕ 4A	
FF-1	2	52.00'	52.03'	26.015'										1
TOT. BMS.	2													
TOT. LINEAR FT.		104.00'												

GENERAL NOTES

1. SPACING OF BARS R & S MAY BE VARIED TO AVOID DIAFRAM HOLES.
2. REINFORCING BARS AND/OR STRANDS MAY COME IN CONTACT WITH MATERIALS USED IN FORMING DIAFRAM HOLES.
3. DIMENSIONS RELATING TO BARS OR STRANDS ARE CENTER TO CENTER.
4. BARS V AND X MAY BE TILTED THUS / OR SKEWED AS REQUIRED TO MAINTAIN 1" MIN. CONCRETE COVER.
5. STRANDS MAY BE SPREAD TO MISS DIAFRAM HOLES.
6. STRANDS MAY BE RECESSED 1/2" MAX INTO END OF BEAM.
7. BEAM ENDS MAY BE FORMED WITH WOOD.
8. BOTTOM CORNERS OF ALL BEAM FLANGES AND OUTSIDE CORNERS OF EXTERIOR BEAM ENDS SHALL BE CHAMFERED OR ROUNDED TO A 3/4" RADIUS. AT FABRICATORS OPTION, ALL VERTICAL EDGES ON ALL BEAMS MAY BE CHAMFERED OR ROUNDED
9. BEAM MARKS TO BE PLACED ON FIXED END OR AS NOTED.
10. ALL DIMENSIONS MEASURED ALONG BOTTOM OF BEAM @ C.L. UNLESS NOTED OTHERWISE

** HAULING OVERHANG		
BEAM MARK	MARK ONE END	TOTAL BOTH ENDS
ALL BEAMS	6'	12'

**FABRICATORS USE ONLY

Figure A.2　High-performance concrete test beam shop drawing (Part 2 of 3)

77

Figure A.3   High-performance concrete test beam shop drawing (Part 3 of 3)

REINFORCING STEEL NOTES:
1. ALL DIMENSIONS ARE CENTER TO CENTER.
2. ALL STEEL TO BE ASTM A-615,GR.60.
3. U BAR SPLICES PERMITTED (40"MIN.
   C-C SPLICES) NO PORTION OF BAR TO BE
   LESS THAN 10'. (2'-5" MIN.)
   DOES NOT INCLUDE LAP.

∠45°

V₁ BAR   R₆ BAR   X₅ BAR   V₁ BAR / W₅ BAR / Y₅ BAR   U₅ BAR

BEAM LGTH. (-3")   2'-5" MIN.

BEAM MARK	ALL BMS				REINFORCING STEEL SCHEDULE & DIMENSIONS							
BAR	SIZE	NO. REQ'D.				TOTAL	LENGTH	∅	A	B	C	D	R
R₆	#4	324				648	8'-3"	—	3 1/4"	3'-8"	4"	—	1"
X₅	#3	54				108	1'-9"	—		11"	6"	—	1"
W₅	#5	4				8	6'-0"	—		1'-6"	2'-3"	—	1"
Y₅	#6	4				8	4'-4"	—		2'-10"	9"	—	3"
V₁	#4	146				292	3'-2"	—	1'-1"	5 1/4"	1'-7 1/4"	—	1"
U₅	#5	2				4	54'-0"	—		— STRAIGHT —		—	

STRANDS

cg=9.60" e=7.49"   CGC   CGS   11 SPA. @ 2" = 1'-10"   C.L. SECTION

cg=9.60" e=7.49"   CGC   CGS   11 SPA. @ 2" = 1'-10"   END VIEW

2'-8"   3'-4"

STRAND PATTERN

NUMBER OF STRANDS	: 20 6/10"∅ 270K @ 43.95K EA.
NUMBER OF STRAIGHT STRANDS	: 20
INITIAL LOAD STRAIGHT STRANDS	: 3000 LBS
CLASS OF CONCRETE	: H
CONCRETE RELEASE STRENGTH	: 4000-5000 PSI
CONCRETE DESIGN STRENGTH @ 28 DAYS	: 5000-7000 PSI

SUBMITTED FOR APPROVAL   DATE: 6/27/95

RELEASED FOR FABRICATION   DATE: _____

BEAM MARK	"C" BEAM DETAIL
FF-2	54' TEST BEAM

TEXAS CONCRETE COMPANY
P.O. DRAWER 1070   VICTORIA, TEXAS 77901

⚠ DELETED H BARS & ADDED MORE R BARS-7/3/95
⚠ CHANGED V1 BARS-6/29/95
⚠ ADD V1,V2 & H BARS-6/28/95

CUSTOMER	UNIV OF TEXAS-FERGUSON LAB	DWN. I.H.
		CHKD R.D.B.
OWNER	UNIVERSITY OF TEXAS	DATE 6/27/95
ENGINEER	PHILL M. FERGUSON STRUCTURAL ENG. LAB.	SHEET NO. F-2
STRUCTURE	TEST BEAMS	DWG. NO. D-2311
LOCATION	AUSTIN, TX.	
PROJECT	RESEARCH BEAMS	JOB NO. 567

Figure A.4   Normal-strength concrete test beam shop drawing (Part 1 of 3)

END VIEW

C.L.
SECTION

END VIEW

● DENOTES CAST CORRECTION ADDED

BEAM SCHEDULE & DIMENSIONS

BEAM MARK	NO. REQ'D	BEAM LENGTHS (ALONG CENTERLINE OF BM.)			INTERIOR DIAFRAMS CHAINED FROM MARKED END (CAST CORRECTION ADDED)								PLAN TYPE
		A	B	C	1	● 1A	2	● 2A	3	● 3A	4	● 4A	
FF-2	2	54.00'	54.03'	27.015'									1
TOT. BMS.	2												
TOT. LINEAR FT.		108.00'											

GENERAL NOTES

1. SPACING OF BARS R & S MAY BE VARIED TO AVOID DIAFRAM HOLES.
2. REINFORCING BARS AND/OR STRANDS MAY COME IN CONTACT WITH MATERIALS USED IN FORMING DIAFRAM HOLES.
3. DIMENSIONS RELATING TO BARS OR STRANDS ARE CENTER TO CENTER.
4. BARS V AND X MAY BE TILTED THUS / OR SKEWED AS REQUIRED TO MAINTAIN 1" MIN. CONCRETE COVER.
5. STRANDS MAY BE SPREAD TO MISS DIAFRAM HOLES.
6. STRANDS MAY BE RECESSED 1/2" MAX INTO END OF BEAM.
7. BEAM ENDS MAY BE FORMED WITH WOOD.
8. BOTTOM CORNERS OF ALL BEAM FLANGES AND OUTSIDE CORNERS OF EXTERIOR BEAM ENDS SHALL BE CHAMFERED OR ROUNDED TO A 3/4" RADIUS. AT FABRICATORS OPTION, ALL VERTICAL EDGES ON ALL BEAMS MAY BE CHAMFERED OR ROUNDED.
9. BEAM MARKS TO BE PLACED ON FIXED END OR AS NOTED.
10. ALL DIMENSIONS MEASURED ALONG BOTTOM OF BEAM @ C.L. UNLESS NOTED OTHERWISE

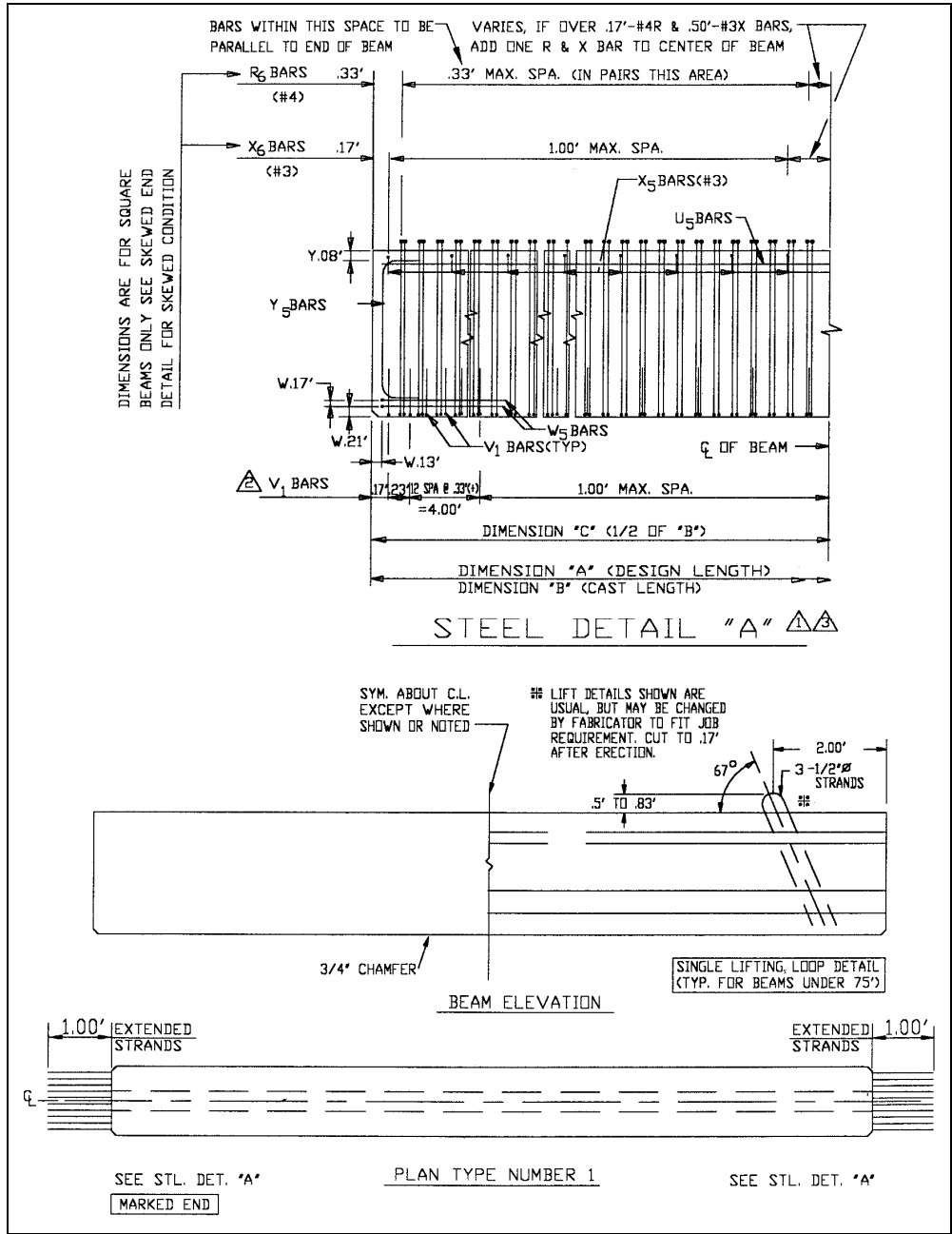| ** HAULING OVERHANG		
BEAM MARK	MARK ONE END	TOTAL BOTH ENDS
ALL BEAMS	6'	12'

**FABRICATORS USE ONLY

Figure A.5   Normal-strength concrete test beam shop drawing (Part 2 of 3)

80

Figure A.6   Normal-strength concrete test beam shop drawing (Part 3 of 3)

APPENDIX B

MATERIAL PROPERTIES

Figure B.1   Strand tensile test results (Sample no. 1)

Figure B.2   Strand tensile test results (Sample no. 2)

83
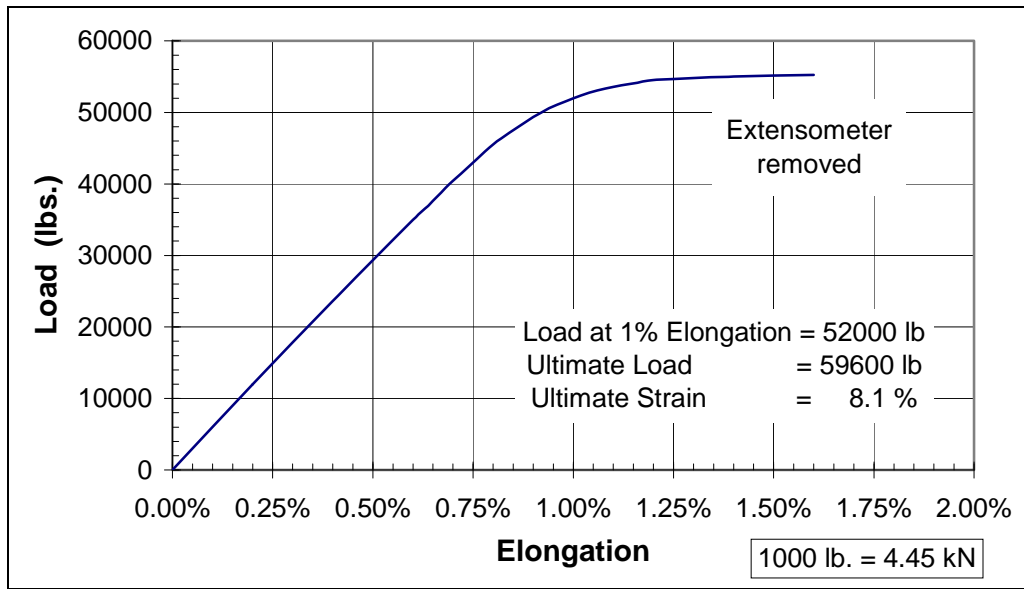
Figure B.3   Strand tensile test results (Sample no. 3)
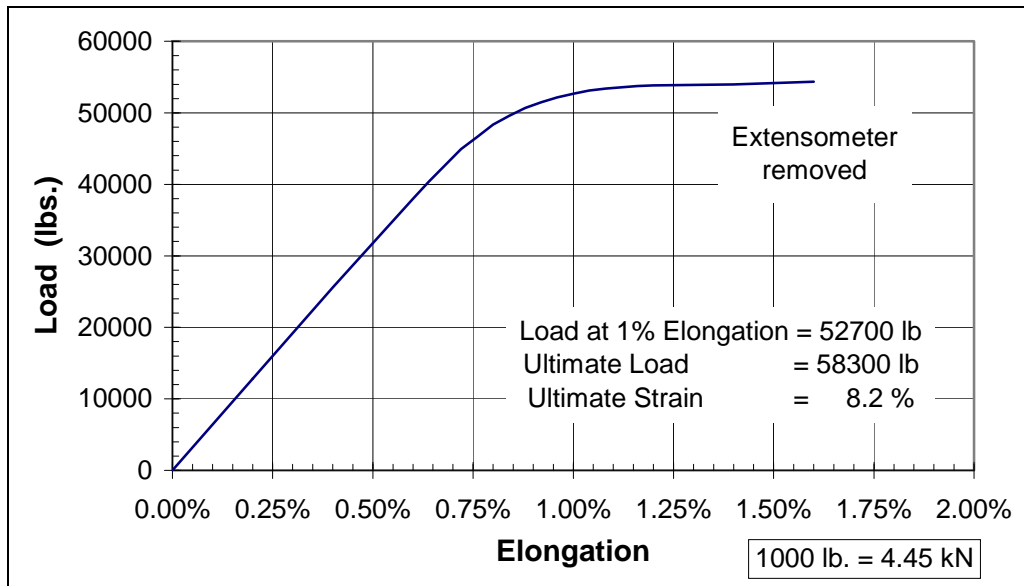
Figure B.4   Strand tensile test results (Sample no. 4)

84
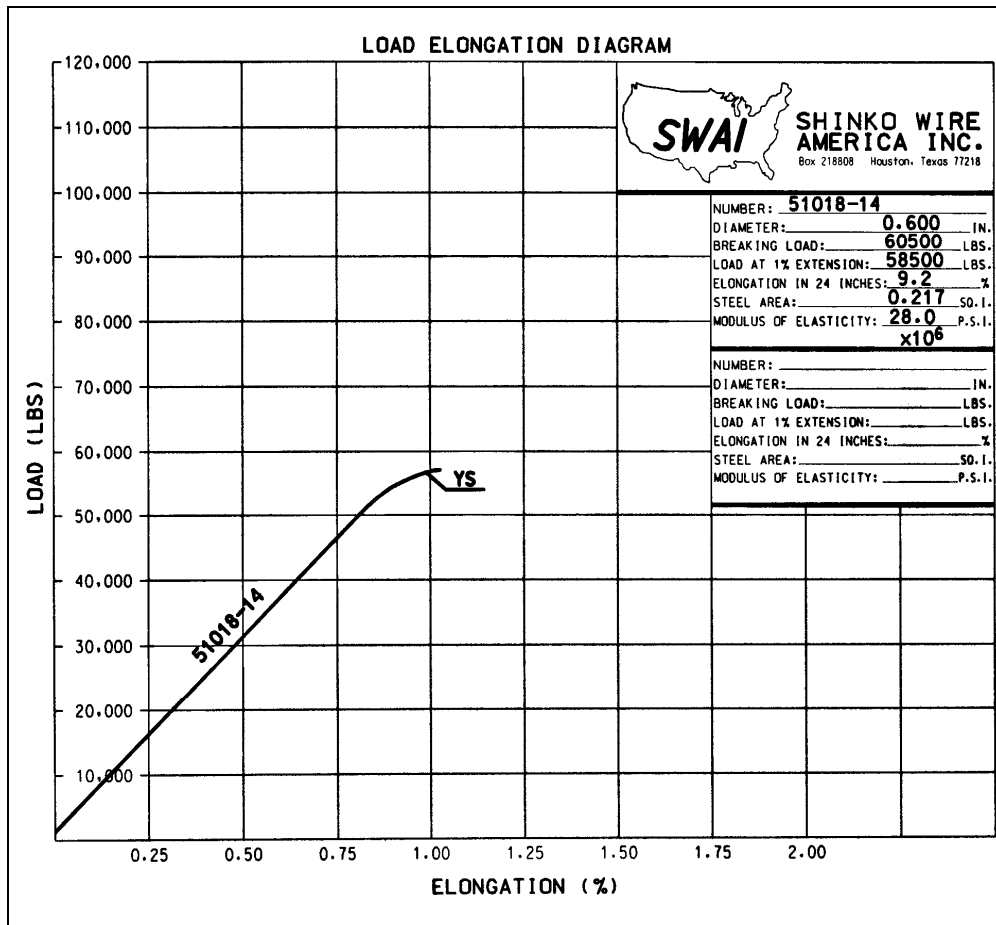
Figure B.5   Strand manufacturer's tension test results
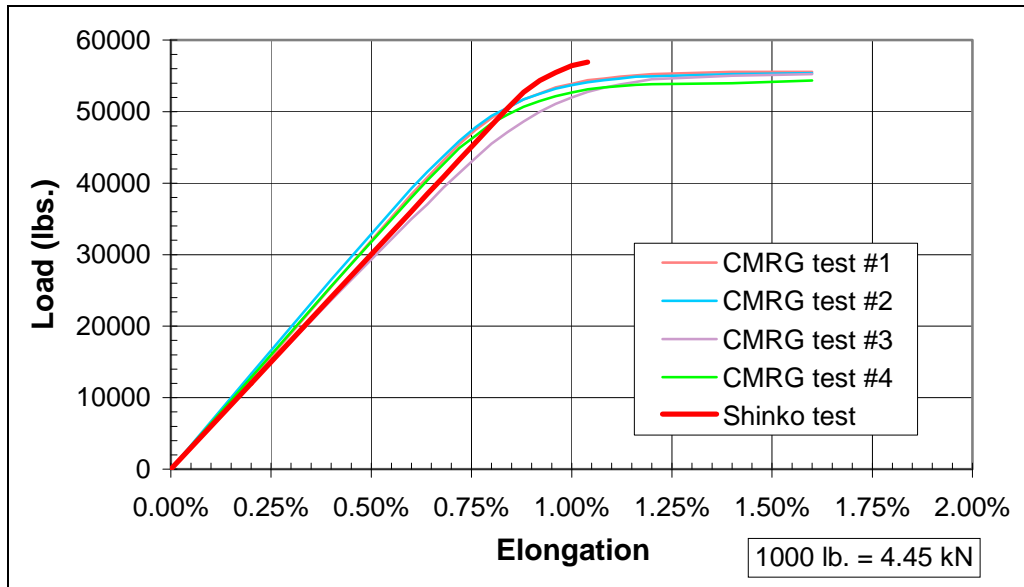
Figure B.6   Strand tensile test results for all samples

Table B.1   Strand tension tests performed at the CMRG Laboratory,
The University of Texas at Austin

Item	Units	Sample #1	Sample #2	Sample #3	Sample #4	Average
Ultimate Load	lbs	59,800	59,300	59,600	58,300	59,300
Ultimate Stress	psi	276	273	275	269	273
Load at 1% Strain	lbs	53,900	53,800	52,000	52,700	53,100
Stress at 1% Strain	psi	248	248	240	243	245
Ultimate Strain	in/in	8.5%	8.7%	8.1%	8.2%	8.4%
Strain at 43,940 lbs.	%	0.693%	0.683%	0.769%	0.703%	0.712%
Modulus of Elasticity	ksi	29,200	29,500	26,600	28,800	28,400
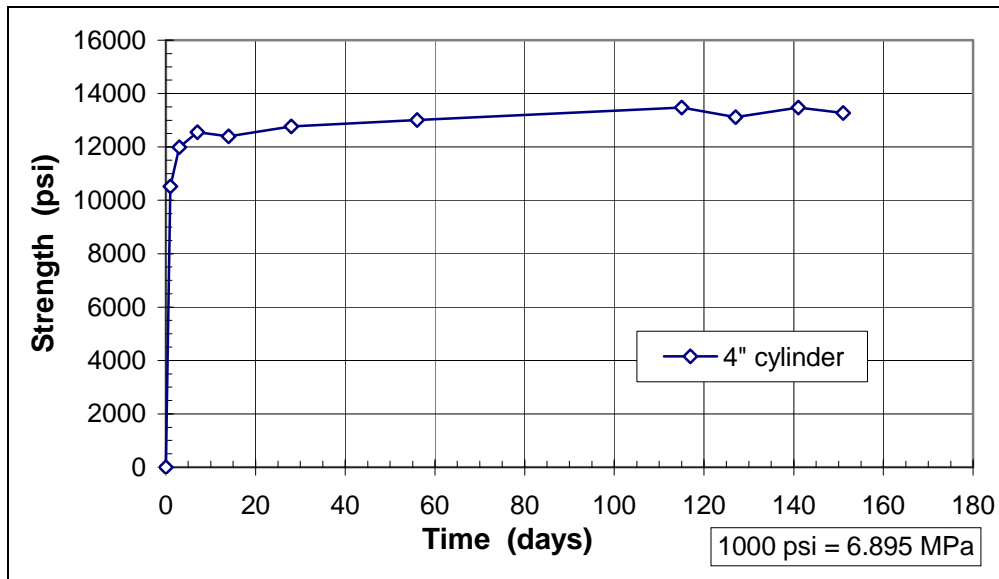
Figure B.7   Concrete compressive strength of HPC beams
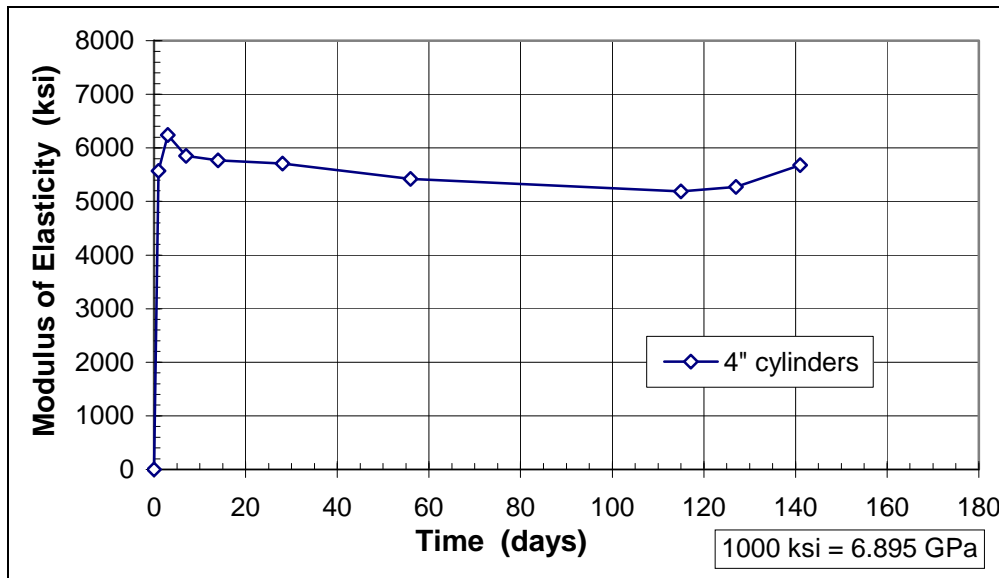
Figure B.8   Concrete modulus of elasticity of HPC beams
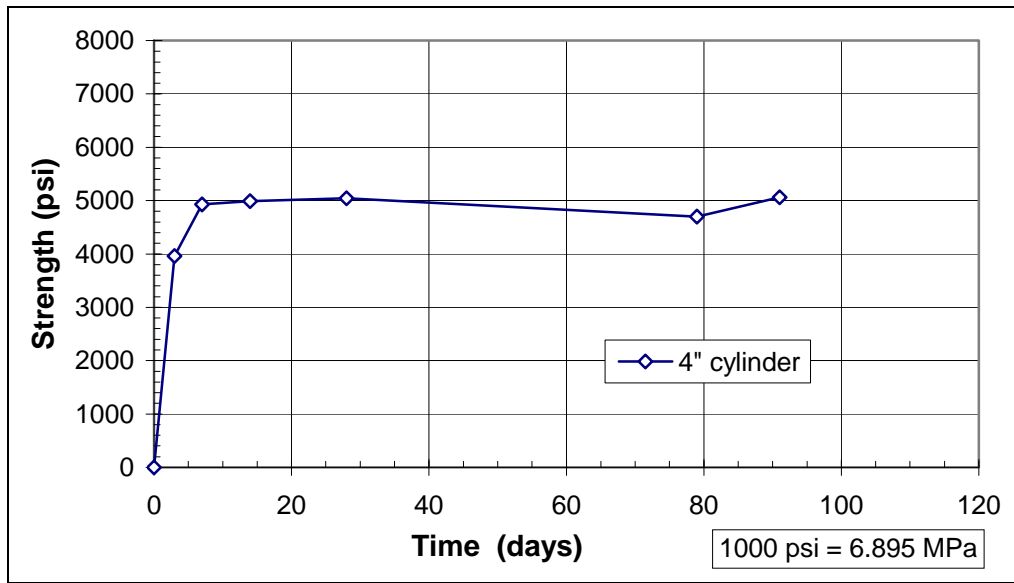
Figure B.9   Concrete compressive strength of composite slab on beam HPC-1
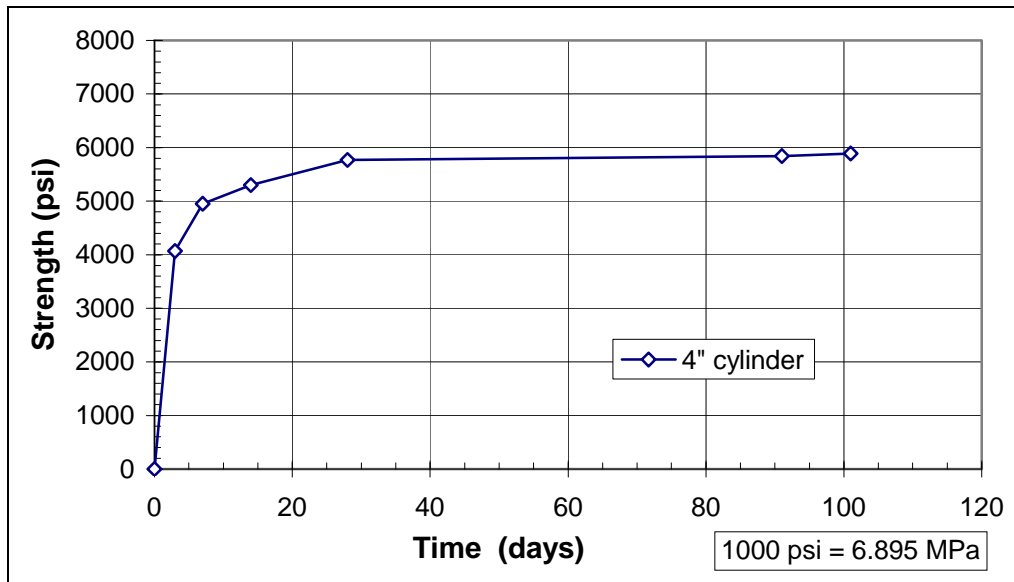
Figure B.10   Concrete compressive strength of composite slab on beam HPC-2
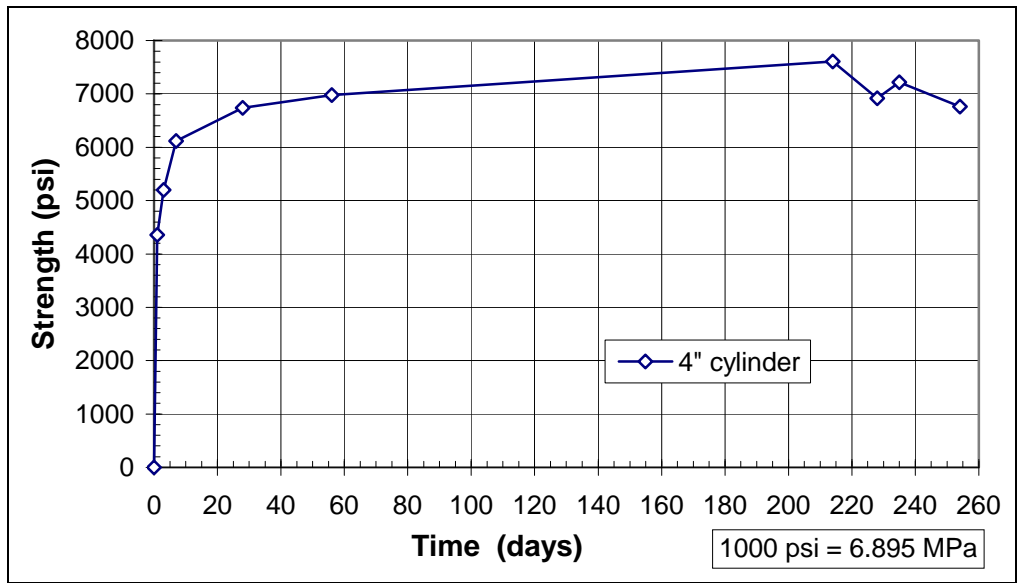
Figure B.11   Concrete compressive strength of NSC beams
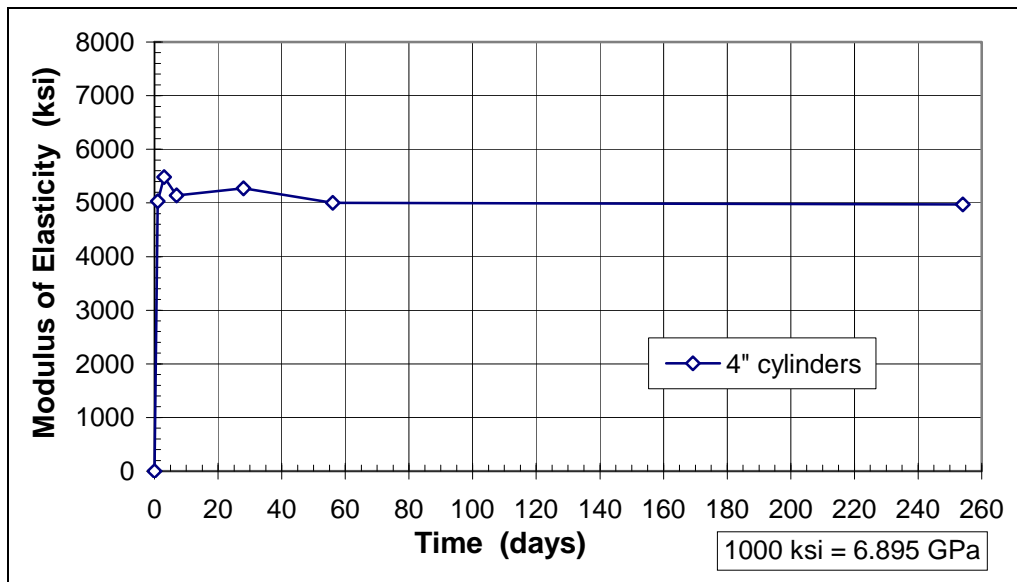
Figure B.12   Concrete modulus of elasticity of NSC beams
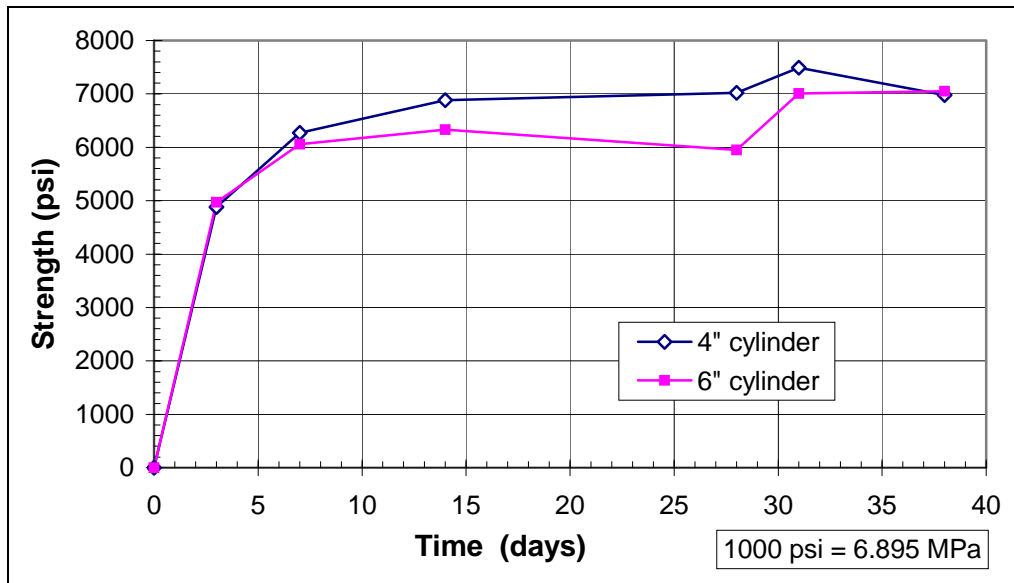
Figure B.13   Concrete compressive strength of composite slab on beam NSC-1
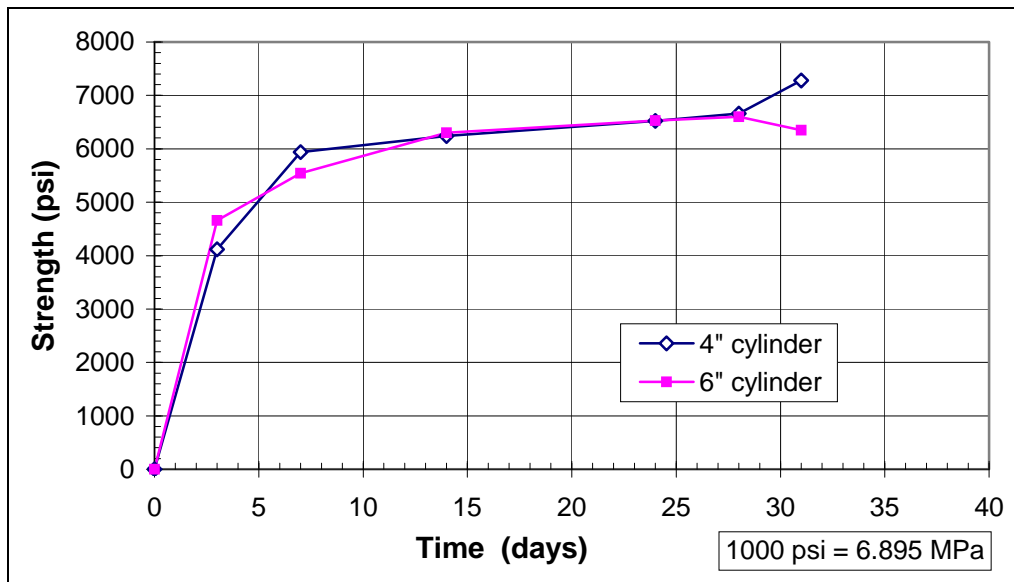
Figure B.14   Concrete compressive strength of composite slab on beam NSC-2

Table B.2   Summary of concrete strengths, modulus of elasticity, and maturity during testing

| Test No.	Date Tested	Beam f_c' 4" cyl psi	Beam E_c 4" cyl 10^6 psi	Slab f_c' 4" cyl psi	Slab f_c' 6" cyl psi	Date Cast Beam	Date Cast Slab	Age at Test Beam days	Age at Test Slab days
1-H1S-120	11/02/95	13,480	5.19	4700	---	07/10/95	08/15/95	115	79
2-H1N-93	11/14/95	13,120	5.27	5060	---	07/10/95	08/15/95	127	91
3-H2N-78	11/28/95	13,480	5.68	5840	---	07/10/95	08/29/95	141	91
4-H2S-72	12/08/95	13,270	---	5890	---	07/10/95	08/29/95	151	101
5-N1S-120	02/09/96	7610	---	7490	7010	07/10/95	01/09/96	214	31
6-N1N-93	02/16/96	---	---	6980	7050	07/10/95	01/09/96	221	38
7-N2S-78	02/23/96	6920	---	6520	6530	07/10/95	01/30/96	228	24
8-N2N-72	03/01/96	7220	---	7280	6350	07/10/95	01/30/96	235	31

Table B.3   Summary of concrete strengths and modulus of elasticity at various ages

Conc. Age days	HPC Beams — Beams f_c' 4" cyl psi	HPC Beams — Beams E_c 4" cyl 10^6 psi	HPC Slab #1 f_c' 4" cyl psi	HPC Slab #2 f_c' 4" cyl psi	NSC Beams — Beams f_c' 4" cyl psi	NSC Beams — Beams E_c 4" cyl 10^6 psi	NSC Slab #1 f_c' 4" cyl psi	NSC Slab #1 f_c' 6" cyl psi	NSC Slab #2 f_c' 4" cyl psi	NSC Slab #2 f_c' 6" cyl psi
1	10,520	5.57	---	---	4360	5.03	---	---	---	---
3	11,990	6.24	3960	4070	5200	5.48	4880	4970	4120	4660
7	12,550	5.85	4930	4950	6120	5.14	6270	6060	5940	5540
14	12,400	5.77	4990	5300	---	---	6880	6330	6240	6300
28	12,770	5.71	5140	5770	6740	5.27	7020	5950	6660	6600
56	13,010	5.42	---	---	6980	5.00	---	---	---	---
254	12,960	5.70	---	---	6760	4.97	---	---	---	---

Table B.4   Mix design for HPC beams

Material	Quantity per Cubic Yard of Concrete
Type III Cement	671 lb.
Fly Ash (Type C)	312 lb.
Water (w/c = 0.251)	247 lb.
Coarse Aggregate (1/2" crushed limestone)	1880 lb.
Fine Aggregate (sand)	1069 lb.
Air	2 %

Admixtures:
    High Range Water Reducer
    Retarder	

Table B.5   Mix design for NSC beams

Material	Quantity per Cubic Yard of Concrete
Type II Cement	452 lb.
Fly Ash (Type F)	122 lb.
Water (w/c = 0.352)	202 lb.
Coarse Aggregate (3/4" rock)	1885 lb.
Fine Aggregate (sand)	1264 lb.
Air	5 %

Admixtures:
    High-Range Water Reducer
    Retarder
    Air Entraining Agent	

Table B.6   Mix design for all composite slabs

Material	Quantity per Cubic Yard of Concrete
Type I Cement	517 lb.
Water (w/c = 0.387)	200 lb.
Coarse Aggregate (3/4" rock)	1869 lb.
Fine Aggregate (sand)	1355 lb.
Admixtures: High-Range Water Reducer	

APPENDIX C

PRESTRESS LOSS CALCULATIONS

The effective prestress after losses was calculated in accordance with the PCI General (Time-Step) Method.[16] The cross section was idealized with uniform top and bottom flange thickness of 7.75 and 10.75 inches (197 and 273 mm), respectively. The other cross section dimensions are shown in Figure 3.1. The bottom corner chamfers were ignored.

The effective prestress of the bottom strands includes a residual stress of about 5 MPa (0.7 ksi) from loads applied and removed at various stages. Typically these residual stresses are insignificant, especially for commercial engineering practice. They were included in the effective prestress calculations of this research for thoroughness of the analysis but justifiably could have been omitted.

Table C.1   Stages for calculation of prestress losses

Item	HPC Beams		NSC Beams	
	Age of Beam days	Age of Slab days	Age of Beam days	Age of Slab days
Stage 1: From tensioning through transfer of P/S.	0	---	0	---
Stage 2: Storage at yard of beam fabricator.	15	---	182	---
Stage 3: Storage at FSEL through placement of shores.	43	0	194	0
Stage 4: From slab conc placement thru removal of shores.	46	3	197	3
Stage 5: Storage until development length tests.	134	91	225	31

Table C.2   Strength and modulus of elasticity of concrete at each stage

Stage No.	HPC Beams				NSC Beams			
	Beams		Slabs		Beams		Slabs	
	f_c' psi	E_c ksi	f_c' psi	E_c ksi	f_c' psi	E_c ksi	f_c' psi	E_c ksi
1	10,520	5,600	---	---	4,360	5,000	---	---
2	12,400	5,650	---	---	7,000	5,000	---	---
3	12,900	5,650	---	---	7,000	5,000	---	---
4	12,900	5,650	4,020	3,600	7,000	5,000	4,500	3,800
5	13,340	5,700	5,370	4,200	7,250	5,000	7,070	4,800

1 psi = 6.894 kPa   1 ksi = 6.894 MPa

Table C.3   Section properties for prestress losses

	HPC Beams			NSC Beams		
	A in^2	y_b in.	I in^4	A in^2	y_b in.	I in^4
Net Section:						
Stage 1 (beam only)	494	17.18	83,400	494	17.20	83,600
Stage 2 (beam only)	494	17.18	83,400	494	17.20	83,600
Stage 3 (beam only)	494	17.18	83,400	494	17.20	83,600
Stage 4 (comp. sect.)	849	28.28	230,600	917	29.43	245,900
Stage 5 (comp. sect.)	902	29.20	242,900	1024	30.93	266,100
Transformed Section:						
Stage 1 (beam only)	516	16.86	88,700	518	16.84	89,500
Stage 2 (beam only)	515	16.87	88,600	518	16.84	89,500
Stage 3 (beam only)	515	16.87	88,600	518	16.84	89,500
Stage 4 (comp. sect.)	870	27.82	242,000	941	28.92	259,800
Stage 5 (comp. sect.)	923	28.75	254,900	1049	30.44	281,500

1 inch = 25.4 mm

Table C.4   Summary of prestress and losses for HPC beams

Item	Top P/S Reinforcement ksi		Bottom P/S Reinf. ksi	
Prestress after anchorage		199.0		199.0
Stage 1 losses, ES		<u>-1.3</u>		<u>-13.4</u>
Initial prestress at transfer, f_{si}		197.7		185.6
Relaxation loss, RET	-2.5		-2.0	
Shrinkage loss, SH	-2.9		-3.0	
Creep loss, CR	<u>-1.6</u>		<u>-5.4</u>	
Stage 2 losses		-7.0		-10.4
Relaxation loss, RET	-0.4		-0.3	
Shrinkage loss, SH	-1.5		-1.5	
Creep loss, CR	<u>-0.7</u>		<u>-2.3</u>	
Stage 3 losses		-2.6		-4.1
Relaxation loss, RET	0.0		0.0	
Shrinkage loss, SH	-0.1		-0.1	
Creep loss, CR	<u>-0.1</u>		<u>-0.2</u>	
Stage 4 losses		-0.2		-0.3
Relaxation loss, RET	-0.4		-0.2	
Shrinkage loss, SH	-1.4		-1.4	
Creep loss, CR	<u>-1.0</u>		<u>-2.4</u>	
Stage 5 losses		-2.8		-4.0
Δf_{se} due to loads		<u>-2.0</u>		<u>+0.6</u>
Total losses		<u>-14.6</u>		<u>-18.2</u>
Effective prestress, f_{se}		183.1		167.4

1 ksi = 6.894 MPa

Table C.5   Summary of prestress and losses for NSC beams

Item	Top P/S Reinforcement			Bottom P/S Reinf.		
	ksi	ksi	ksi	ksi	ksi	ksi
Prestress after anchorage			199.0			199.0
Stage 1 losses, ES			<u>-1.4</u>			<u>-14.8</u>
Initial prestress at transfer, f_{si}			197.6			184.2
Relaxation loss, RET	-3.5			-2.8		
Shrinkage loss, SH	-6.3			-6.3		
Creep loss, CR	<u>-3.9</u>			<u>-12.0</u>		
Stage 2 losses		-13.7			-21.1	
Relaxation loss, RET	0.0			0.0		
Shrinkage loss, SH	-0.1			-0.1		
Creep loss, CR	<u>-0.1</u>			<u>-0.2</u>		
Stage 3 losses		-0.2			-0.3	
Relaxation loss, RET	0.0			0.0		
Shrinkage loss, SH	0.0			-0.0		
Creep loss, CR	<u>0.0</u>			<u>-0.1</u>		
Stage 4 losses		0.0			-0.1	
Relaxation loss, RET	0.0			0.0		
Shrinkage loss, SH	-0.3			-0.3		
Creep loss, CR	<u>-0.1</u>			<u>-0.2</u>		
Stage 5 losses		-0.4			-0.5	
Δf_{se} due to loads		<u>-2.6</u>			<u>+0.7</u>	
Total Losses			<u>-16.9</u>			<u>-21.3</u>
Effective prestress, f_{se}			180.7			162.9

1 ksi = 6.894 MPa

APPENDIX D

MOMENT-CURVATURE ANALYSIS

Moment-curvature relationships were calculated for the composite section in accordance with the procedure presented by Lin and Burns.[13] The assumed stress-strain relationship for strand shown below is a modified form of an equation in the PCI Design Handbook.[21]

$$f_{ps} = E_{ps} \cdot \varepsilon_{ps} \qquad \text{for} \quad \varepsilon_{ps} \leq 0.0086$$

$$f_{ps} = f_{pu} - \left[\frac{0.048}{(\varepsilon_{ps} - 0.007)} \right] \qquad \text{for} \quad \varepsilon_{ps} > 0.0086$$

where E_{ps} = 28,000 ksi (193 GPa) and f_{pu} = 270 ksi (1860 MPa).
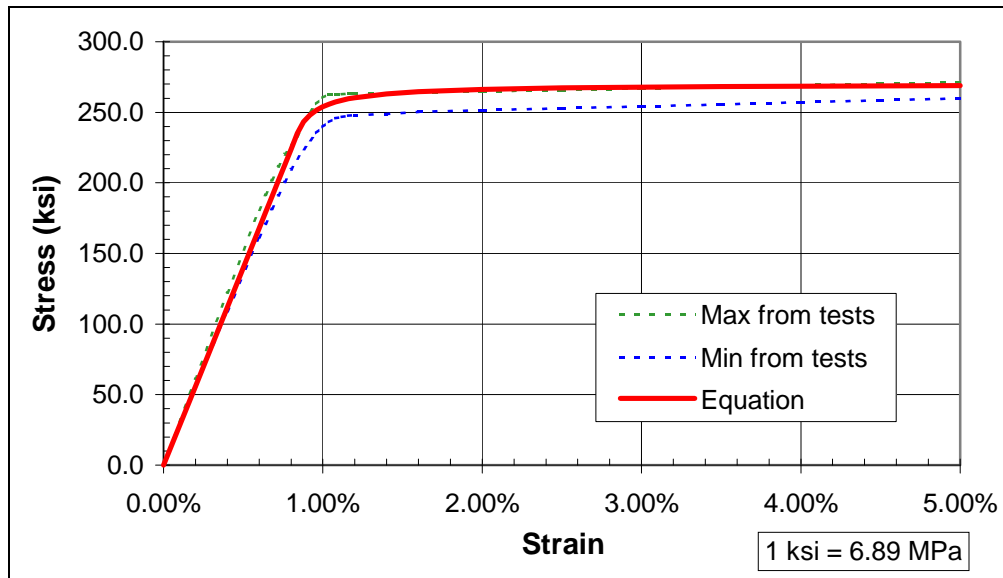
Figure D.1   Assumed prestressing steel stress-strain relationship

This modified equation appeared to be a good fit of the strand tensile test data as shown in Figure D.1. The initial prestress in the strand was based on the prestress losses calculated in Appendix C. The prestress in the strand was rounded off to the values shown in Table D.1.

A linear stress-strain relationship was used for the concrete prior to cracking. After cracking, the following concrete stress-strain relationship based on the Hognestad model was used.[13]

$$f_c = f_c' \cdot \left[\frac{2\varepsilon}{\varepsilon_o} - \left(\frac{\varepsilon}{\varepsilon_o} \right)^2 \right]$$

Table D.1　Effective prestress

HPC Beams		NSC Beams	
Top Strands	Bottom Strands	Top Strands	Bottom Strands
ksi (MPa)	ksi (MPa)	ksi (MPa)	ksi (MPa)
183.0 (1262)	167.0 (1151)	181.0 (1248)	163.0 (1124)

where ε is the concrete strain at any location and ε_o is the concrete strain when the concrete stress, f_c, is equal to the concrete compressive strength, f_c'. This assumed concrete stress-strain relationship is plotted in Figure D.2. The concrete compressive strengths and the moduli of elasticity are listed in Table D.2.

Figure D.2　Assumed concrete stress-strain relationship

Table D.2   Compressive strength and moduli of elasticity of the concrete

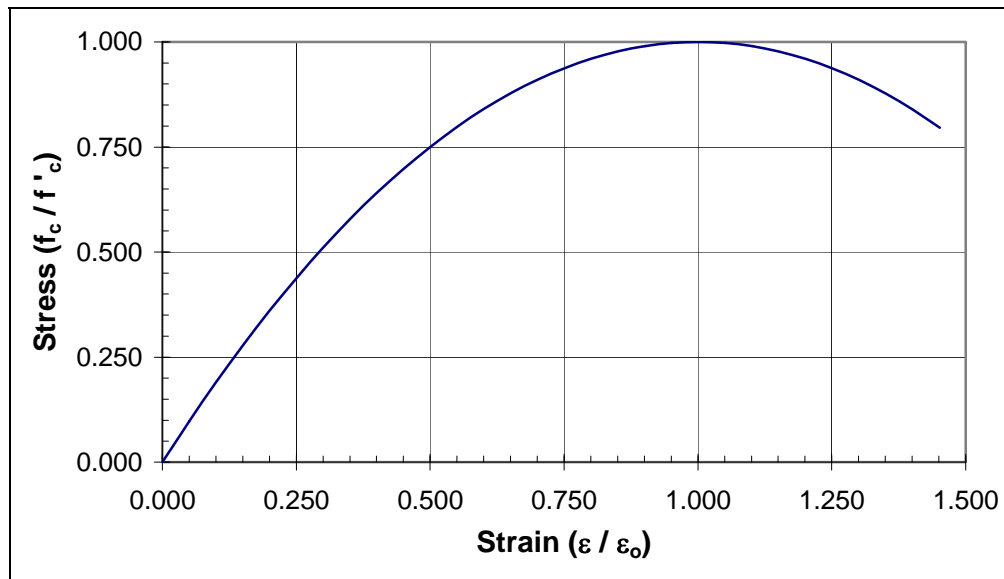| HPC Beams				NSC Beams			
Beams		Slabs		Beams		Slabs	
f_c'	E_c	f_c'	E_c	f_c'	E_c	f_c'	E_c
psi (MPa)	ksi (GPa)	psi (MPa)	ksi (GPa)	psi (MPa)	ksi (GPa)	psi (MPa)	ksi (GPa)
13,340 (92.0)	5,700 (39.3)	5,370 (37.0)	4,200 (29.0)	7,250 (50.0)	5,000 (34.4)	7,070 (48.7)	4,800 (33.1)

For a rectangular piece of the cross section where the stress and strain are zero along one horizontal boundary, the resultant compressive force, C_c, and the location of that force, $\overline{x}$, are given by the following expressions.[13]   The location of the resultant force is with respect to the boundary with zero strain.

$$C_c = b \cdot f_c' \cdot c \cdot \left[\frac{(3\varepsilon_0 \varepsilon - \varepsilon^2)}{3\varepsilon_0^2} \right]$$

$$\overline{x} = c \cdot \left[\frac{(8\varepsilon_0 - 3\varepsilon)}{(12\varepsilon_0 - 4\varepsilon)} \right]$$

where b is the width of the rectangular piece, c is the depth, and ε is the non-zero strain along the horizontal boundary.

Similarly, for a rectangular piece of the cross section with non-zero strains, ε_1 and ε_2, along the horizontal boundaries, the resultant compressive force and the location of that force are given by the following expressions.

$$C_c = b \cdot f_c' \cdot c \cdot \left[\frac{(3\varepsilon_2^2 \varepsilon_0 - \varepsilon_2^3 - 3\varepsilon_1^2 \varepsilon_0 + \varepsilon_1^3)}{3\varepsilon_0^2 \cdot (\varepsilon_2 - \varepsilon_1)} \right]$$

$$\overline{x} = \frac{c}{(\varepsilon_2 - \varepsilon_1)} \cdot \left[\frac{(8\varepsilon_2^3 \varepsilon_0 - 3\varepsilon_2^4 - 8\varepsilon_1^3 \varepsilon_0 + 3\varepsilon_1^4)}{(12\varepsilon_2^2 \varepsilon_0 - 4\varepsilon_2^3 - 12\varepsilon_1^2 \varepsilon_0 + 4\varepsilon_1^3)} - \varepsilon_1 \right]$$

Note, ε_1 is the lesser strain, $(\varepsilon_1 \leq \varepsilon_2)$. The resultant force is located with respect to the horizontal boundary that has the lesser strain, ε_1.

The non-prestressed reinforcement was assumed to have elastic-plastic behavior. The tensile yield strength was assumed to be 60.0 ksi (414 MPa) and the modulus of elasticity was assumed to be 29,000 ksi (200 GPa).

The beam section was idealized with uniform top and bottom flange thickness of 7.75 and 10.75 inches (197 and 273 mm), respectively. The other cross section dimensions are shown in Figure 3.1. The bottom corner chamfers were ignored. The net and transformed section properties are shown in Table D.3.

Some residual stresses existed from the self-weight of the beam. The stresses induced by the beam self-weight were calculated at midspan of the simple span member using the non-composite beam section properties. To get to the initial unloaded state for the beginning of the moment-curvature calculations, the self-weight of the beam must be subtracted. When the beam self-weight is subtracted, the composite section properties must be used. As a result, some residual stresses were locked in. The beams were shored prior to casting the slab concrete, so the weight of the slab did not induce any residual stresses.

The numerical results of the moment-curvature calculations are shown in Tables D.4 through D.7 for assumed moduli of rupture, f_r, of $7.5\sqrt{f_c'}$ and $10\sqrt{f_c'}$ where the units of f'_c are pounds per square inch. The assumption for the modulus of rupture only affects the moment-curvature relationship up to cracking. Moment-curvature diagrams are shown in Figures D.3 and D.4 for a modulus of rupture of $7.5\sqrt{f_c'}$. The diagrams for a

Table D.3   Section properties for moment-curvature calculations

Item	HPC Beams			NSC Beams		
	A in^2	y_b in.	I in^4	A in^2	y_b in.	I in^4
Net Section:						
Beam only	494	17.18	83,400	494	17.20	83,600
Composite section	902	29.20	242,900	1024	30.93	266,100
Transformed Section:						
Beam only	515	16.87	88,600	518	16.84	89,500
Composite section	923	28.75	254,900	1049	30.44	281,500

1 in. = 25.4 mm

modulus of rupture of $10\sqrt{f_c'}$ do not look significantly different.

The tables and diagrams mentioned above ignore slab shrinkage. Russell and Burns[17] found that slab shrinkage can significantly affect the cracking load, and hence, the cracking moment. To account for the effect of slab shrinkage on the moment-curvature relationship, a procedure similar to that discussed by Russell and Burns was used.

Beam cambers were measured from a time before shores were placed under the beam until some time before the load tests were conducted. The measured cambers are shown in Table D.8. The measured deflections from the maximum camber to the final camber are shown in Table D.8 and Figure D.5.

Cambers of beam HPC-1 were measured with a tensioned wire system. At one end of the beam, the wire was attached to an expansion anchor at the centroid of the beam cross section. At the other end, the wire passed over a roller. The wire was tensioned for all readings with the same mass, which weighed approximately 15 pounds (6.8 kg mass). The deflections were measured with a scale epoxied to the face of the beam at midspan. A mirror was attached to the scale to eliminate a potential parallax error. The readings from the tensioned wire system were accurate to the nearest 0.01 inch. To obtain greater accuracy, deflections for the remaining three beams were calculated from displacements measured with dial gauges at midspan and at the neoprene bearing pad supports.

Placement of the shores caused an upward deflection. The heat of hydration of the slab concrete also caused an upward deflection. Within a few hours, the upward deflection of beam HPC-1 from the heat of hydration exceeded the upward deflection from the installation of the shores. The shores were re-tightened. Shores for the remaining three beams were installed tighter than they had been for beam HPC-1, so re-tightening of the shores after placement of the concrete slab was unnecessary.

The upward load caused by the installation of the shores can be determined from the increase in camber when the shores were installed. The upward deflection due to the installation of the shores is shown in Table D.8 and Figure D.5. After the shores were
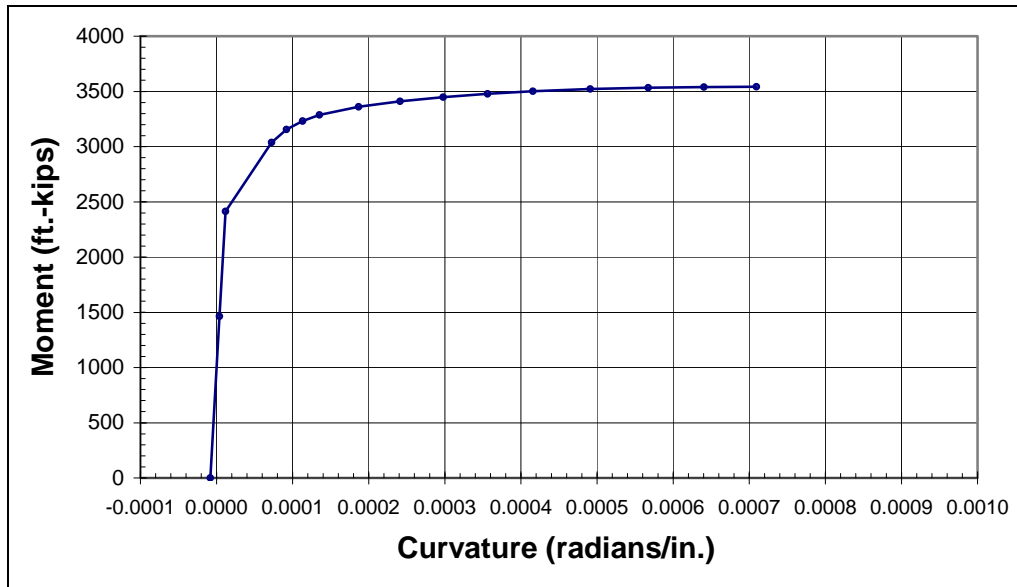
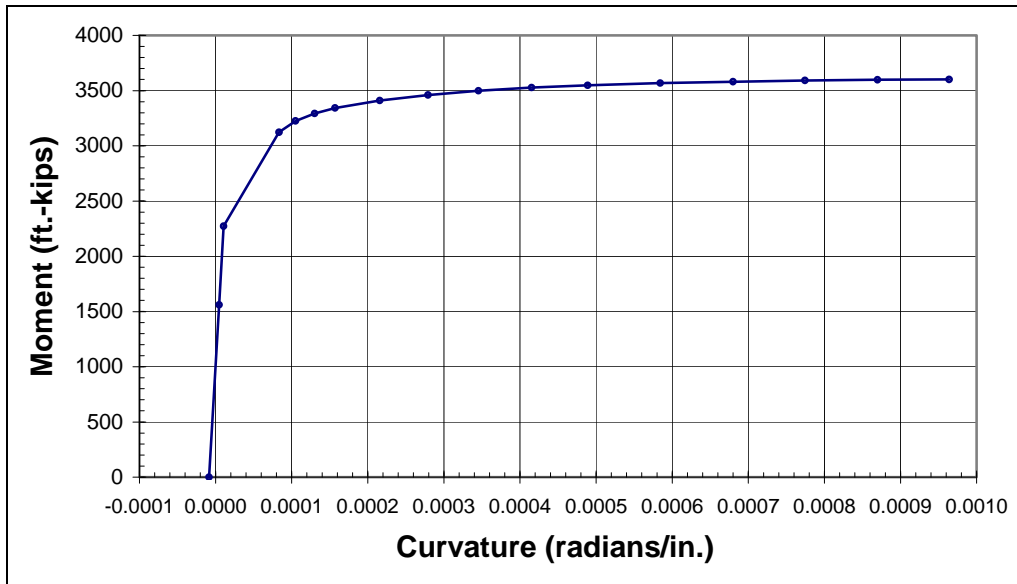*Figure D.3   Moment-curvature diagram for HPC beams*

Figure D.4   Moment-curvature diagram for NSC beams

Table D.4   Moment-curvature points for HPC beams for $f_r = 7.5\sqrt{f'_c}$

Strain at Top of Slab	Curvature	Moment	Strain of Bottom Strands	Stress in Bottom Strands	Strain of Top Strands	Stress in Top Strands	Depth of Compression Block
in./in.	rad./in.	kip-ft.	%	ksi	%	ksi	in.
-0.000027	-0.0000082	0	0.596%	167.0	0.654%	183.0	7.50[1]
0.000200	0.0000039	1463	0.628%	175.8	0.644%	180.2	47.50
0.000347	0.0000117	2412	0.648%	181.5	0.637%	178.4	34.54
0.000700	0.0000722	3038	0.884%	243.8	0.665%	186.3	10.50
0.000800	0.0000920	3155	0.962%	251.7	0.676%	189.3	9.33
0.000900	0.0001133	3232	1.047%	256.2	0.688%	192.8	7.50
0.001000	0.0001354	3286	1.137%	259.0	0.702%	196.5	7.03
0.001200	0.0001866	3361	1.345%	262.6	0.735%	205.9	6.21
0.001400	0.0002411	3411	1.569%	264.5	0.773%	216.4	5.65
0.001600	0.0002980	3449	1.804%	265.7	0.812%	227.5	5.25
0.001800	0.0003561	3479	2.044%	266.4	0.853%	239.0	4.96
0.002000	0.0004156	3501	2.290%	267.0	0.896%	245.5	4.74
0.002250	0.0004910	3521	2.603%	267.5	0.950%	250.8	4.52
0.002500	0.0005670	3533	2.918%	267.8	1.005%	254.3	4.36
0.002750	0.0006403	3540	3.221%	268.1	1.057%	256.5	4.25
0.003000	0.0007092	3543	3.504%	268.3	1.104%	258.1	4.19

Note: [1] The entire slab is in tension in the initial condition.

Table D.5   Moment-curvature points for HPC beams for $f_r = 10\sqrt{f'_c}$

Strain at Top of Slab	Curvature	Moment	Strain of Bottom Strands	Stress in Bottom Strands	Strain of Top Strands	Stress in Top Strands	Depth of Compression Block
in./in.	rad./in.	kip-ft.	%	ksi	%	ksi	in.
-0.000027	-0.0000082	0	0.596%	167.0	0.654%	183.0	7.50[1]
0.000200	0.0000039	1463	0.628%	175.8	0.644%	180.2	47.50
0.000380	0.0000135	2626	0.653%	182.8	0.636%	178.0	32.48
0.000700 to 0.003000	The values for this table are the same as those in the table above.						

Note: [1] The entire slab is in tension in the initial condition.

Table D.6   Moment-curvature points for NSC beams for $f_r = 7.5\sqrt{f_c'}$

Strain at Top of Slab	Curvature	Moment	Strain of Bottom Strands	Stress in Bottom Strands	Strain of Top Strands	Stress in Top Strands	Depth of Compression Block
in./in.	rad./in.	kip-ft.	%	ksi	%	ksi	in.
-0.000027	-0.0000086	0	0.582%	163.0	0.646%	181.0	7.50[1]
0.000200	0.0000048	1561	0.619%	173.3	0.638%	178.6	47.50
0.000304	0.0000108	2273	0.636%	178.0	0.634%	177.4	35.70
0.000700	0.0000834	3124	0.921%	248.3	0.670%	187.7	9.39
0.000800	0.0001052	3225	1.009%	254.4	0.683%	191.3	7.13
0.000900	0.0001302	3293	1.110%	258.3	0.699%	195.8	6.56
0.001000	0.0001572	3342	1.221%	260.8	0.718%	201.0	6.09
0.001200	0.0002158	3412	1.464%	263.7	0.759%	212.6	5.39
0.001400	0.0002791	3461	1.727%	265.3	0.806%	225.6	4.89
0.001600	0.0003454	3499	2.003%	266.3	0.855%	239.5	4.54
0.001800	0.0004152	3529	2.296%	267.0	0.909%	247.0	4.26
0.002000	0.0004889	3549	2.606%	267.5	0.966%	252.0	4.03
0.002250	0.0005842	3568	3.007%	267.9	1.041%	255.9	3.81
0.002500	0.0006799	3582	3.410%	268.2	1.117%	258.5	3.64
0.002750	0.0007744	3592	3.808%	268.5	1.191%	260.2	3.52
0.003000	0.0008697	3599	4.210%	268.6	1.266%	261.5	3.42
0.003250	0.0009640	3601	4.607%	268.8	1.340%	262.5	3.35

Note: [1] The entire slab is in tension in the initial condition.

Table D.7   Moment-curvature points for NSC beams for $f_r = 10\sqrt{f_c'}$

Strain at Top of Slab	Curvature	Moment	Strain of Bottom Strands	Stress in Bottom Strands	Strain of Top Strands	Stress in Top Strands	Depth of Compression Block
in./in.	rad./in.	kip-ft.	%	ksi	%	ksi	in.
-0.000027	-0.0000086	0	0.582%	163.0	0.646%	181.0	7.50[1]
0.000200	0.0000048	1561	0.619%	173.3	0.638%	178.6	47.50
0.000327	0.0000122	2437	0.640%	179.1	0.633%	177.2	33.57
0.000700 to 0.003250	The values for this table are the same as those in the table above.						

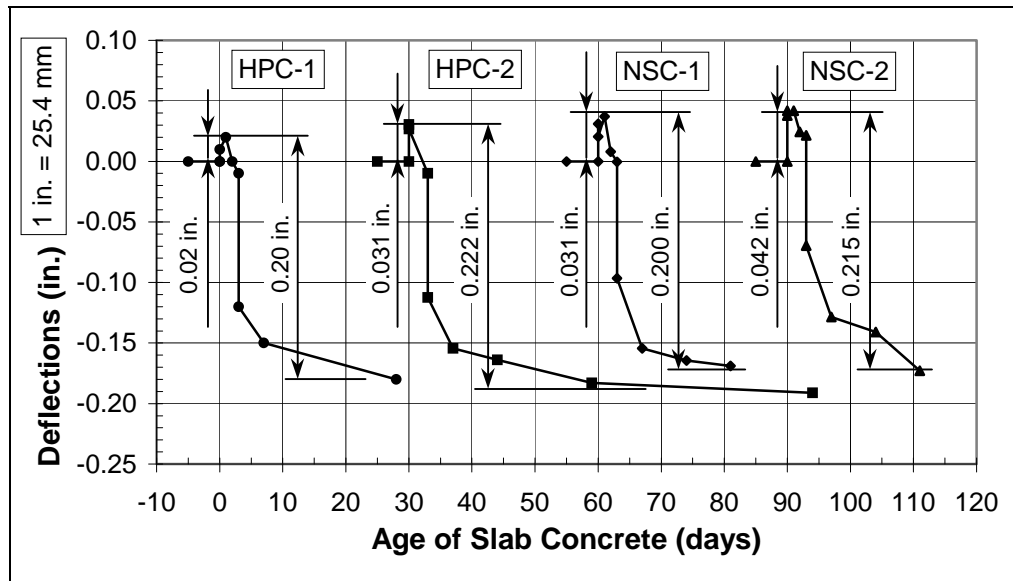Note: [1] The entire slab is in tension in the initial condition.

Figure D.5   Beam deflection data for calculation of slab shrinkage effects

installed, the decrease in camber was due to time-dependent effects. Time-dependent effects include relaxation of the prestressing strand, concrete creep, and concrete shrinkage. The effects of relaxation, creep and beam shrinkage were included in the prestress loss calculations, but slab shrinkage was not. Since relaxation, creep and beam shrinkage were included in the prestress losses, their effect on camber had to be subtracted from the measured deflections to get the net deflection due to slab shrinkage.

When the shores were removed, there was an instantaneous deflection that included the effects of the shoring force induced by their installation, the weight of the slab, and an additional force that had accumulated in the shores. The additional force was from the restraint of the shores against downward deflections caused by slab shrinkage and other time-dependent effects.

Table D.8 shows the calculated deflections that were predicted for the forces mentioned above when the shores were removed. The initial upward shoring force became a downward load on the composite section when the shores were removed. The calculated deflection for the weight of the slab assumed the shores supported the entire load and the beams supported none of it. The shores were short, 4 inch (100 mm) nominal, square wood posts spaced at 5 feet (1.5 m) center-to-center. They were

107

assumed to be much stiffer than the simply supported non-composite beam. A deflection was also calculated for the prestress losses that occurred over the period of time for which the cambers were measured. The prestress losses over that time period caused minor beam deflection (sag). The prestress losses (Table D.9) were calculated using the PCI General (Time-Step) Method[16] that was used to calculate the total losses in Appendix C.

The measured deflection (i.e., the change in camber) was reduced by the

Table D.8   Measured and calculated deflections prior to development length load tests

Item	Units	HPC-1	HPC-2	NSC-1	NSC-2
Measurements:					
Camber before installation of shores	in.	0.43	0.390	0.410	0.420
Max. camber after shore installation/slab cast	in.	0.45	0.421	0.441	0.462
Camber just before removal of shores	in.	0.42	0.380	0.410	0.442
Camber just after removal of shores	in.	0.31	0.278	0.314	0.350
Final measured camber	in.	0.25	0.199	0.241	0.247
Upward deflection due to installation of shores	in.	0.02	0.031	0.031	0.042
Upward load on beam from shoring	k/ft	0.066	0.101	0.078	0.106
Load from slab on composite section	k/ft	0.563	0.563	0.563	0.563
SUM of loads	k/ft	0.629	0.664	0.641	0.669
Calculated deflection upon removal of shores:					
from initial shoring load	in.	0.01	0.011	0.010	0.013
from weight of slab	in.	0.06	0.059	0.071	0.071
from accumulated prestress losses	in.	0.01	0.012	0.002	0.002
SUM (due to shore removal and P/S losses)	in.	0.08	0.082	0.083	0.086
Measured deflect from max camber to final camber	in.	0.20	0.222	0.200	0.215
Calc'd deflect. due to shore removal and P/S loss	in.	-0.08	-0.082	-0.083	-0.086
Net deflection due to slab shrinkage	in.	0.12	0.140	0.117	0.129
Age of slab concrete at final camber measurement	days	28	64	21	21
Average age of slab concrete during load tests	days	85	96	35	28

1 in. = 25.4 mm   1 ft. = 0.3048 m   1 kip = 4.448 kN

108

predicted deflections discussed above to obtain the net deflection due to slab shrinkage shown at the bottom of Table D.8. The time period over which the cambers were measured is also shown at the bottom of the table. For beam HPC-1, cambers were measured for only the first 28 of 85 days that passed until the load

tests were conducted. For beam HPC-2, cambers were measured for the first 64 of 96 days, that is, about two thirds of the time. The net deflection due to shrinkage was taken as 0.14 inch (3.6 mm) for both HPC beams. Similarly, the net deflection for the NSC beams was taken as 0.13 inch (3.3 mm).

The net deflections were substituted into the following equation[17] to obtain the curvature due to slab shrinkage, ϕ_{sh}.

$$\Delta_{sh} = \frac{\phi_{sh} \cdot L^2}{8} \quad \Rightarrow \quad \phi_{sh} = \frac{8 \cdot \Delta_{sh}}{L^2}$$

where L is the span length and Δ_{sh} is the deflection due to shrinkage.

The equivalent force in the slab due to shrinkage, F_{sh}, is calculated from the following equation.[17]

$$\phi_{sh} = \frac{F_{sh} \cdot e_{sl}}{(E \cdot I)_{comp}} \quad \Rightarrow \quad F_{sh} = \frac{\phi_{sh} \cdot (E \cdot I)_{comp}}{e_{sl}}$$

where e_{sl} is the eccentricity of the slab shrinkage, that is, the distance from the center of the slab to the centroid of the composite section. The equivalent shrinkage force, F_{sh}, is used to calculate the strains in the concrete. The stresses are calculated using the appropriate modulus of elasticity, E_c, of the beam or slab. Russell and Burns[17] provide a more complete explanation of the procedure.

The stresses from the slab shrinkage must be added to the stresses from the prestress and the residual stresses from the self-weight of the beam discussed previously to obtain the initial unloaded state for the beginning of the moment-curvature calculations. The slab shrinkage effects were not included in the prestress loss

Table D.10   Effective prestress including slab shrinkage effects

HPC Beams		NSC Beams	
Top Strands ksi (MPa)	Bottom Strands ksi (MPa)	Top Strands ksi (MPa)	Bottom Strands ksi (MPa)
181.1 (1249)	167.5 (1155)	179.6 (1238)	163.4 (1127)

calculations in Appendix C. Including the slab shrinkage effects in the losses yields the prestress values shown in Table D.10.

The upward deflection caused by the installation of the shores was included with the slab shrinkage effects. The shoring uplifted the beam while it was non-composite by 0.02 to 0.042 inch (0.5 to 1.07 mm) as shown in Table D.8 and Figure D.5. When the shoring was removed the section was composite. In the calculations, the uplift due to shoring was taken as 0.03 and 0.04 inch (0.8 and 1.0 mm) for the HPC and NSC beams, respectively. The effect of the installation of the shores was not significant. The discussion of Chapter 4 stated that slab shrinkage decreased the calculated cracking moment, $M_{cr,calc}$, by 3% to 5%. If the upward deflection from the installation of the shores had not been included, the calculated cracking moments would have decreased by 4% to 6%. The conclusions regarding the slab shrinkage effects in this study would be unchanged.

The numerical results of the moment-curvature calculations including the effects of slab shrinkage (and the uplift from the installation of the shores) are shown in Tables D.11 through D.14.

Table D.11   Moment-curvature points for HPC beams for $f_r = 7.5\sqrt{f_c'}$ with slab shrinkage

Strain at Top of Slab	Curvature	Moment	Strain of Bottom Strands	Stress in Bottom Strands	Strain of Top Strands	Stress in Top Strands	Depth of Compression Block
in./in.	rad./in.	kip-ft.	%	ksi	%	ksi	in.
-0.000039	-0.0000057	0	0.598%	167.5	0.647%	181.1	7.50[1]
0.000200	0.0000070	1541	0.631%	176.8	0.636%	178.2	47.50
0.000318	0.0000133	2304	0.648%	181.4	0.631%	176.7	36.09
0.000700	0.0000752	3034	0.887%	244.3	0.658%	184.3	11.47
0.000800	0.0000944	3150	0.963%	251.7	0.668%	187.1	10.19
0.000900	0.0001152	3227	1.045%	256.1	0.680%	190.4	7.34
0.001000	0.0001368	3283	1.132%	258.9	0.693%	194.0	6.93
0.001200	0.0001881	3359	1.342%	262.5	0.727%	203.4	6.14
0.001400	0.0002430	3409	1.568%	264.5	0.764%	214.0	5.59
0.001600	0.0003004	3447	1.804%	265.7	0.804%	225.2	5.20
0.001800	0.0003589	3477	2.046%	266.4	0.846%	236.8	4.91
0.002000	0.0004186	3499	2.293%	267.0	0.889%	244.5	4.69
0.002250	0.0004937	3520	2.604%	267.5	0.942%	250.2	4.49
0.002500	0.0005702	3532	2.922%	267.8	0.998%	253.9	4.33
0.002750	0.0006438	3539	3.226%	268.1	1.050%	256.3	4.22
0.003000	0.0007130	3543	3.511%	268.3	1.098%	257.9	4.16

Note: [1] The entire slab is in tension in the initial condition.

Table D.12   Moment-curvature points for HPC beams for $f_r = 10\sqrt{f_c'}$ with slab shrinkage

Strain at Top of Slab	Curvature	Moment	Strain of Bottom Strands	Stress in Bottom Strands	Strain of Top Strands	Stress in Top Strands	Depth of Compression Block
in./in.	rad./in.	kip-ft.	%	ksi	%	ksi	in.
-0.000039	-0.0000057	0	0.598%	167.5	0.647%	181.1	7.50[1]
0.000200	0.0000070	1541	0.631%	176.8	0.636%	178.2	47.50
0.000351	0.0000151	2517	0.652%	182.7	0.630%	176.3	34.07
0.000700 to 0.003000	The values for this table are the same as those in the table above.						

Note: [1] The entire slab is in tension in the initial condition.

Table D.13   Moment-curvature points for NSC beams for $f_r = 7.5\sqrt{f_c'}$ with slab shrinkage

Strain at Top of Slab	Curvature	Moment	Strain of Bottom Strands	Stress in Bottom Strands	Strain of Top Strands	Stress in Top Strands	Depth of Compression Block
in./in.	rad./in.	kip-ft.	%	ksi	%	ksi	in.
-0.000032	-0.0000066	0	0.584%	163.4	0.641%	179.6	7.50[1]
0.000200	0.0000069	1592	0.621%	173.9	0.632%	177.1	47.50
0.000288	0.0000121	2198	0.635%	177.9	0.629%	176.1	36.95
0.000700	0.0000846	3118	0.919%	248.0	0.664%	185.9	10.16
0.000800	0.0001060	3220	1.004%	254.2	0.676%	189.4	7.03
0.000900	0.0001308	3290	1.106%	258.2	0.692%	193.9	6.49
0.001000	0.0001578	3340	1.216%	260.7	0.711%	199.0	6.04
0.001200	0.0002169	3409	1.460%	263.7	0.753%	210.8	5.34
0.001400	0.0002805	3459	1.726%	265.3	0.800%	223.9	4.85
0.001600	0.0003472	3497	2.004%	266.3	0.850%	237.9	4.51
0.001800	0.0004171	3527	2.297%	267.0	0.903%	246.4	4.24
0.002000	0.0004908	3548	2.607%	267.5	0.960%	251.6	4.01
0.002250	0.0005865	3567	3.010%	267.9	1.036%	255.7	3.79
0.002500	0.0006826	3581	3.415%	268.2	1.112%	258.3	3.62
0.002750	0.0007773	3592	3.814%	268.5	1.186%	260.1	3.50
0.003000	0.0008712	3599	4.209%	268.6	1.260%	261.4	3.41
0.003250	0.0009658	3601	4.607%	268.8	1.334%	262.4	3.34

Note: [1] The entire slab is in tension in the initial condition.

Table D.14   Moment-curvature points for NSC beams for $f_r = 10\sqrt{f_c'}$ with slab shrinkage

Strain at Top of Slab	Curvature	Moment	Strain of Bottom Strands	Stress in Bottom Strands	Strain of Top Strands	Stress in Top Strands	Depth of Compression Block
in./in.	rad./in.	kip-ft.	%	ksi	%	ksi	in.
-0.000032	-0.0000066	0	0.584%	163.4	0.641%	179.6	7.50[1]
0.000200	0.0000069	1592	0.621%	173.9	0.632%	177.1	47.50
0.000312	0.0000135	2362	0.639%	179.0	0.628%	175.9	34.89
0.000700 to 0.003250	The values for this table are the same as those in the table above.						

Note: [1] The entire slab is in tension in the initial condition.

APPENDIX E

TRANSFER LENGTH MEASUREMENTS

Figure E.1   Concrete strain profile for beam end H1S

Figure E.2   Concrete strain profile for beam end H1N
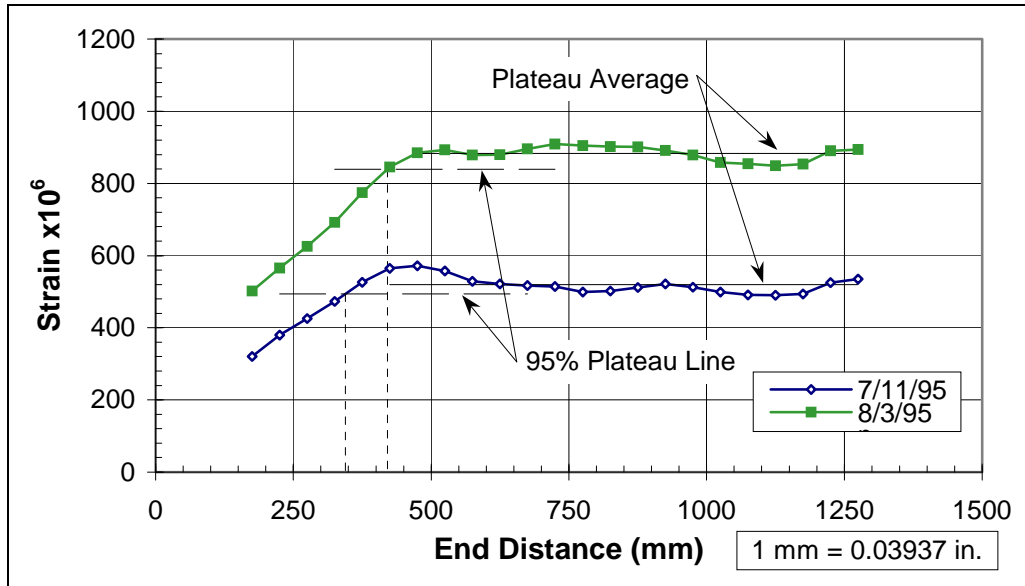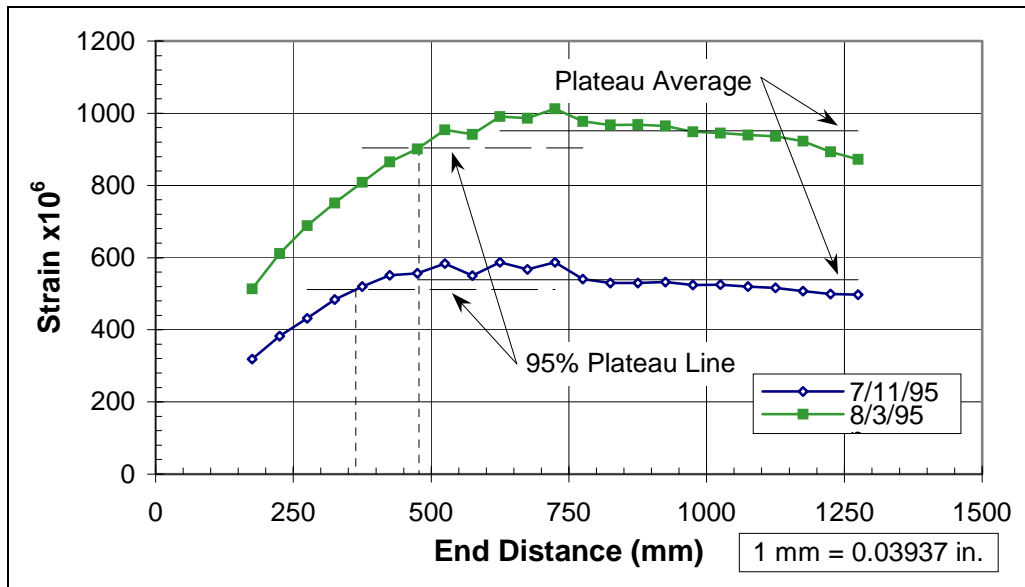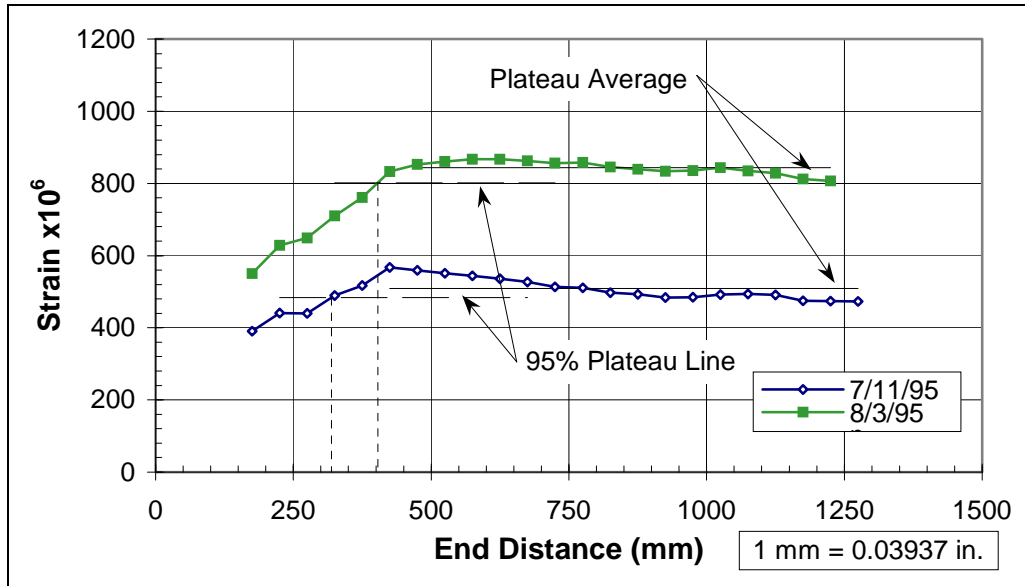
114

Figure E.3   Concrete strain profile for beam end H2S
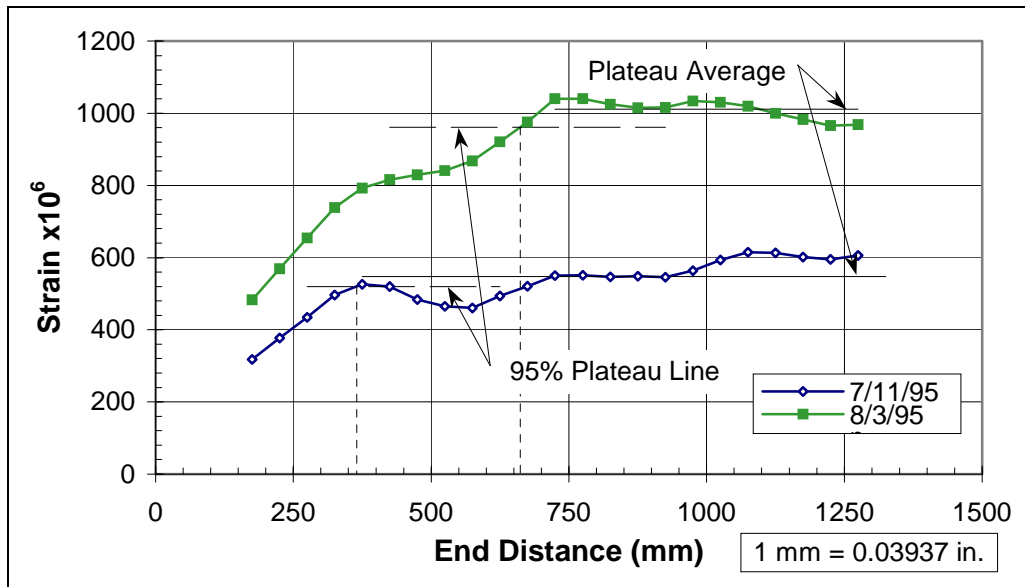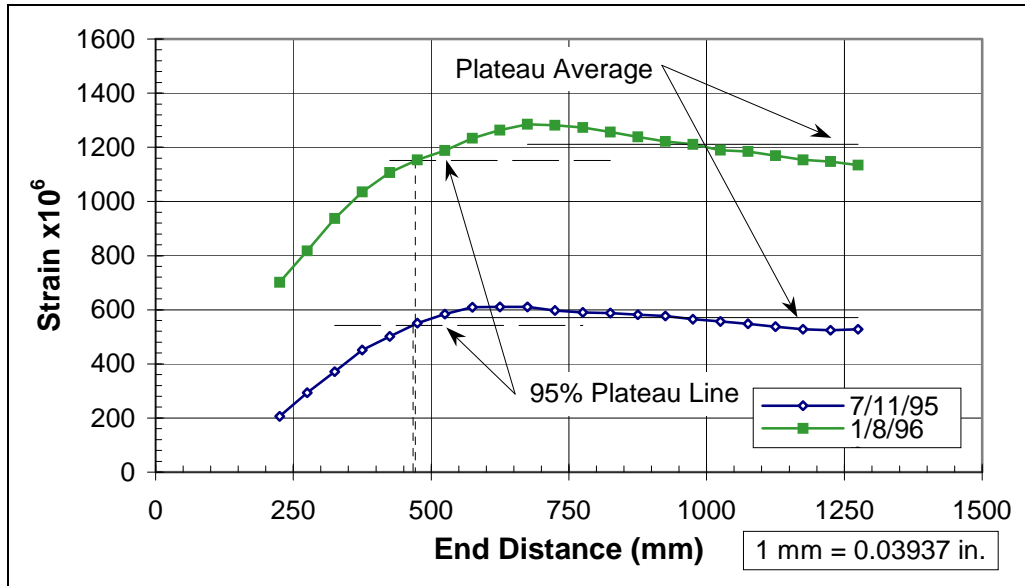

Figure E.4   Concrete strain profile for beam end H2N

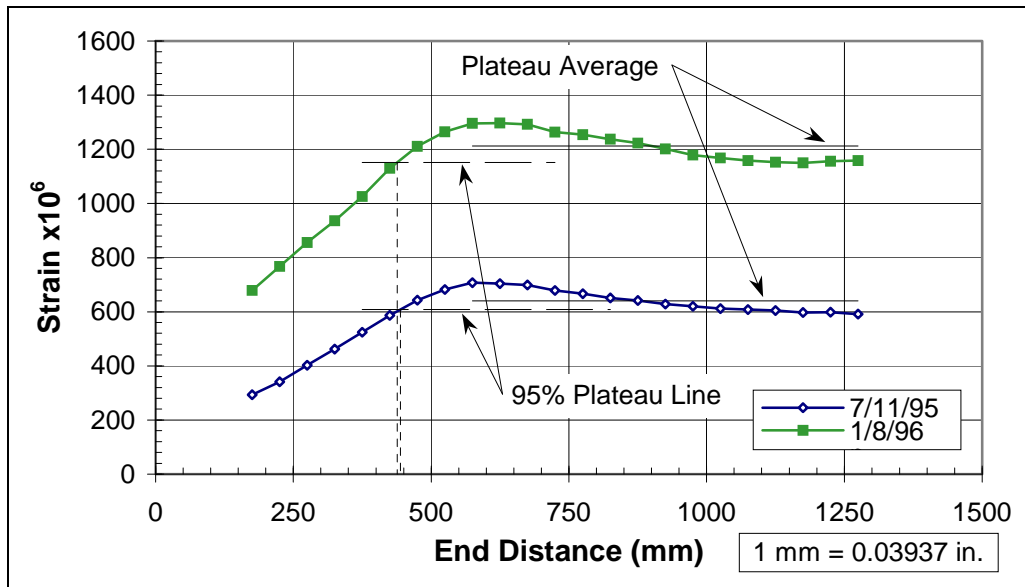*Figure E.5   Concrete strain profile for beam end N1S*

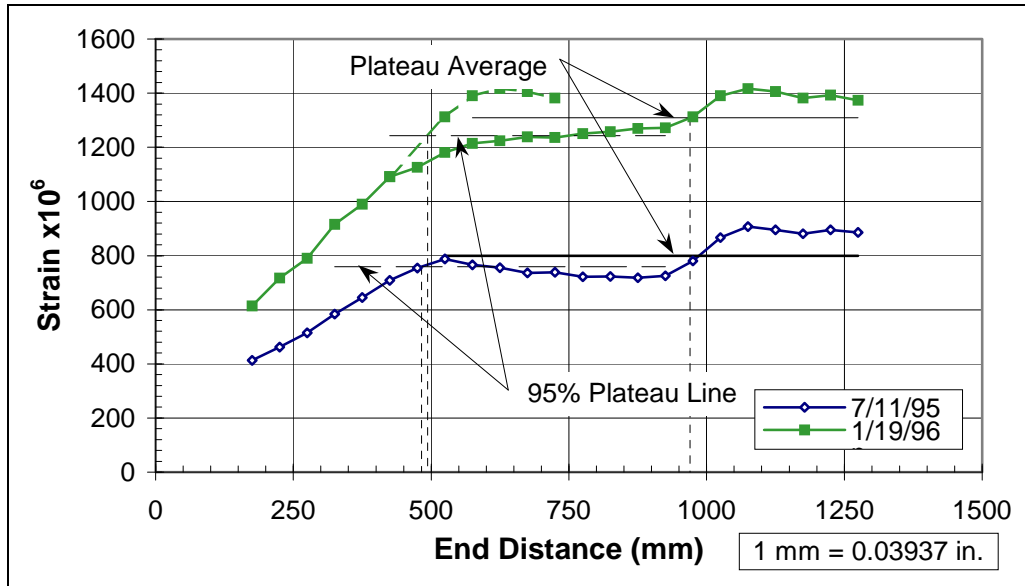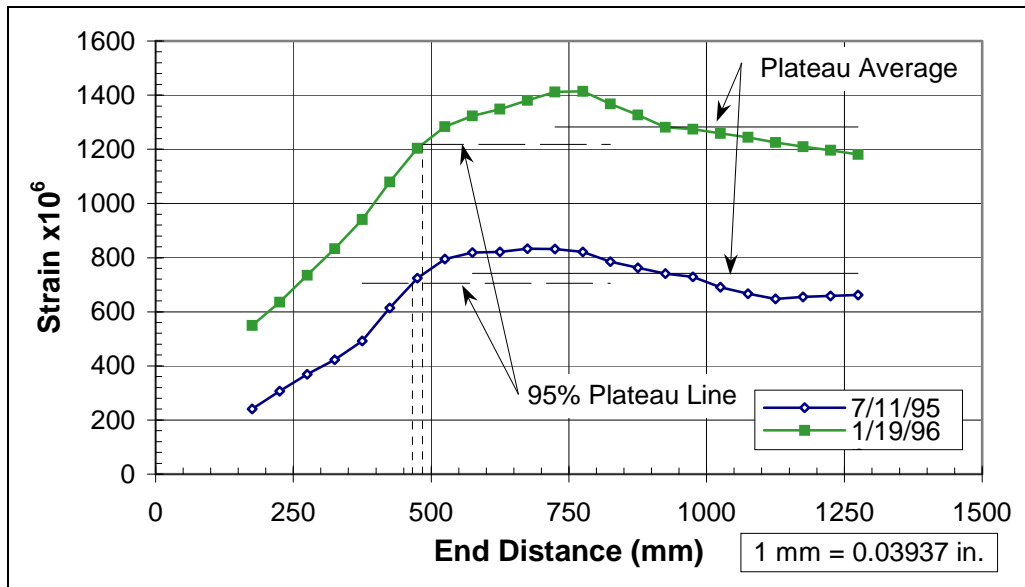*Figure E.6   Concrete strain profile for beam end N1N*

116

Figure E.7   Concrete strain profile for beam end N2S

Figure E.8   Concrete strain profile for beam end N2N

117

Table E.1   Concrete strains at level of bottom strands for beam end H1S

End	Measured Strain				Average		Smoothed	
Distance	East Face		West Face		Strain		Average Strain	
	7/11/95	8/3/95	7/11/95	8/3/95	7/11/95	8/3/95	7/11/95	8/3/95
mm	με	με	με	με	με	με	με	με
125	236	356	264	492	250	424		
175	308	412	340	584	324	498	321	502
225	380	508	396	660	388	584	380	565
275	404	536	452	692	428	614	425	625
325	416	556	504	800	460	678	473	692
375	540	724	524	844	532	784	526	775
425	624	820	548	904	586	862	565	845
475	600	844	552	936	576	890	572	885
525	580	876	528	932	554	904	557	893
575	560	868	524	904	542	886	529	879
625	476	796	504	896	490	846	521	880
675	552	916	512	900	532	908	517	895
725	544	956	512	908	528	932	515	909
775	464	872	504	904	484	888	499	905
825	464	868	508	920	486	894	502	902
875	564	940	508	908	536	924	512	901
925	524	872	504	900	514	886	521	891
975	520	832	508	896	514	864	513	879
1025	524	904	496	868	510	886	499	858
1075	456	792	488	856	472	824	491	855
1125	472	828	512	880	492	854	490	849
1175	520	880	492	856	506	868	493	853
1225	484	844	480	832	482	838	525	890
1275	652	1036	520	892	586	964	535	894
1325	584	944	488	816	536	880		

Table E.2   Concrete strains at level of bottom strands for beam end H1N

End Distance	Measured Strain				Average Strain		Smoothed Average Strain	
	East Face		West Face					
	7/11/95	8/3/95	7/11/95	8/3/95	7/11/95	8/3/95	7/11/95	8/3/95
mm	με	με	με	με	με	με	με	με
125	256	308	244	492	250	400		
175	360	--- [1]	296	568	328	515	319	513
225	396	616	360	632	378	624	383	611
275	460	--- [1]	424	724	442	694	431	689
325	480	712	468	784	474	748	483	752
375	560	--- [1]	508	848	534	813	520	809
425	588	844	516	888	552	866	551	866
475	588	888	548	948	568	918	557	901
525	568	872	532	968	550	920	583	954
575	732	1064	532	984	632	1024	550	941
625	388	728	548	1032	468	880	587	991
675	812	1128	508	1008	660	1068	567	987
725	644	1000	504	1024	574	1012	587	1012
775	548	880	504	1032	526	956	540	977
825	556	924	484	1004	520	964	529	967
875	572	936	512	1028	542	982	529	969
925	556	920	496	1000	526	960	533	965
975	540	892	520	1012	530	952	524	949
1025	516	864	516	1004	516	934	525	945
1075	556	908	504	988	530	948	520	939
1125	524	864	504	1008	514	936	516	936
1175	540	876	468	972	504	924	507	923
1225	524	844	484	972	504	908	499	893
1275	520	836	456	856	488	846	497	872
1325	524	848	476	876	500	862		

Note: [1] No data were recorded for these strands, because the DEMEC point was damaged. To calculate the average strain and the smoothed average strain, a value for the measured strain was interpolated from preceding and succeeding values.

Table E.3   Concrete strains at level of bottom strands for beam end H2S

End Distance	Measured Strain				Average Strain		Smoothed Average Strain	
	East Face		West Face					
	7/11/95	8/3/95	7/11/95	8/3/95	7/11/95	8/3/95	7/11/95	8/3/95
mm	με	με	με	με	με	με	με	με
125	280	316	392	604	336	460		
175	372	420	440	704	406	562	390	550
225	416	484	440	--- [1]	428	628	441	628
275	472	548	504	840	488	694	440	649
325	212	328	596	924	404	626	489	710
375	536	684	616	936	576	810	517	761
425	548	740	592	956	570	848	567	833
475	540	728	572	952	556	840	559	853
525	548	776	556	964	552	870	551	861
575	524	772	568	972	546	872	544	867
625	524	768	544	952	534	860	536	867
675	504	768	552	968	528	868	527	863
725	512	772	524	948	518	860	513	857
775	492	756	496	928	494	842	511	858
825	516	788	524	956	520	872	497	845
875	476	756	480	888	478	822	493	839
925	476	752	484	896	480	824	483	834
975	476	--- [1]	508	956	492	855	485	835
1025	480	--- [1]	484	900	482	827	492	843
1075	504	756	500	940	502	848	494	834
1125	472	724	524	932	498	828	491	829
1175	468	--- [1]	476	892	472	810	475	813
1225	440	--- [1]	468	868	454	800	474	807
1275	516	736	476	884	496	810	473	
1325	480	--- [1]	460	844	470			

Note: [1] No data were recorded for these strands, because the DEMEC point was damaged. To calculate the average strain and the smoothed average strain, a value for the measured strain was interpolated from preceding and succeeding values.

Table E.4   Concrete strains at level of bottom strands for beam end H2N

End Distance	Measured Strain				Average Strain		Smoothed Average Strain	
	East Face		West Face					
	7/11/95	8/3/95	7/11/95	8/3/95	7/11/95	8/3/95	7/11/95	8/3/95
mm	με	με	με	με	με	με	με	με
125	248	308	276	496	262	402		
175	324	400	304	544	314	472	318	483
225	372	484	384	664	378	574	377	569
275	416	548	460	772	438	660	435	655
325	464	636	512	824	488	730	496	739
375	532	696	592	956	562	826	526	793
425	536	736	520	908	528	822	520	816
475	588	696	352	904	470	800	484	829
525	532	792	376	940	454	866	465	841
575	584	788	356	924	470	856	461	868
625	556	828	360	936	458	882	494	921
675	680	1104	428	944	554	1024	521	975
725	664	1096	436	944	550	1020	550	1040
775	680	1088	412	1064	546	1076	551	1041
825	728	1052	388	1000	558	1026	547	1025
875	728	1016	344	932	536	974	548	1015
925	764	1176	336	912	550	1044	545	1016
975	772	1176	328	884	550	1030	563	1034
1025	792	1148	388	908	590	1028	593	1030
1075	820	1092	460	972	640	1032	615	1019
1125	736	1008	492	988	614	998	613	1000
1175	688	952	480	988	584	970	601	983
1225	748	996	464	964	606	980	595	966
1275	680	940	508	956	594	948	606	969
1325	704	972	532	984	618	978		

Table E.5   Concrete strains at level of bottom strands for beam end N1S

End Distance	Measured Strain				Average Strain		Smoothed Average Strain	
	East Face		West Face					
	7/11/95	1/8/96	7/11/95	1/8/96	7/11/95	1/8/96	7/11/95	1/8/96
mm	με	με	με	με	με	με	με	με
125	--- [1]	--- [1]	212	504				
175	32	532	260	664	146	598		
225	84	580	340	--- [1]	212	681	206	702
275	144	752	376	900	260	826	293	818
325	256	876	556	1016	406	946	371	937
375	352	1012	540	1064	446	1038	451	1035
425	400	1076	604	1164	502	1120	502	1107
475	480	1128	636	1200	558	1164	550	1154
525	508	1144	672	1212	590	1178	584	1188
575	524	1168	684	1276	604	1222	609	1234
625	576	1304	688	1300	632	1302	611	1263
675	520	1208	672	1324	596	1266	611	1285
725	540	1232	668	1344	604	1288	597	1281
775	524	1248	660	1332	592	1290	590	1273
825	512	1228	636	1256	574	1242	587	1257
875	548	1252	644	1224	596	1238	582	1239
925	512	1220	640	1252	576	1236	577	1221
975	508	1172	612	1208	560	1190	565	1211
1025	504	1184	616	1228	560	1206	556	1190
1075	496	1096	600	1252	548	1174	548	1185
1125	484	1168	588	1184	536	1176	537	1169
1175	472	1160	584	1156	528	1158	527	1153
1225	452	1084	584	1168	518	1126	524	1147
1275	472	1136	580	1180	526	1158	528	1135
1325	480	1112	600	1128	540	1120		

Note: [1] No data were recorded for these strands, because the DEMEC point was damaged. To calculate the average strain and the smoothed average strain, a value for the measured strain was interpolated from preceding and succeeding values.

Table E.6   Concrete strains at level of bottom strands for beam end N1N

End Distance	Measured Strain				Average Strain		Smoothed Average Strain	
	East Face		West Face					
	7/11/95	1/8/96	7/11/95	1/8/96	7/11/95	1/8/96	7/11/95	1/8/96
mm	με	με	με	με	με	με	με	με
125	308	724	200	480	254	602		
175	312	676	252	640	282	658	293	679
225	392	848	296	704	344	776	341	767
275	432	904	364	828	398	866	402	856
325	520	1012	408	840	464	926	461	935
375	560	1032	484	996	522	1014	525	1026
425	628	1188	548	1088	588	1138	587	1130
475	712	1244	588	1232	650	1238	643	1211
525	728	1264	652	1252	690	1258	682	1265
575	736	1312	676	--- [1]	706	1299	707	1296
625	792	1344	656	1320	724	1332	703	1297
675	720	1276	640	1244	680	1260	699	1292
725	736	1240	648	1328	692	1284	679	1264
775	688	1216	640	--- [1]	664	1247	667	1254
825	672	1232	616	1228	644	1230	651	1237
875	676	1212	612	1256	644	1234	641	1223
925	696	1244	576	1168	636	1206	629	1202
975	660	1172	552	1160	606	1166	620	1179
1025	644	1132	592	1196	618	1164	612	1168
1075	640	1160	584	1188	612	1174	608	1158
1125	616	1096	572	1176	594	1136	604	1152
1175	644	1124	568	1168	606	1146	597	1150
1225	648	1176	536	1160	592	1168	598	1156
1275	640	1156	552	1152	596	1154	591	1159
1325	628	1152	544	1156	586	1154		

Note: [1] No data were recorded for these strands, because the DEMEC point was damaged. To calculate the average strain and the smoothed average strain, a value for the measured strain was interpolated from preceding and succeeding values.

Table E.7   Concrete strains at level of bottom strands for beam end N2S

End Distance	Measured Strain				Average Strain		Smoothed Average Strain	
	East Face		West Face					
	7/11/95	1/19/96	7/11/95	1/19/96	7/11/95	1/19/96	7/11/95	1/19/96
mm	με	με	με	με	με	με	με	με
125	580	740	192	356	386	548		
175	568	684	256	488	412	586	413	613
225	624	812	256	600	440	706	462	717
275	656	976	412	740	534	858	514	789
325	688	836	448	772	568	804	584	916
375	800	1304	500	868	650	1086	645	989
425	856	1176	576	980	716	1078	708	1091
475	880	1220	636	1000	758	1110	754	1127
525	900	1248	676	1136	788	1192	788	1181
575	924	1292	712	1188	818	1240	766	1215
625	692	1216	692	1208	692	1212	755	1225
675	780	1204	732	1240	756	1222	736	1238
725	804	1276	716	1284	760	1280	738	1236
775	700	1172	696	1240	698	1206	722	1251
825	684	1196	732	1336	708	1266	723	1258
875	820	1312	708	1292	764	1302	718	1269
925	668	1224	696	1256	682	1240	725	1272
975	736	1220	720	1328	728	1274	780	1313
1025	1176	1628	684	1224	930	1426	866	1390
1075	1204	1680	676	1260	940	1470	907	1417
1125	1056	1500	648	1208	852	1354	895	1406
1175	1144	1612	644	1176	894	1394	881	1383
1225	1148	1608	648	1192	898	1400	895	1393
1275	1148	1604	640	1164	894	1384	886	1373
1325	1088	1532	644	1140	866	1336		

Table E.8   Concrete strains at level of bottom strands for beam end N2N

End Distance	Measured Strain				Average Strain		Smoothed Average Strain	
	East Face		West Face					
	7/11/95	1/19/96	7/11/95	1/19/96	7/11/95	1/19/96	7/11/95	1/19/96
mm	με	με	με	με	με	με	με	με
125	144	372	240	636	192	504		
175	112	364	288	616	200	490	240	549
225	312	644	344	664	328	654	306	636
275	380	728	400	800	390	764	368	735
325	320	676	452	896	386	786	423	833
375	456	896	528	1000	492	948	492	941
425	564	960	632	1216	598	1088	614	1079
475	808	1208	696	1196	752	1202	724	1204
525	876	1344	768	1300	822	1322	795	1285
575	868	1356	752	1304	810	1330	818	1324
625	880	1352	764	1288	822	1320	821	1349
675	896	1412	768	1380	832	1396	833	1381
725	920	1428	772	1428	846	1428	832	1413
775	868	1384	768	1444	818	1414	821	1414
825	840	1364	756	1436	798	1400	785	1368
875	744	1248	732	1332	738	1290	762	1327
925	788	1248	712	1332	750	1290	741	1282
975	744	1156	728	1376	736	1266	729	1275
1025	680	1172	724	1364	702	1268	691	1259
1075	552	1112	716	1372	634	1242	667	1245
1125	632	1116	696	1332	664	1224	647	1226
1175	628	1140	660	1284	644	1212	655	1210
1225	636	1100	676	1288	656	1194	658	1197
1275	652	1024	696	1344	674	1184	662	1181
1325	636	1056	676	1272	656	1164		
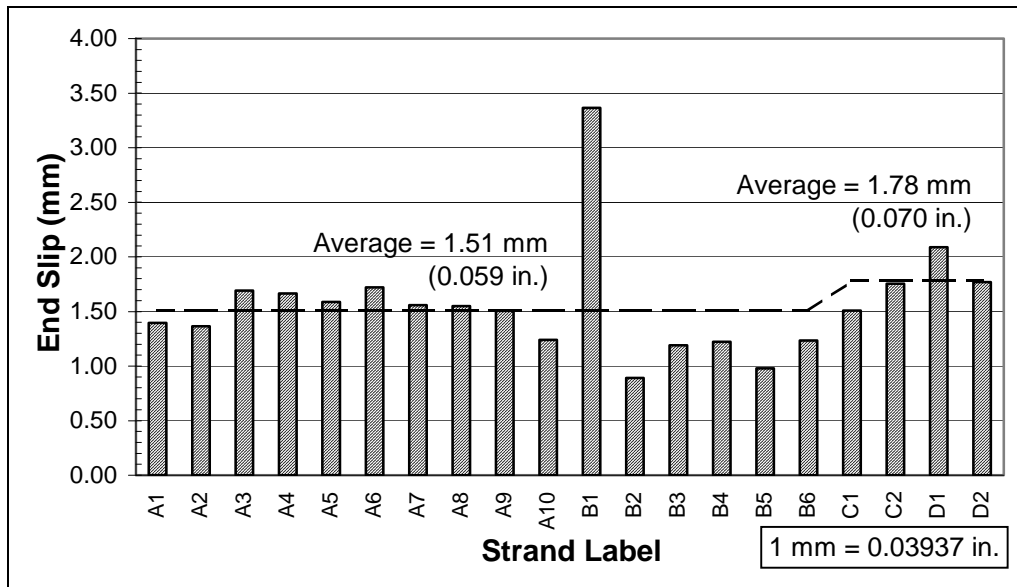
Figure E.9   Strand end slips at beam end H1S measured just after transfer
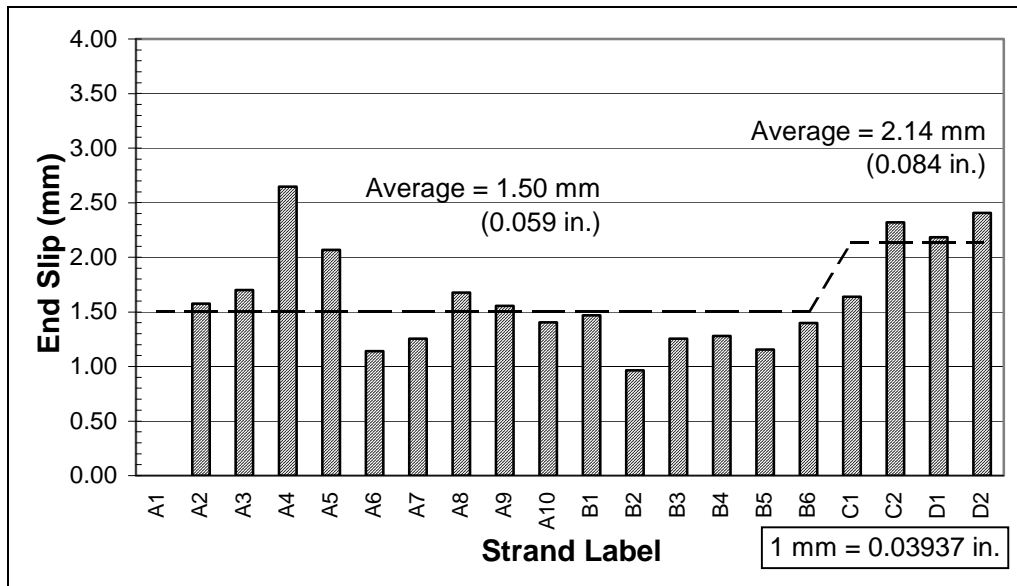
Figure E.10   Strand end slips at beam end H1N measured just after transfer

126
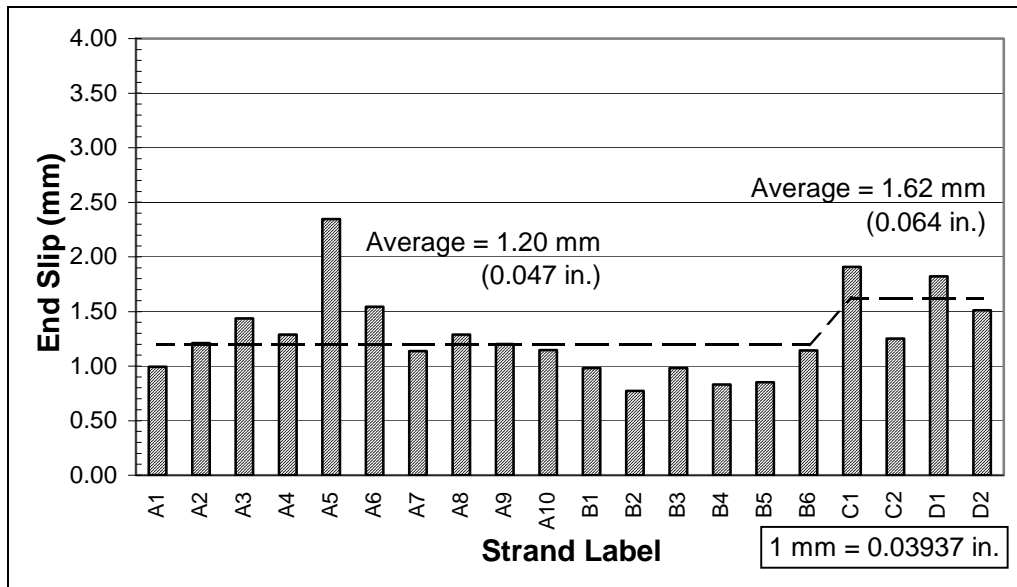
Figure E.11   Strand end slips at beam end H2S measured just after transfer
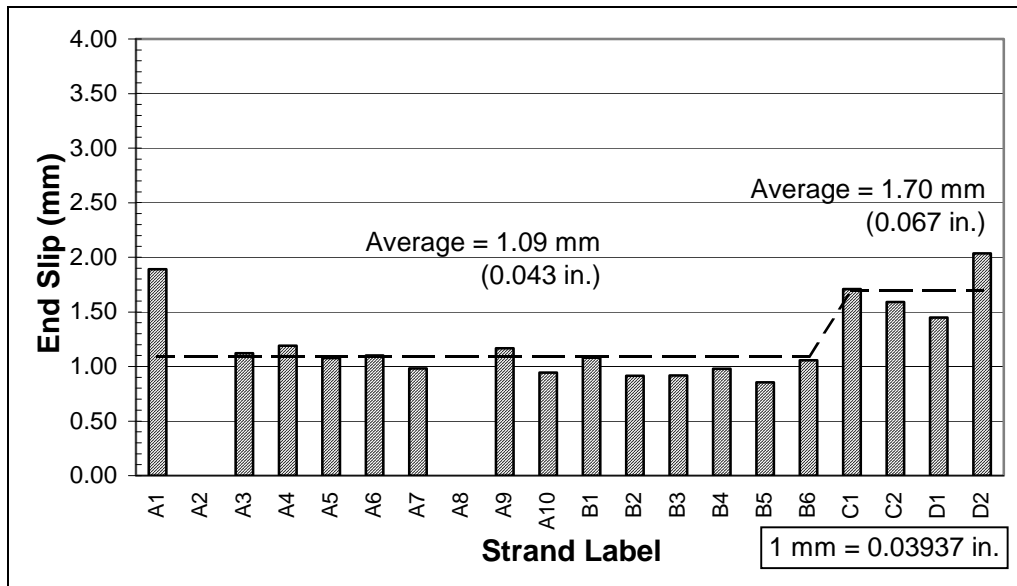
Figure E.12   Strand end slips at beam end H2N measured just after transfer

127
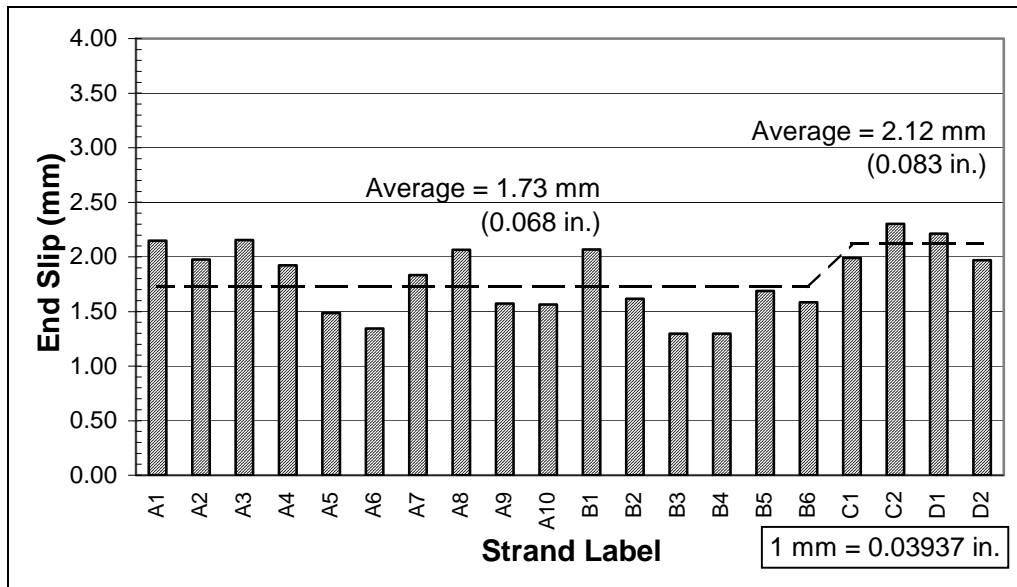
Figure E.13   Strand end slips at beam end N1S measured just after transfer
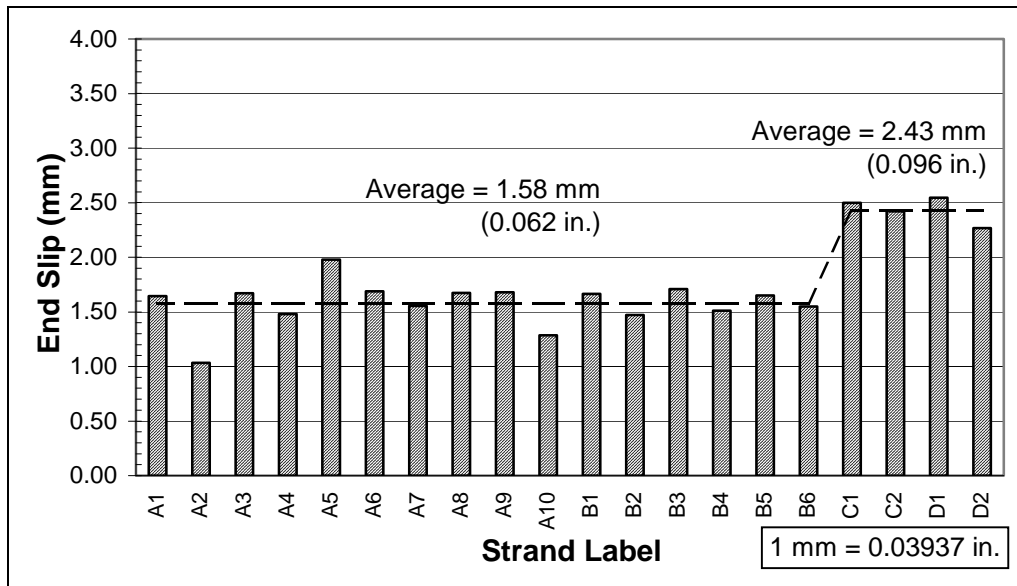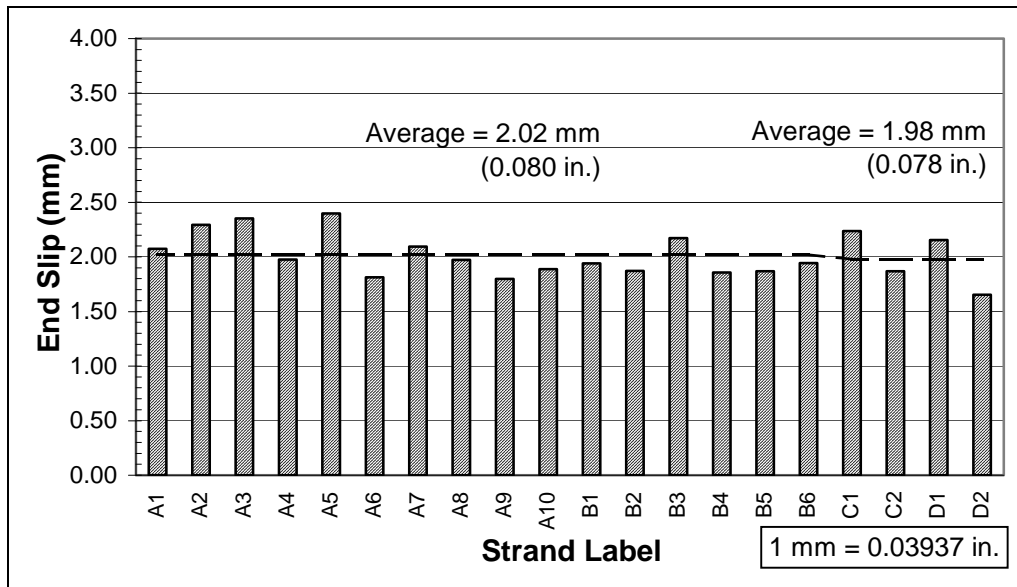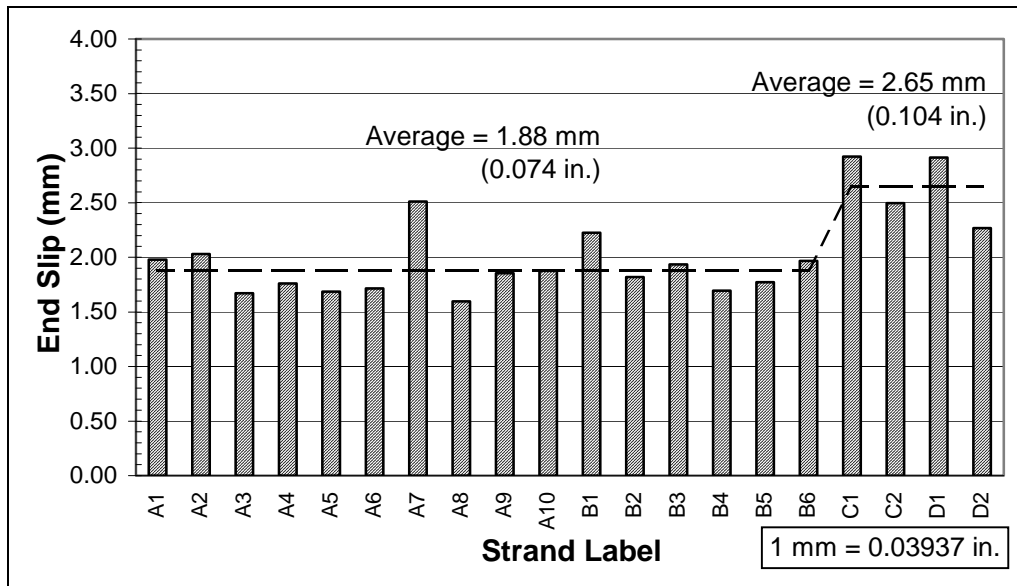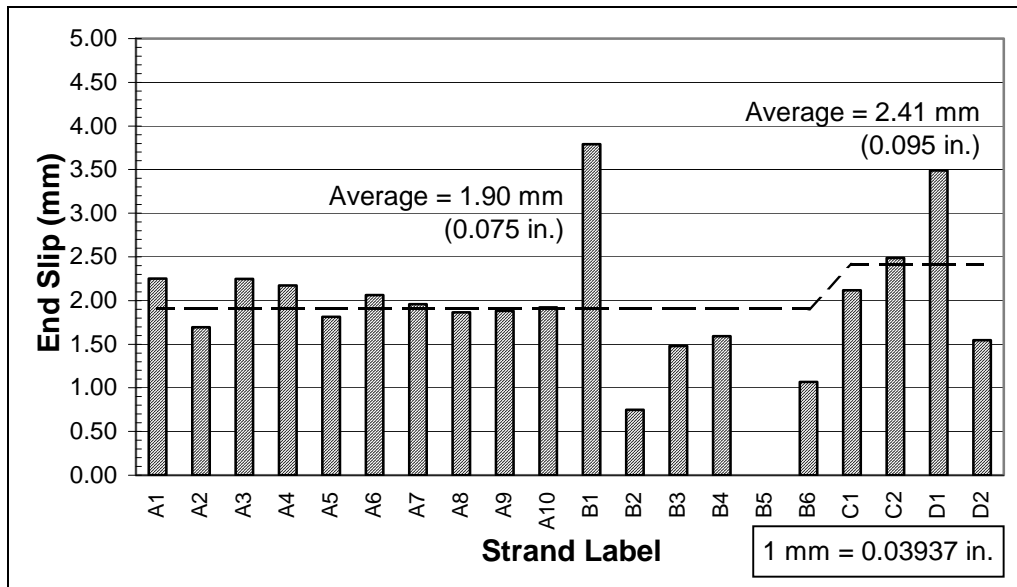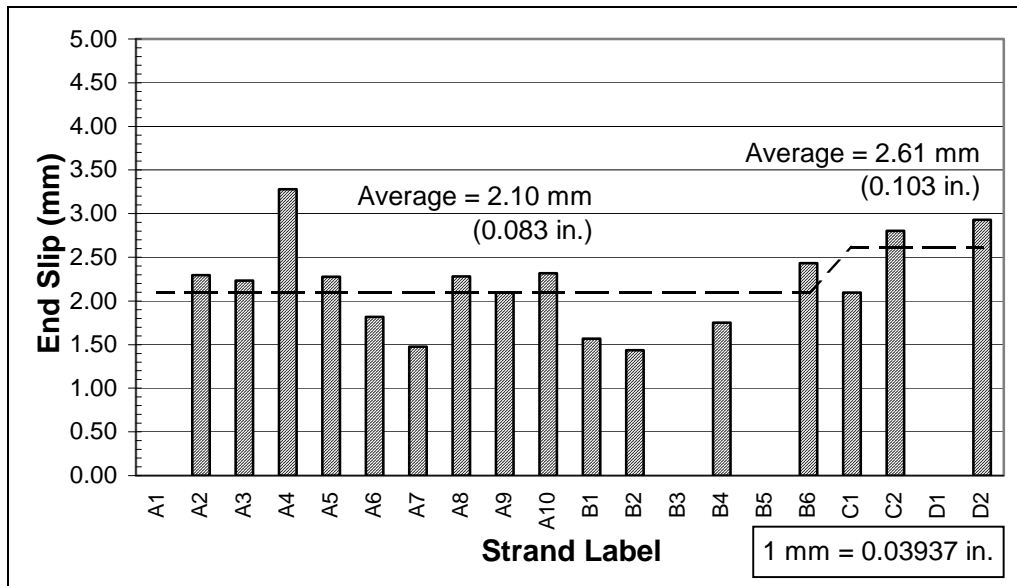

Figure E.14   Strand end slips at beam end N1N measured just after transfer

128

Figure E.15   Strand end slips at beam end N2S measured just after transfer

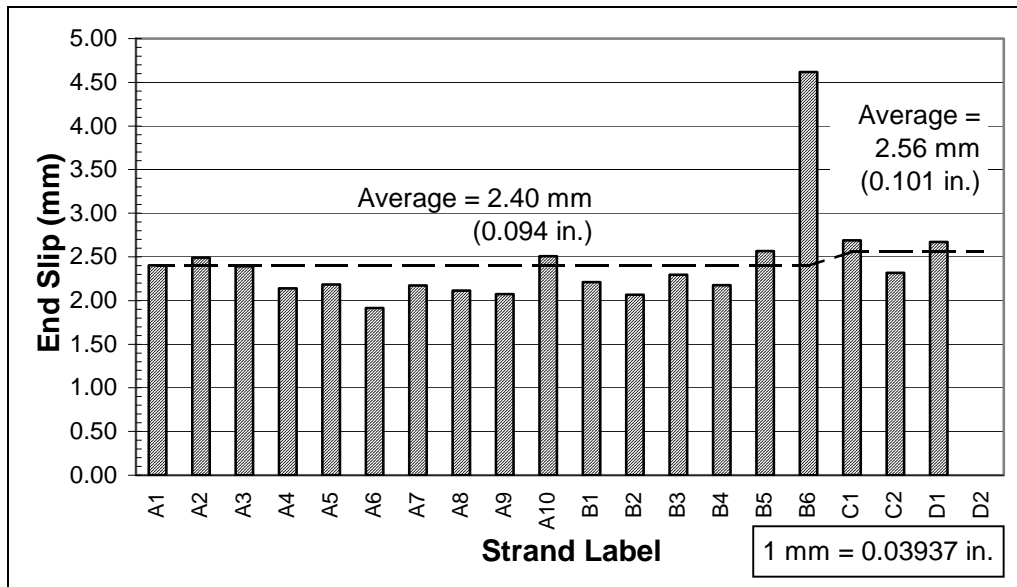*Figure E.16   Strand end slips at beam end N2N measured just after transfer*

129

Figure E.17   Strand end slips at beam end H1S measured after placement of the slab

Figure E.18   Strand end slips at beam end H1N measured after placement of the slab
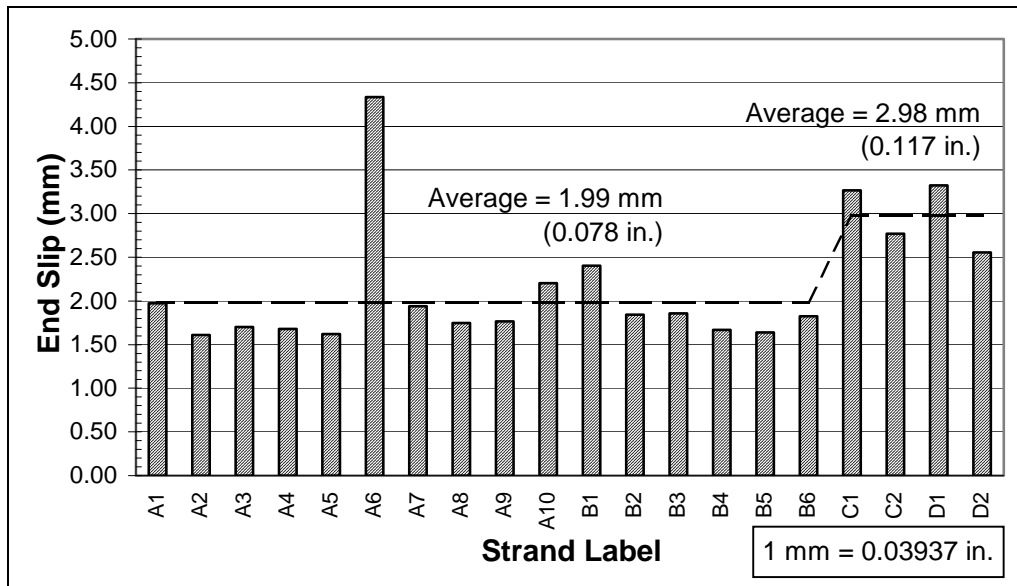
130
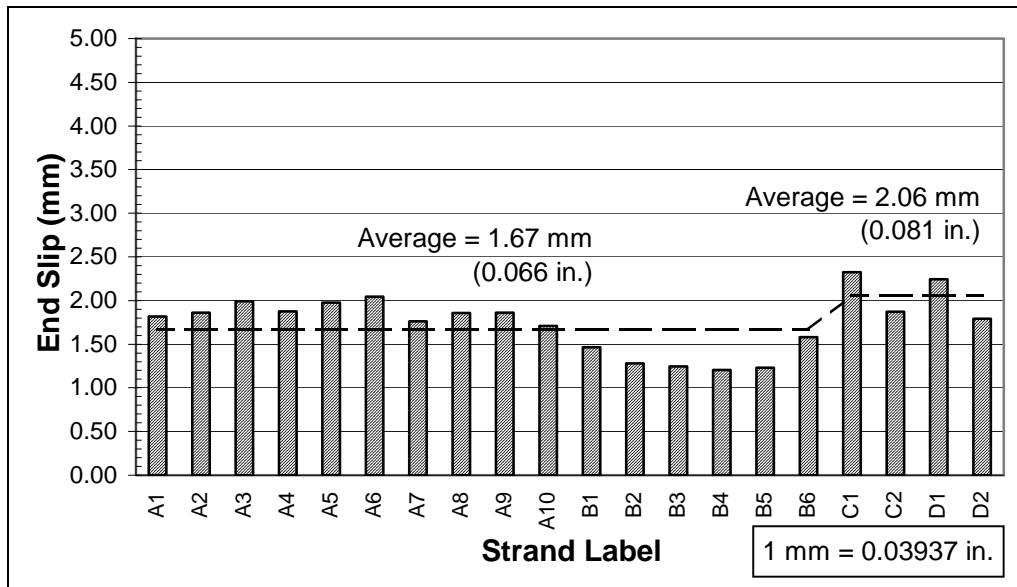
Figure E.19 Strand end slips at beam end H2S measured after placement of the slab
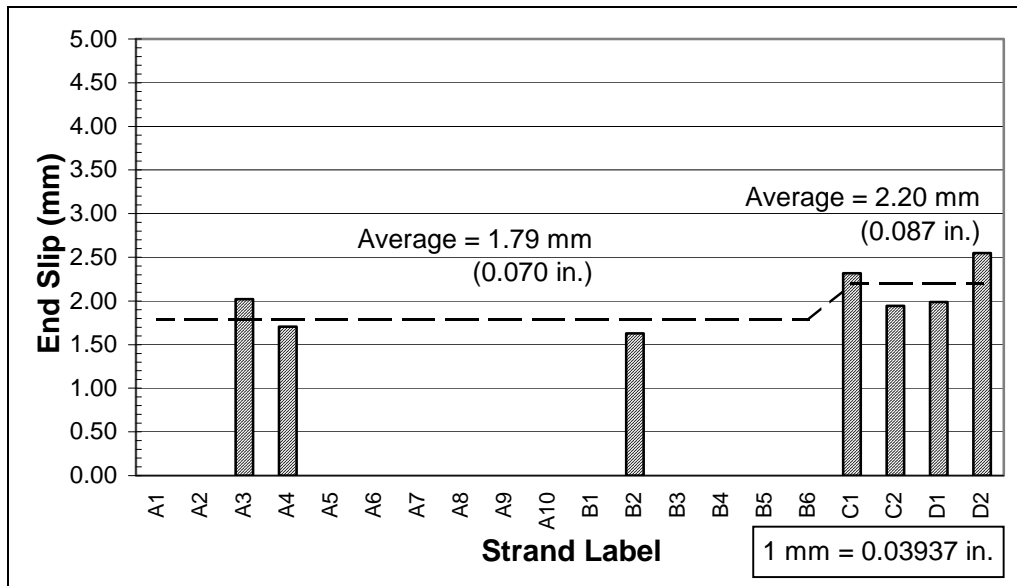
Figure E.20 Strand end slips at beam end H2N measured after placement of the slab

Figure E.21   Strand end slips at beam end N2S measured after placement of the slab

Figure E.22   Strand end slips at beam end N2N measured after placement of the slab

Table E.9   Strand end slips measured just after transfer

Strand Label	Beam End							
	H1S mm	H1N mm	H2S mm	H2N mm	N1S mm	N1N mm	N2S mm	N2N mm
A1	1.39	--- [1]	0.99	1.89	2.15	1.64	2.08	1.98
A2	1.36	1.58	1.21	--- [1]	1.98	1.03	2.29	2.03
A3	1.69	1.70	1.44	1.12	2.15	1.67	2.35	1.67
A4	1.67	2.65	1.29	1.19	1.92	1.48	1.98	1.76
A5	1.59	2.07	2.35	1.08	1.49	1.98	2.40	1.69
A6	1.72	1.14	1.54	1.10	1.34	1.69	1.81	1.71
A7	1.56	1.26	1.14	0.98	1.83	1.56	2.10	2.51
A8	1.55	1.68	1.29	--- [1]	2.07	1.67	1.97	1.60
A9	1.50	1.56	1.20	1.17	1.57	1.68	1.80	1.86
A10	1.24	1.40	1.14	0.94	1.56	1.28	1.89	1.88
B1	3.37	1.47	0.98	1.08	2.07	1.66	1.94	2.23
B2	0.89	0.97	0.77	0.91	1.62	1.47	1.87	1.82
B3	1.19	1.26	0.98	0.92	1.30	1.71	2.17	1.93
B4	1.22	1.28	0.83	0.98	1.30	1.51	1.86	1.70
B5	0.98	1.15	0.85	0.85	1.69	1.65	1.87	1.77
B6	1.24	1.40	1.14	1.06	1.59	1.55	1.94	1.97
Avg. for Bottom Strands	1.51	1.50	1.20	1.09	1.73	1.58	2.02	1.88
C1	1.51	1.64	1.91	1.71	1.99	2.50	2.24	2.92
C2	1.75	2.32	1.25	1.59	2.30	2.42	1.87	2.50
D1	2.09	2.18	1.82	1.45	2.21	2.55	2.16	2.91
D2	1.77	2.41	1.51	2.03	1.97	2.27	1.65	2.27
Avg. for Top Strands	1.78	2.14	1.62	1.70	2.12	2.43	1.98	2.65

Note: [1] No data were recorded for these strands, because the aluminum U-shaped guides caught on the formwork when the prestressing force was released.

Table E.10   Strand end slips measured after placement of the slab

Strand Label	Beam End					
	H1S 10/19/95 mm	H1N 11/6/95 mm	H2S 11/16/95 mm	H2N 11/16/95 mm	N2S 2/19/96 mm	N2N 2/19/96 mm
A1	2.25	--- [1]	1.82	--- [1]	2.41	1.97
A2	1.70	2.30	1.86	--- [1]	2.49	1.61
A3	2.25	2.23	1.99	2.02	2.39	1.70
A4	2.17	3.28	1.88	1.71	2.14	1.68
A5	1.81	2.28	1.98	--- [1]	2.19	1.62
A6	2.06	1.82	2.04	--- [1]	1.91	4.33
A7	1.96	1.48	1.76	--- [1]	2.18	1.94
A8	1.87	2.28	1.86	--- [1]	2.11	1.75
A9	1.88	2.10	1.86	--- [1]	2.07	1.77
A10	1.92	2.32	1.71	--- [1]	2.51	2.20
B1	3.79	1.57	1.47	--- [1]	2.21	2.41
B2	0.75	1.44	1.28	1.63	2.07	1.84
B3	1.48	--- [1]	1.25	--- [1]	2.30	1.86
B4	1.59	1.75	1.21	--- [1]	2.18	1.67
B5	--- [1]	--- [1]	1.23	--- [1]	2.57	1.64
B6	1.07	2.43	1.58	--- [1]	4.62	1.82
Avg. for Bottom Strands	1.90	2.10	1.67	1.79	2.40	1.99
C1	2.12	2.10	2.32	2.32	2.69	3.27
C2	2.49	2.81	1.87	1.94	2.32	2.77
D1	3.49	--- [1]	2.25	1.99	2.67	3.32
D2	1.55	2.93	1.79	2.55	--- [1]	2.56
Avg. for Top Strands	2.41	2.61	2.06	2.20	2.56	2.98

Note: [1] No data were recorded for these strands, because the aluminum U-shaped
guides were dislodged during transportation of the beams.

[2] A second set of final measurements was not taken for beam ends N1S or N1N.

APPENDIX F

DEVELOPMENT LENGTH TEST MEASUREMENTS

Table F.1   Maximum concrete strains at the top of the slab during load tests

ERSG Label	Load Test Designation							
	1-H1S-120	2-H1N-93	3-H2N-78	4-H2S-72	5-N1S-120	6-N1N-93	7-N2S-78	8-N2N-72
	με	με	με	με	με	με	με	με
1A	-3076	-2047	-2981	-2216	-2856	-2507	-2331	-2132
1B		-1886	-2359	-2733	-2867	-2569	-2645	-2724
2A	-2307	-2376	-1705	-1636	-2360	-1945	-2063	-1450
2B	-2179	-2673	-2261	-2287	-2915	-2445	-2482	-1896
2C	-2260		-1996	-1963	-2490	-2286	-2380	-1889
2D	-2429		-1563	-1648	-2307	-2133	-2292	-1645
2E	-2325							
2F	-1822							
3A	-2443	-1947	-1998	-1952	-2565	-2627	-2668	-1874
3B		-1911	-1978	-2112	-2735	-2163	-2183	-1597
Averages								
Row 1	-3076	-1966	-2670	-2475	-2862	-2538	-2488	-2428
Row 2	-2220	-2524	-1881	-1883	-2518	-2202	-2304	-1720
Row 3	-2443	-1929	-1988	-2032	-2650	-2395	-2425	-1736

Table F.2   Maximum strand end slips during load tests

Strand Label	Load Test Designation							
	1-H1S-120 mm	2-H1N-93 mm	3-H2N-78 mm	4-H2S-72 mm	5-N1S-120 mm	6-N1N-93 mm	7-N2S-78 mm	8-N2N-72 mm
A1	0.02	0.05	0.09	0.41	0.00	0.01	0.19	0.74
A2	0.00	0.05	0.01	0.02	0.00	0.05	0.04	0.03
A3	0.01	0.20	0.15	0.05	0.12	0.10	0.10	0.15
A4	0.00	0.12	0.31	0.02	0.00	0.02	0.38	0.55
A5	0.10	0.63	0.53	0.06	0.04	0.05	0.71	0.82
A6	0.04	0.33	0.14	0.59	0.00	0.34	0.55	0.92
A7	0.00	0.06	0.04	0.12	0.00	0.03	0.07	0.26
A8	0.00	0.07	0.00	0.00	0.00	0.00	0.09	0.07
A9	0.03	0.04	0.01	0.02	0.00	0.01	0.10	0.01
A10	0.01	0.08	0.37	0.29	0.01	0.01	0.39	0.44
B1	0.06	0.54	0.65	1.11	0.16	0.09	0.47	1.13
B2	0.10	0.79	0.40	0.62	0.05	0.05	0.67	0.44
B3	0.28	1.22	0.97	0.55	0.01	0.54	0.86	1.40
B4	0.12	1.19	0.21	1.22	0.05	0.49	0.70	1.03
B5	0.08	0.58	0.40	0.81	0.00	0.10	0.76	0.70
B6	0.06	0.44	0.70	0.88	0.01	0.15	1.24	0.82
Max. for Bottom Strands	0.28	1.22	0.97	1.22	0.16	0.54	1.24	1.40
C1	0.01	0.00	0.00	0.00	0.00	0.01	0.00	0.00
C2	0.01	0.05	0.04	0.00	0.00	0.05	0.00	0.05
D1	0.01	0.03	0.24	0.00	0.00	0.04	0.05	0.08
D2	0.00	0.01	0.00	0.00	0.00	0.01	0.00	0.00
Max. for Top Strands	0.01	0.05	0.24	0.00	0.00	0.05	0.05	0.08
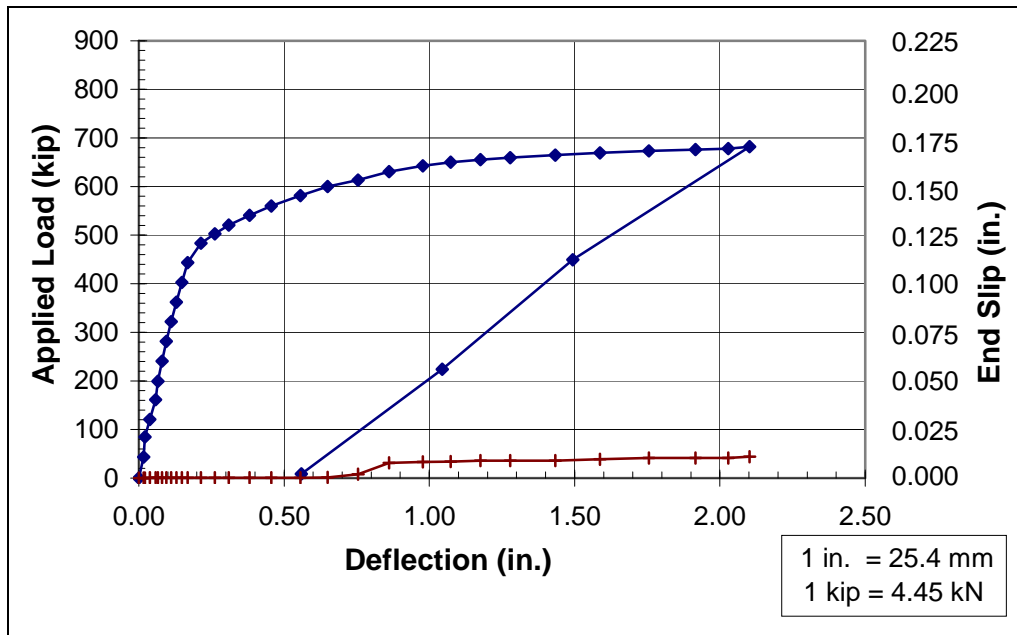
Figure F.1   Load-deflection curve for test no. 1-H1S-120
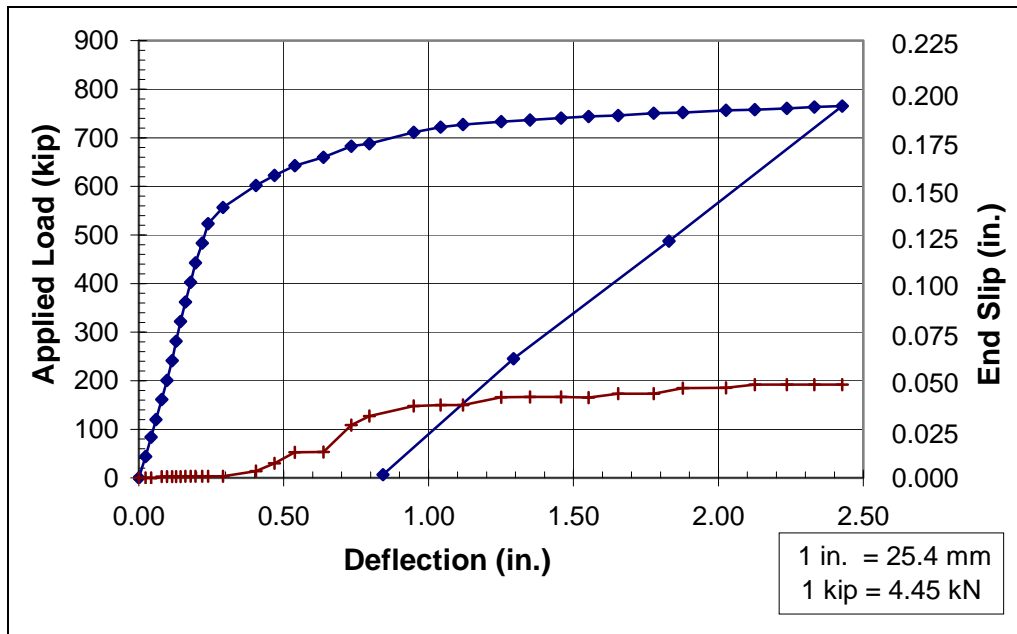
Figure F.2   Load-deflection curve for test no. 2-H1N-93
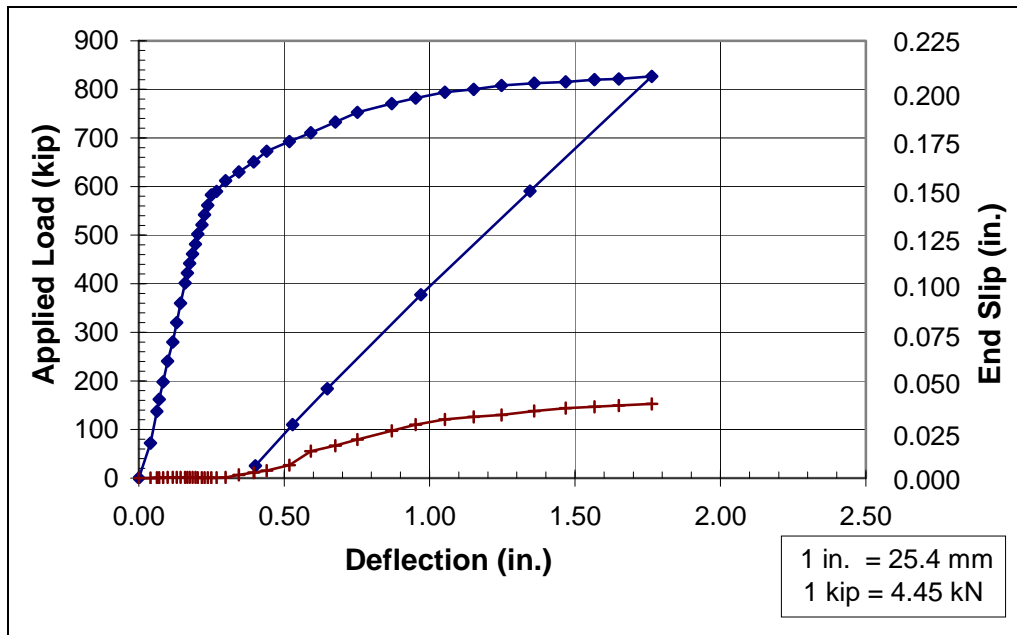
138

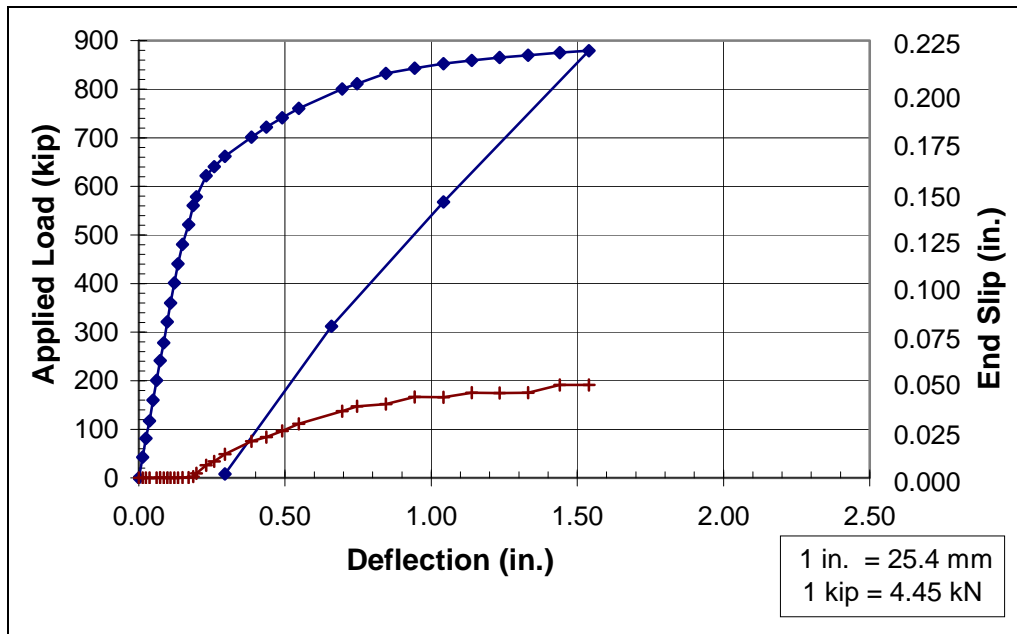*Figure F.3 Load-deflection curve for test no. 3-H2N-78*

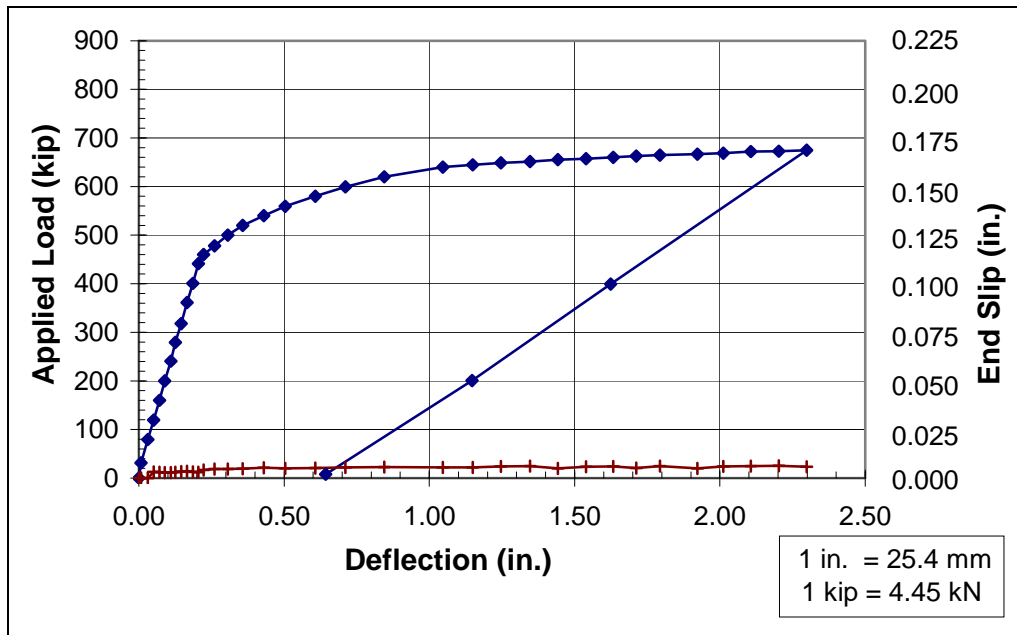*Figure F.4 Load-deflection curve for test no. 4-H2S-72*
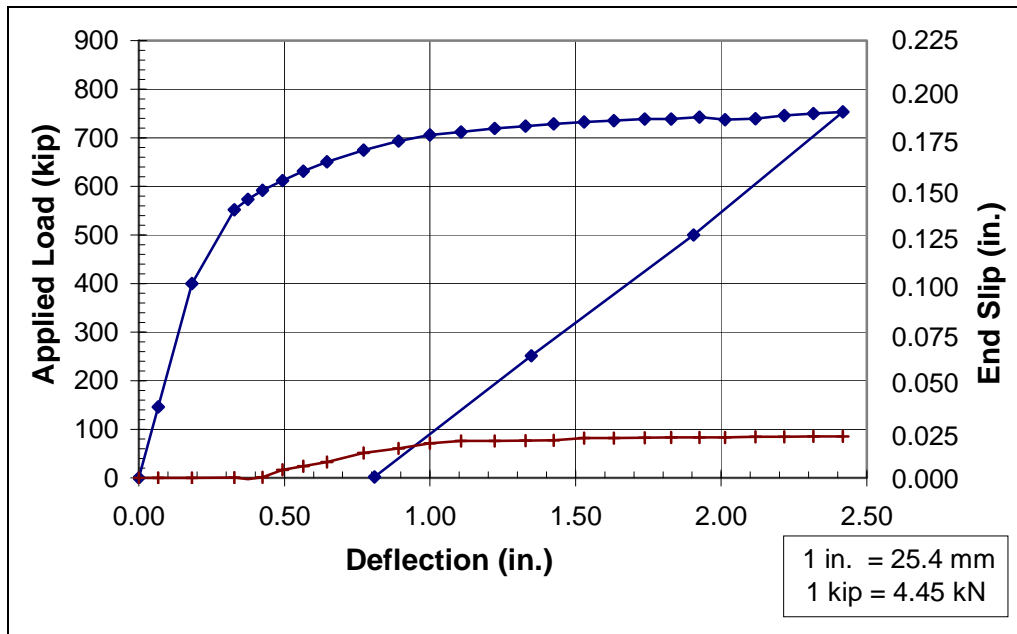
Figure F.5   Load-deflection curve for test no. 5-N1S-120
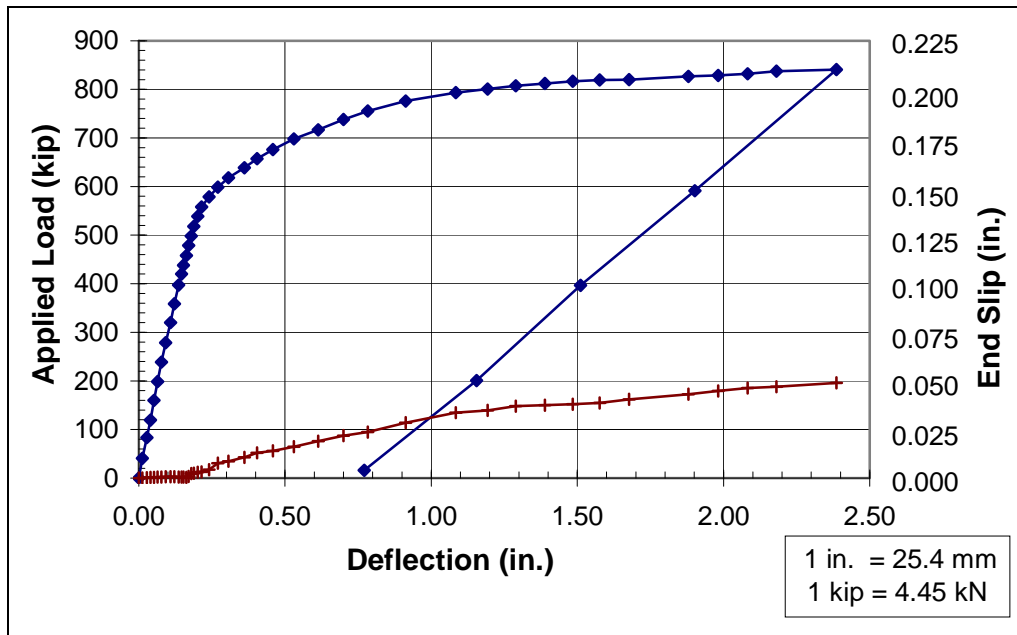

Figure F.6   Load-deflection curve for test no. 6-N1N-93

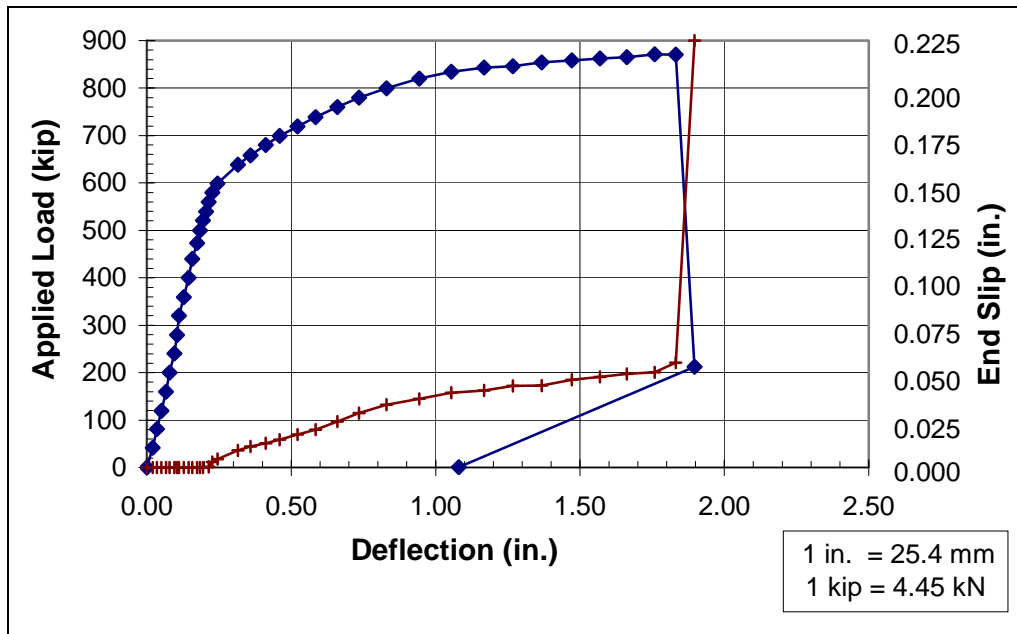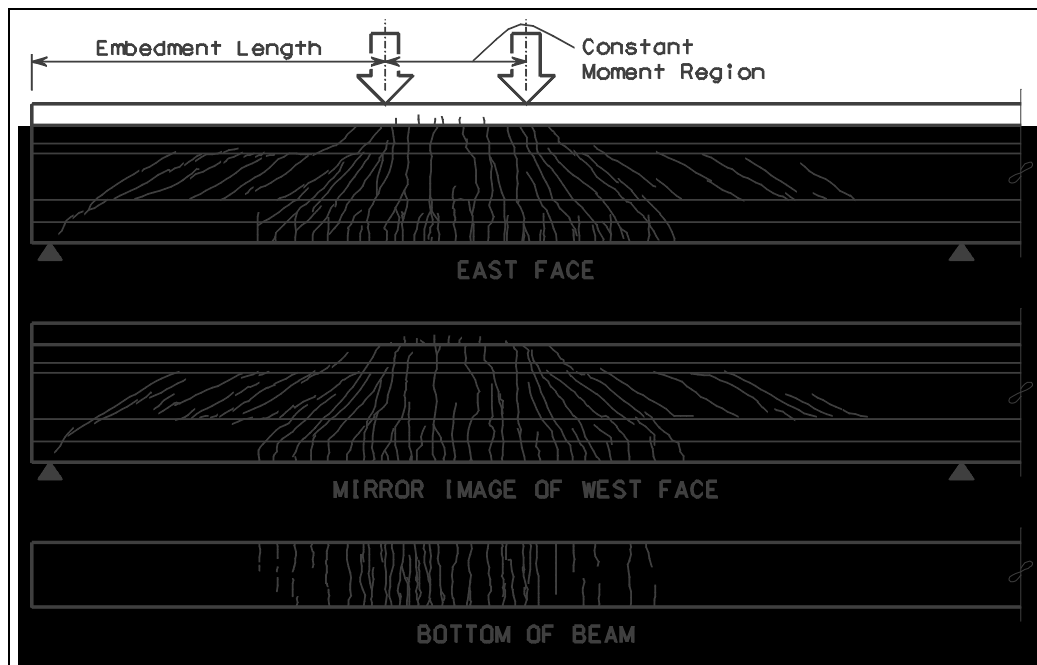*Figure F.7   Load-deflection curve for test no. 7-N2S-78*

Figure F.8   Load-deflection curve for test no. 8-N2N-72
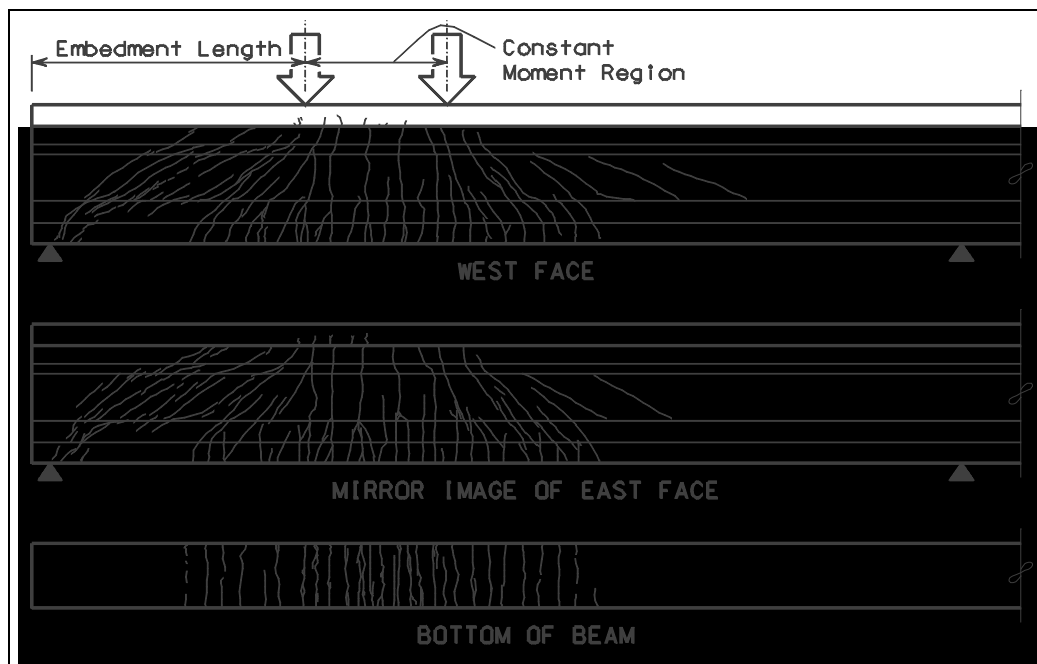
Figure F.9   Crack pattern for test no. 1-H1S-120

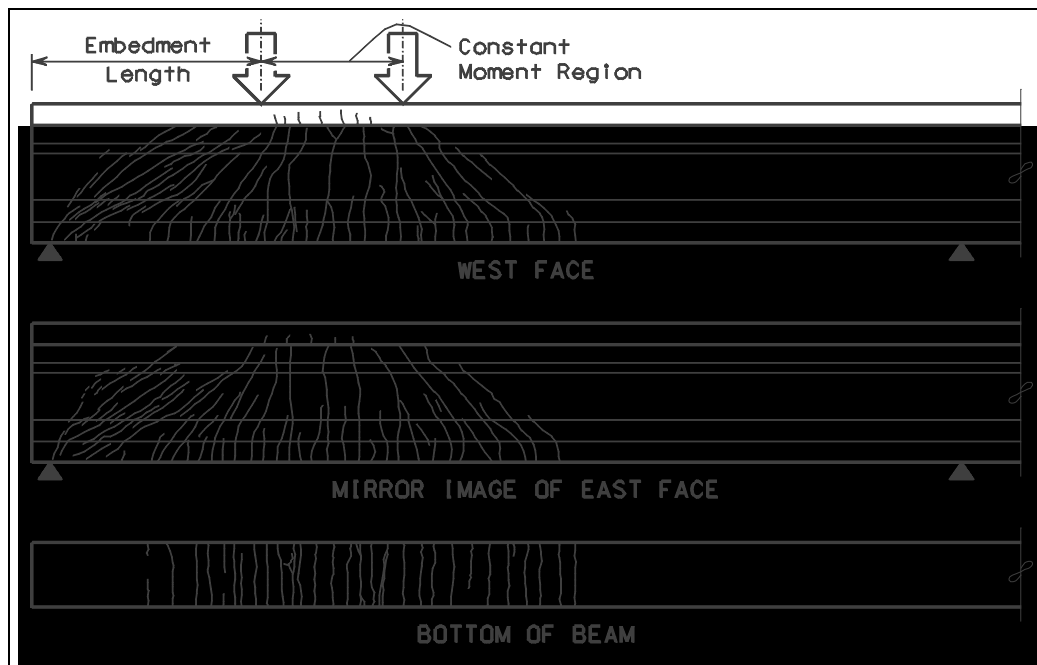*Figure F.10   Crack pattern for test no. 2-H1N-93*

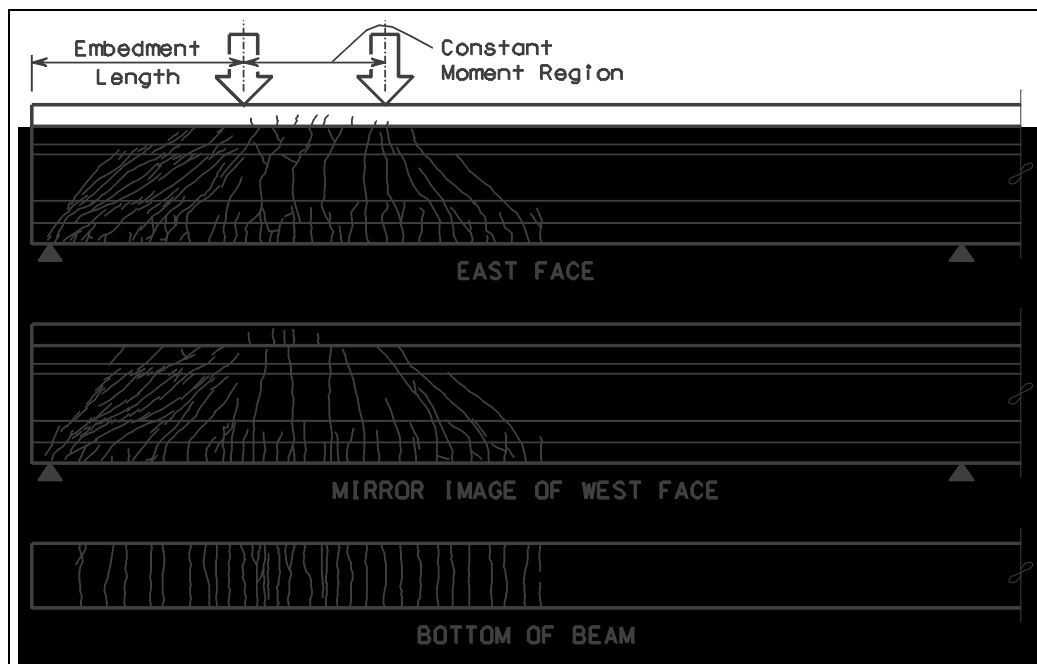*Figure F.11   Crack pattern for test no. 3-H2N-78*

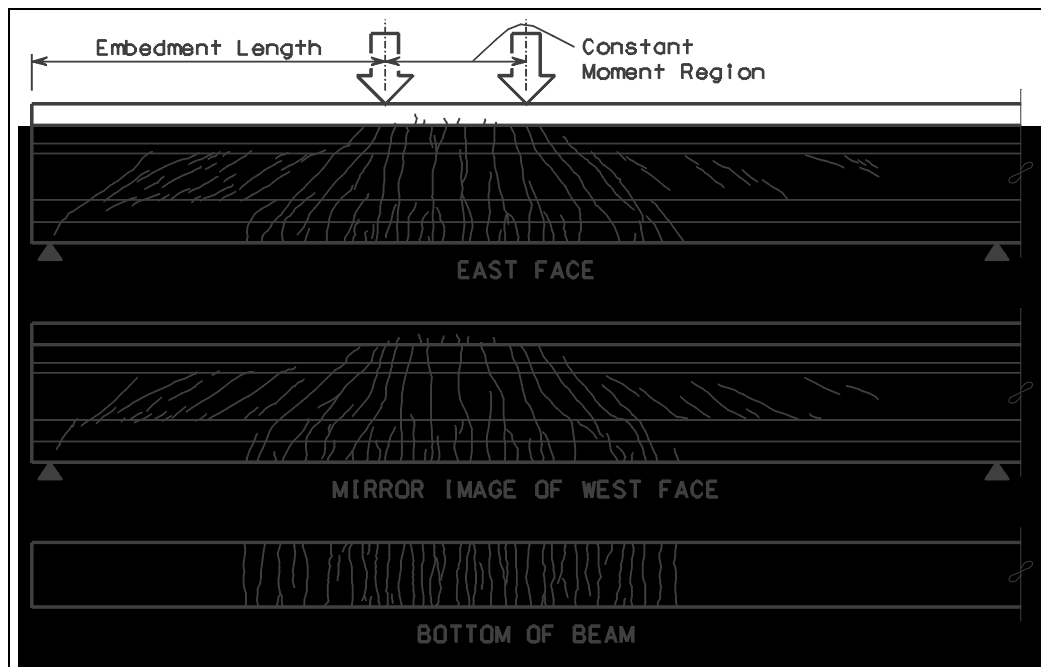*Figure F.12   Crack pattern for test no. 4-H2S-72*
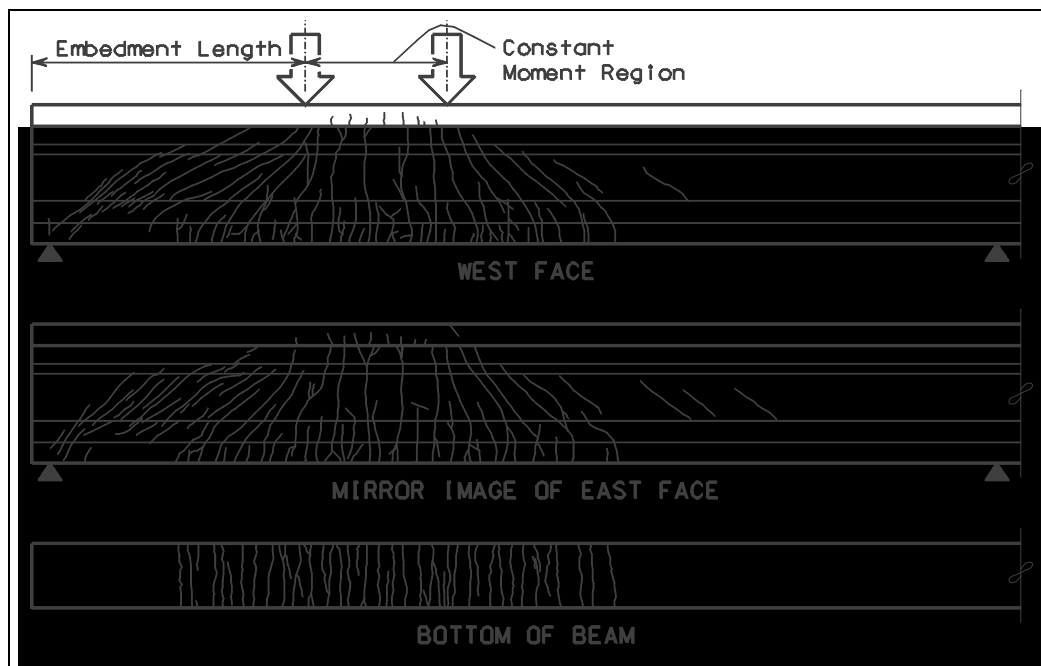
Figure F.13   Crack pattern for test no. 5-N1S-120

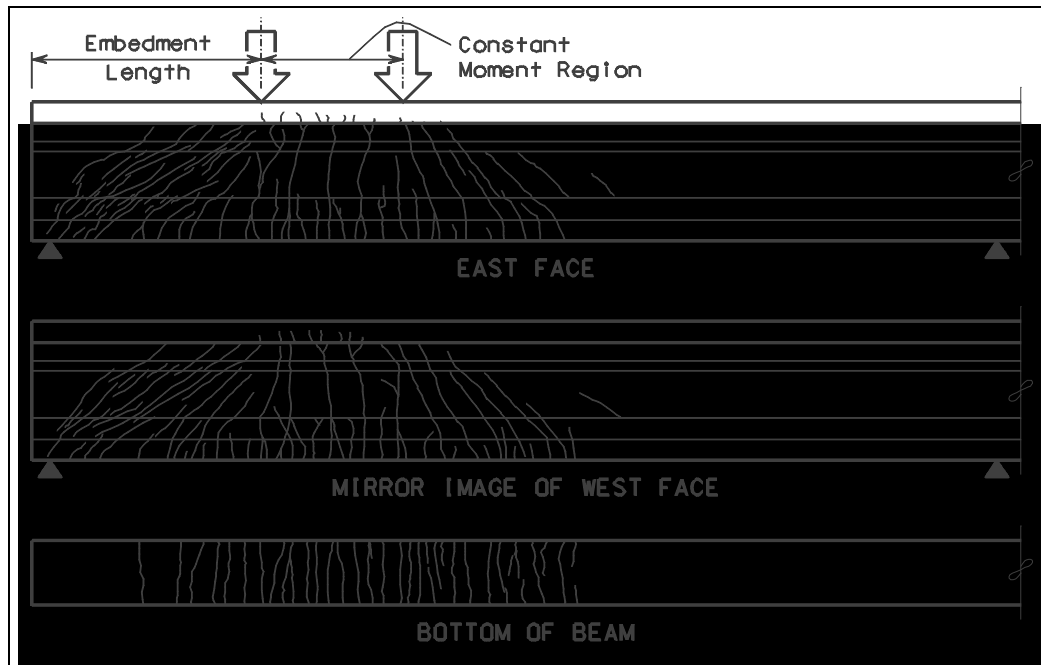*Figure F.14   Crack pattern for test no. 6-N1N-93*

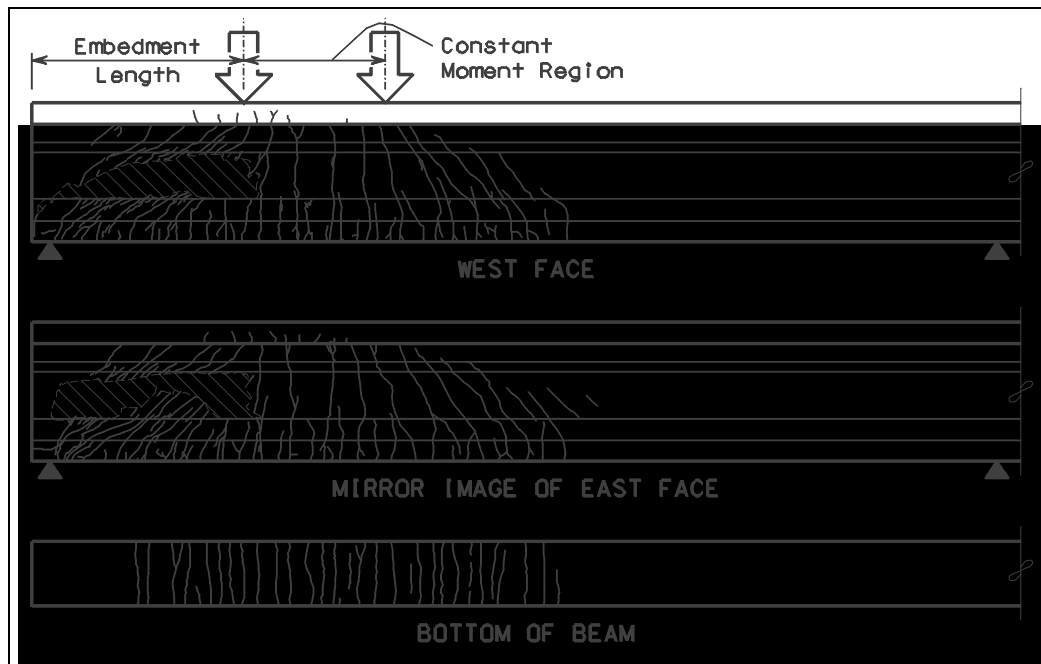*Figure F.15   Crack pattern for test no. 7-N2S-78*

Figure F.16   Crack pattern for test no. 8-N2N-72

APPENDIX G

NOTATION

Report Notation	ACI Notation	AASHTO Notation	Description
A			Area of cross section.
A_{ps}	A_{ps}	A_s^*	Area of prestressing strand.
B			Bond stress factor in transfer length equation proposed by Cousins et al.[5]
b			Width of rectangular piece in moment-curvature calculations.
c			Depth of rectangular piece in moment-curvature calculations.
d_b	d_b	D	Diameter of prestressing strand.
E_c	E_c	E_c	Modulus of elasticity of concrete.
E_{ci}	E_{ci}	E_{ci}	Modulus of elasticity of concrete at transfer.
E_{ps}		E_s	Modulus of elasticity of prestressing strand.
E_s		E_s	Modulus of elasticity of non-prestressed reinforcement.
f_c	f_c	f_c	Stress in concrete.
f_{po}			Stress in pretensioned strand immediately before release (i.e., at anchorage).
f_{ps}	f_{ps}	f_{su}^*	Stress in pretensioned strand at nominal flexural strength of cross section.
f_{pu}	f_{pu}	f'_s	Ultimate tensile strength of prestressing strands.
f_{py}	f_{py}	f_y^*	Specified yield strength of prestressing strands.
f_r	f_r	f_r	Modulus of rupture of concrete.
f_{se}	f_{se}	f_{se}	Effective prestress, i.e., stress in pretensioned strands after all losses.
f_{si}			Initial prestress, i.e., stress in pretensioned strands immediately after release.
f_{strand}			Stress in prestressing strand during pull out tests.
f'_c	f'_c	f'_c	Concrete compressive strength.
f'_{ci}	f'_{ci}	f'_{ci}	Concrete compressive strength at transfer.
I	I	I	Moment of inertia of cross section.
L_b			Length of debonding for debonded strands in development length criteria proposed by Russell and Burns.[17]
L_d	ℓ_d		Development length of prestressing strands.
L_e			Embedment length of prestressing strands.
L_t			Transfer length of prestressing strands.
M_{cr}	M_{cr}	M_{cr}^*	Cracking moment of cross section.
M_n	M_n	M_n	Nominal flexural strength of cross section.
M_{test}			Maximum total moment at a section during load tests.
n	n	n	Modular ratio, E_s/E_c or E_{ps}/E_c.
Q			First moment of area used in calculation of nominal web shear strength, V_{cw}.
U'_d			Strand surface coeff. in development length equation proposed by Cousins et al.[5]

U'_t			Strand surface coefficient in transfer length equation proposed by Cousins et al.[5]
V_{cw}	V_{cw}	V_{cw}	Nominal web shear strength of cross section.
V_{test}			Maximum total shear at a section during load tests.
y_b			Dimension from the bottom of the cross section to the center of gravity.
β_1	β_1	β_1	Depth of equivalent rectangular stress block / Depth of neutral axis.
γ_p	γ_p	γ^*	Constant for strand type (0.28 for Grade 270).
ε			Concrete strain at any location in the moment-curvature calculations.
ε_{ci}			Strain in concrete at level of pretensioned strands immediately after release.
ε_o			Concrete strain when the concrete stress, f_c, is equal to the concrete compressive strength, f'_c, in the moment-curvature calculations.
ε_{po}			Strain in pretensioned strands immediately before release (i.e., at anchorage).
ε_{ps}			Strain in pretensioned strands at nominal flexural strength of the cross section.
ε_{se}			Strain in pretensioned strands after losses (due to prestressing only).
ε_{si}			Strain in pretensioned strands immediately after release.
$\varepsilon_1, \varepsilon_2$			Concrete strain at the top and bottom of a rectangular piece of the cross section (where $\varepsilon_1 \geq \varepsilon_2$) in the moment-curvature calculations.
ϕ_{sh}			Curvature of cross section due to slab shrinkage used in moment-curvature calculations.
Δf_{se}			Change in effective prestress of pretensioned strand due to losses.
Δ_{sh}			Measured beam deflection due to slab shrinkage.
λ			Factor to increase flexural bond length in development length equation proposed by Buckner.[3]
ω_p	ω_p	ω_p	Reinforcement index.

Note: This list of notation was adopted from Buckner[3].

REFERENCES

1. *Building Code Requirements for Reinforced Concrete*, (ACI 318-95), American Concrete Institute, Detroit, Michigan, 1995.

2. *Standard Specifications for Highway Bridges*, 15th Edition, American Association of State Highway and Transportation Officials, Washington, D.C., 1992.

3. Buckner, C.D., "An Analysis of Transfer and Development Lengths for Pretensioned Concrete Structures," Final Report FHWA-RD-94-049, Department of Civil and Environmental Engineering, Virginia Military Institute, December 1994.

4. Carrasquillo, R.L., Nilson, A.H., and Slate, F.O., "Properties of High-strength concrete Subject to Short-Term Loads," ACI Journal, Vol. 78, No. 3, May-June 1981, pp. 171-178.

5. Cousins, T., Johnston, D., and Zia, P., "Transfer and Development Length of Epoxy Coated Prestressing Strand," PCI Journal, Vol. 35, No. 4, July-August 1990, pp. 92-103.

6. Deatherage, J.H., Burdette, E.G., and Chew, C.K., "Development Length and Lateral Spacing Requirements of Prestressing Strand for Prestressed Concrete Bridge Girders," PCI Journal, Vol. 39, No. 1, January-February 1994, pp. 70-83.

7. Gross, S.P. and Burns, N.H., "Transfer and Development Length of 15.2 mm (0.6 in.) Diameter Prestressing Strand in High Performance Concrete: Results of the Hoblitzell-Buckner Beam Tests," Research Report 580-2, Center for Transportation Research, The University of Texas at Austin, June 1995.

8. Hanson, N.W., "Influence of Surface Roughness of Prestressing Strand in Bond Performance," PCI Journal, Vol. 14, No. 1, January-February 1969, pp. 32-45.

9. Hanson, N.W. and Kaar, P.H., "Flexural Bond Tests of Pretensioned Prestressed Beams," ACI Journal, Vol. 55, No. 7, January 1959, pp. 783-803.

10. Janney, J.R., "Nature of Bond in Pre-Tensioned, Prestressed Concrete," ACI Journal, Vol. 50, 1954, pp. 717-736.

11. Kaar, P.H., LaFraugh, R.W., and Mass, M.A., "Influence of Concrete Strength on Strand Transfer Length," PCI Journal, Vol. 8, No. 5, October 1963, pp. 47-67.

12. Lane, S. N., "Transfer Lengths in Regular Prestressed Concrete Concentric Beams," Public Roads - A Journal of Highway Research and Development, Federal Highway Administration, Vol. 56, No. 2, September 1992, pp. 67-71.

13. Lin, T.Y. and Burns, N.H., *Design of Prestressed Concrete Structures*, 3rd Edition, John Wiley and Sons, New York, 1981.

14. Martin, L.D. and Scott, N.L., "Development of Prestressing Strand in Pretensioned Members," ACI Journal, Vol. 73, No. 8, August 1976, pp. 453-456.

15. Mitchell, D., Cook, W. D., Khan, A.A., and Tham, T., "Influence of High Strength Concrete on Transfer and Development Length of Pretensioning Strand," PCI Journal, Vol. 38, No. 3, May-June 1993, pp. 52-66.

16. PCI Committee on Prestress Losses, "Recommendations for Estimating Prestress Losses," PCI Journal, Vol. 21, No. 4, July-August 1975, pp. 44-75.

17. Russell, B.W. and Burns, N.H., "Design Guidelines for Transfer, Development, and Debonding of Large Diameter Seven Wire Strands in Pretensioned Concrete Girders," Research Report 1210-5F, Center for Transportation Research, The University of Texas at Austin, January 1993.

18. Shahawy, M.A., Issa, M., and Batchelor, B., "Strand Transfer Lengths in Full Scale AASHTO Prestressed Concrete Girders," PCI Journal, Vol. 37, No. 3, May-June 1992, pp. 84-96.

19. Tawfiq, K., "Cracking and Shear Capacity of High Strength Concrete Girders," Final Report, Department of Civil Engineering, FAMU/FSU College of Engineering, January 1995.

20. Zia, P., and Mostafa, T., "Development of Prestressing Strands," PCI Journal, Vol. 22, No. 5, September-October 1977, pp. 54-65.

21. *PCI Design Handbook – Precast and Prestressed Concrete*, 4th Edition, Precast/Prestressed Concrete Institute, Chicago, Illinois, 1992.

22. Cordova Alvestegui, C., "Transfer and Development Length of 0.6-Inch Diameter Prestressing Strand at Two Inch Spacing in Fully Bonded Normal Strength Concrete Composite Texas Type C Beams," Master's Thesis, The University of Texas at Austin, August 1996.

23. Shah, A., "Bond Behavior of 0.6-Inch Diameter Prestressing Strand at Two Inch Grid Spacing in Fully Bonded High Strength and Normal Strength Composite Texas Type C Beams," Master's Departmental Report, August 1996.

VITA

Michael Owen Braun was born in Milwaukee, Wisconsin on May 28, 1953, the son of Henry William Braun and Ruth Amolia Braun. After graduation from Kettle Moraine High School, Wales, Wisconsin in 1971, he attended the University of Wisconsin at Platteville where he graduated Summa cum Laude with a Bachelor of Science Degree in Civil Engineering in 1975. From 1976 to 1978, he studied graduate level courses in environmental engineering at Utah State University in Logan, Utah. Beginning in 1979, he worked as a design engineer and a Registered Professional Engineer for structural consulting engineering firms in San Antonio, Texas. In 1991, he joined the Bridge Design Section in the Houston District Office of the Texas Department of Transportation. After completing several graduate level civil engineering courses at The University of Texas at Austin in the early 1980's and the University of Houston in 1994, he reentered the Graduate School at The University of Texas in 1995 as a participant in the MSCE Graduate Program of the Texas Department of Transportation. Currently, he is a Registered Professional Engineer with Atwood Hinzman, Inc., Consulting Engineers in Spokane, Washington.

Permanent Address: 1118 Droester Road

Madison, Wisconsin 53716

This thesis was typed by the author.